Development of an On-Animal Separation Based Sensor using On-line Microdialysis Sampling Coupled to Microchip Electrophoresis with Electrochemical Detection

David E. Scott

Submitted to the Department of Chemistry and the Faculty of the Graduate School of the University of Kansas in Partial Fulfillment of the Requirements for the Degree of Doctor of Philosophy

Dissertation Committee

Chair, Susan M. Lunte, Ph.D.

Craig E. Lunte, Ph.D.

Cindy L. Berrie, Ph.D.

Christopher G. Elles, Ph.D.

Brian D. Ackley, Ph.D.

Date Defended: January 30, 2014

The Dissertation Committee for David Emmanuele Scott certifies that this is the approved version of the following dissertation:

Development of an On-Animal Separation Based Sensor using On-line Microdialysis Sampling Coupled to Microchip Electrophoresis with Electrochemical Detection

Dissertation Committee

Chair, Susan M. Lunte, Ph.D.

Date Approved: February 04, 2014

Abstract

Microdialysis is a sampling technique that can be employed for the continuous monitoring of compounds both *in vivo* and *in vitro*. The online-coupling of microdialysis to microchip electrophoresis provides an attractive technology for near real time monitoring of drugs and neurotransmitters in pharmacokinetic and behavioral studies. These on-line systems for the analysis of microdialysis samples allow for the development of selective and sensitive separation based sensors with the capability of preserving high temporal resolution. Electrochemical detection is well suited for these separation-based sensors due to the possibility of integrating the working and reference electrodes directly into the chip as well as the availability of a miniaturized isolated potentiostat.

This dissertation primarily focuses on the development of an on-animal separation-based sensor using microdialysis coupled to microchip electrophoresis with amperometric detection. The system consists of an on-line interface to couple the microdialysis to microchip electrophoresis, high voltage power supplies, and an electrically isolated potentiostat. Initial studies were focused on developing and fabricating an all glass microfluidic device. This system was evaluated *in vitro* for the continuous monitoring of the enzymatic production of hydrogen peroxide.

The system was optimized for the *in vivo* analysis of nitrite on a *freely roaming* animal. The system incorporates telemetry for remote control, data acquisition, and has been optimized for the continuous on-line analysis of microdialysis samples obtained using a linear probe following nitroglycerin administration. The on-line microdialysis-

microchip electrophoresis system was fabricated using an all glass substrate that includes an electrophoresis separation channel, integrated platinum working and reference electrodes, as well as an interface for direct coupling of the chip to the microdialysis probe. This dissertation describes the development of the integrated system including optimization of the electrophoresis conditions, injection of samples into the chip using the on-line microdialysis-microchip electrophoresis interface, and evaluation of the overall ruggedness of the system. The ultimate goal is to use the separation based sensor for on-animal *in vivo* analysis of drugs and neurotransmitters in order to correlate neurochemistry and/or metabolism with behavior in *freely roaming* animals.

Acknowledgements

I would like to first thank Dr. Susan Lunte for putting up with me over the past five years. It has become clear to me that I can be extremely opinionated an equally difficult to work with. Through Sue's constant "encouragement" and motivation I have been able to develop greatly here at KU. Sue has given me wonderful opportunities to collaborate with individuals at other universities and well as to reach out and speak about our research with others. These have been invaluable experiences in expanding my breadth of knowledge in the scientific arena.

I must give a sincere thanks to Dr. James Chapman for all of his encouragement during my undergraduate education. He fostered a passion for knowledge in me and believed in my ability in a laboratory setting. If it were not for his extreme brilliance and passion as an educator and kindness as an individual I would not have accomplished as much as I have been able to. I must also thank Dr. Dale Harrak, and Dr. Anne Lee for being amazing educators and driving their passion for chemistry into all of their students.

Dr. Fatemah Nichols, Where can I even begin? She is such a strong woman and tough educator that truly believes in knowledge and understanding and is willing to instill that passion for knowledge into her students. My first chemistry class, ever, was with her and I will never forget that very intense summer semester. She made such a dramatic impression upon me and gave me the confidence to continue on and further my education in chemistry. Her strength, knowledge, and passion are unequal.

Table of Contents

List of Figures

Chapter 1

Introduction

1.1 Microdialysis sampling

In 1966, Bito and collaborators described the first application of dialysis sampling in the brain.[1] Sterile dialysis membranes filled with a six percent dextran saline solution were implanted into the parenchyma of the brain and neck of dogs. Ten weeks later, the implanted dialysis membranes were removed and samples were collected for analysis. The ability to continuously sample through the dialysis membrane in an effort to measure a "time-course" of infused and recovered compounds was later reported by Delgado *et al*. (1972).[2] Delgado reported on a "dialytrode" which was a small push-pull perfusion cannula with a small semipermeable membrane sack attached to its tip that was used for long-term intracerebral perfusion in conscious monkeys. Two years later, Ungerstedt and Pycock (1974) published the seminal paper that established modern microdialysis (MD) sampling. They described a simple hollow fiber dialysis probe that was implanted into the striatum of a rat.[3] The dialysis probe of this design is still being marketed by Bioanalytical Systems (BASi) and CMA microdialysis, as seen in Figure 1.1, and is considered one of the most popular commercially available MD probes on the market.[4] These probes are typically 15 mm long and implanted vertically in the brain. They consist of two concentric tubes with one small inner tube for perfusion and a larger outer tube for recovery, with a 2-5 mm long dialysis membrane secured to the bottom of the outer tube.

Since then, more than 13,000 scientific papers have been published using microdialysis sampling.[2,5] This technique has become a widely used and pervasive technology in part due to rapid advances in the development of highly sensitive analytical

techniques as well as the ability to easily manufacture small-bore dialysis tubing first described by Ungerstedt and Pycock in 1974.[3,6] Since then, microdialysis has become an extremely powerful tool for continuously sampling and monitoring biological compound release in the fields of neurochemistry and pharmacology. MD sampling also allows for the assessment of drug metabolism in living tissue, which provides more clinically relevant information than can be gained from testing blood samples.[4,7]

Microdialysis is a technique that can provide some of the most comprehensive data on intrinsic changes at the cellular level while still preserving physiological and behavioral functions. MD is a minimally invasive technique that allows for *in-vivo* sampling of molecular transport within the extracellular space of virtually any tissue or organ in the body. It has also been used for sampling biologically relevant fluids such as blood, urine, and cerebral spinal fluid.[8] Microdialysis provides a unique ability to gain insight into neurological functions through the ability to monitor and collect relevant data regarding neurotransmitters from biological systems under basal, non-stimulated conditions as well as under stimulated conditions. This technique also makes it possible to observe the release of neurotransmitters in response to stimuli and drugs, providing a starting point for analyzing neuroactivity as it relates to the role of various brain structures and receptors. MD, as a continuous sampling technique, has been extensively tested for *in-vivo* and *in-vitro* methods.[9-12]

Microdialysis has been extensively used for *in-vivo* monitoring of endogenous compounds, as well as drug delivery and metabolism in multiple tissues including liver, kidney, heart, lungs, and brain structures.[8] The analysis of microdialysis samples has been accomplished with a wide variety of analytical systems including liquid

chromatography (LC) and capillary electrophoresis (CE) using laser-induced fluorescence (LIF), mass spectrometry (MS), contactless conductivity (C4D), and electrochemical (EC) detection.[13]

The principles of MD sampling are relatively simple. The MD probe is initially implanted into the tissue of interest. A solution of similar osmolality and composition to that of the extracellular fluid of the tissue being sampled is pumped through the MD probe. Compounds from the extracellular fluid diffuse across the probe membrane as illustrated in Figure 1.1. Microdialysis sampling is driven by the diffusion of molecules across the membrane based on the concentration gradient. The concentration gradient causes the diffusion of analytes from areas of high concentration to areas of low concentration between the fluid that is perfused through the probe against the extracellular fluid which is separated by the semipermeable membrane.

The MD probe also serves as a molecular weight filter in which analytes above the molecular weight cut off of the MD probe, such as large proteins and protein complexes, are unable to pass through the membrane. Molecules move in both directions across the membrane, which allows for the recovery of endogenous compounds while also giving the option for the simultaneous local delivery of drugs through the probe directly to the sampling area. One of the major uses cited for MD sampling is to measure *in-vivo* concentrations of endogenous compounds such as neurotransmitters and biogenic amines along with the concentration of drugs and their metabolites.[13]

A fundamental objective in microdialysis sampling is to maximize the recovery of the analyte of interest during sampling. Recovery is theoretically defined by the following equation:[14,15]

$$Recovery = 1 - \exp\left\{\frac{-1}{[Q_d(R_d+R_m+R_e)]}\right\} \quad (1)$$

In this equation Q_d = dialysate/perfusate flow rate; R = mass transfer resistance with subscripts d = dialysate, m = membrane and e = external surrounding medium. The most readily controlled variables within this equation are Qd and Rm, where Rm is the resistance of the membrane and is defined by the molecular weight cut-off or the pore size of the MD membrane. The working dimensions of the probe, such as membrane length and total area of the probe, also factor into the Rm variable. Qd represents the volumetric flow rate of the fluid through the probe. With lower flow rates Qd decreases which, in turn, increases the recovery.

The parameters which are less easily controlled for system analysis, are Re and Rd. Re defines the rate of diffusion for the analyte of interest through the extracellular matrix, the rate of metabolism for the analyte of interest, and other reactions that may take place as defined by the system being monitored. Rd is the rate of diffusion of the analyte of interest in the perfusate.

Many factors can affect recovery such as placement of the probe, the diffusion coefficient of the analyte in the matrix, the size and mobility of the analyte, along with any metabolic transformations due to enzymatic reactions that may occur before the analyte diffuses across the membrane. Understanding all of these factors impresses upon one why probe calibration is extremely important and should ideally be done before and after an experiment to be able to properly calculate analyte concentration as a function of

time.

A commonly used experimental approach for probe calibration, and determination of experimental recovery is to calculate the extraction efficiency (EE). The extraction efficiency consists of measuring the response of a compound with a known concentration from a matrix. The EE is directly proportional to the concentration gradient established at the membrane. Extraction efficiency can be determined based on the concentration of analyte present in the dialysate versus that available in the sample. Meaning that *in-vivo* the relative recovery (RR) of a compound can be calculated by:

$$\text{Relative Recovery} = 100 \text{ x} \frac{C_{dialysate}}{C_{sample}} \quad (2)$$

For *in-vivo* studies, retrodialysis which takes advantage of an internal standard, is commonly used and relies on the assumption that diffusion is equal in both directions.[15] In this case, the internal standard must possess analogous properties to the analyte of interest. A known concentration of the compound is added to the perfusate and the rate of disappearance or *in vivo* loss is calculated based on the recovery of the compound verses its loss from the perfusate.[16]

1.1.1 Description of different microdialysis probes

The construction of a microdialysis probe is pretty basic. The probe consists of a semipermeable dialysis membrane connected to solid construction tubing for perfusion and sample collection. There are a few basic types of MD probes: concentric cannula,

side-by-side, flexible, linear, and shunt probes.[4,7,13] Each geometric type is designed and used for specific application types and has distinct advantages and disadvantages.

Concentric cannula and side-by-side probes are often used in conjunction with a guide cannula, which increases the rigidity of the probe as well as allows for a longer recovery time between surgical procedure to the actual experiment (Figure 1.2-A). The guide cannula is normally inserted into the surgical site prior to the actual experiment and remains until the experimental procedure begins. These probes are most commonly used in the brain for monitoring neurochemical processes. More recently, a Metaquant™ concentric probe has been developed which has a secondary inlet that is used as a dilution flow (Figure 1.2-B).[17] This secondary makeup flow makes it possible to use a very low flow rate for sampling to increase recovery while providing enough sample volume for analysis by standard analytical methods such as CE.[18]

The flexible probe, which is very similar in geometry to the concentric probe, was originally described by Telting-Diaz *et al*. (1992) for continuous monitoring of the concentration of analyte in the blood.[19] As its name suggests, instead of being rigid in construction, this probe is flexible and can move with the tissue (Figure 1.2-C). This flexible construction helps minimize damage to the probe site caused by movement, allowing the probe to be placed within a blood vessel, where analyte recoveries are reported to be higher, without severely damaging or destroying the blood vessel.

The linear probe allows for bilateral sampling and has been used in many modes of research. These probes are also commonly referred to as loop probes (Figure 1.2-D). The difference between the two designs is that the loop probe has a metal wire support inside the probe for structural support (Figure 1.2-E). The loop microdialysis probe was

used extensively in the research presented within this dissertation. These probes lend themselves well to subcutaneous sampling and investigations of transdermal delivery due to a variety of membrane sizes and lengths being commercially available and their ease of implantation. However, the probe's horizontal geometry can restrict the placement of the probe and limits its use for monitoring some biological tissues.

Shunt probes have proven to be very useful for sampling moving fluids such as bile. It has been used to monitor endogenous compounds and drug metabolites in bile and follow rapid changes in the concentration of target analytes (Figure 1.2-F). A shunt, very similar to that used to expand and open arteries, carries the bile flow through the shunt, which has a linear microdialysis probe suspended inside of it.[20] These probes can be used to continuously monitor analytes within the bile duct without causing loss of bile or interfering with liver function.[21]

Microdialysis membranes come in a variety of physical configurations along with geometric configurations. Membranes can be customized to specific lengths in an effort to tailor the membrane for optimal recovery and experimental purposes; they also come in a variety of materials. Membranes are available with different molecular weight cut-offs ranging from 20,000 to 60,000 Daltons.[22] Microdialysis probes are available at specific molecular weight cutoff so as to maximize recovery of the target analytes and exclude larger molecules from reaching the analytical system. Probes can also be made with membranes of varying chemical composition that can be chosen and tailored to the experimental design and sampling environment. Early studies describing the effects of membrane composition have shown that the composition of the membrane greatly affects the rate of recovery for specific analytes of interest *in vivo* and *in vitro*.[5]

1.2 Capillary electrophoresis (CE)

Modern capillary electrophoresis (CE) has become a widely used analytical technique for the separation of charged compounds since it was first introduced by Jorgenson and Lukacs in the 1980s.[23] The separation of charged compounds in fused silica capillaries is based on their mobility through a conductive fluid under the influence of an electric field (Figure 1.3). CE has been used for a wide variety of analytical applications ranging from drug discovery to genetic analysis. Its versatility is exemplified by its many diverse modes:[24]

- capillary zone electrophoresis (CZE),
- capillary gel electrophoresis (CGE),
- capillary isoelectric focusing (CIEF),
- isotachophoresis (ITP),
- micellar electrokinetic capillary chromatography (MEKC), and
- non-aqueous capillary electrophoresis (NACE).

It has been said “There are only three problems with capillary electrophoresis: injection, separation, and detection!”[24] A standard CE instrument, when broken down to the basic components, is comprised of a fused-silica capillary with both ends of the capillary immersed in a vial containing buffer solution, a high voltage power supply that applies a voltage across the capillary, and a detector at one end of the capillary (Figure 1.4). At the end of the capillary is the detector, which can be attached either on-line or

off-line. Conventional CE has been coupled to a wide variety of detection schemes with UV, LIF, MS, C^4D, and EC all being cited in literature.[24] The solution used within the capillary consists of a background electrolyte (BGE) that must be ionic. The BGE serves as the matrix in which the separation occurs. Therefore, one must carefully consider the conductivity of the BGE when choosing one for a separation. The BGE conducts an electrical current, which results in the generation of heat due to friction. A high conductivity BGE will increase the current generated, which is directly proportional to the amount of heat generated. This process is called joule heating. The production of heat inside the capillary will eventually cause the buffer solution to boil and degas.[24]

Sample introduction into the capillary can be accomplished by either a pressure injection where a discrete sample plug is pushed into the capillary, or via electrokinetic injection where the sample is injected into the capillary by applying a voltage across the capillary. In electrokinetic injections, analytes are introduced into the capillary based on their electrophoretic mobility and the electroosmotic flow. If there is no electroosmotic flow, then only positively charged compounds will be injected in a normal polarity system, and only negatively charged compounds are injected in a reverse polarity system. If there is electroosmotic flow an unequal concentration of positive, neutral, and negative compounds will be injected into the capillary based on their electrophoretic mobility and their size to charge ratio.

Once the sample plug is inside the capillary, a voltage is applied across the capillary in order to induce the electrophoretic separation. The CE separation is accomplished based on the difference in the combined effects of the electrophoretic mobility of the charged compounds. Electrophoretic mobility is defined as the rate of

migration of charged particles under the influence of an electric field.[25] This movement is based on the molecules size-to-charge ratio with the hydrated radius of the molecule dictating the size component. Thus, negatively charged compounds are attracted to the positive pole (anode) of the induced electric field, while the positively charged compounds move towards the negative pole (cathode), and the neutral compounds are left unaffected by the applied electric field. The velocity of an ion through the buffer solution can be calculated by its electrophoretic mobility (μ), represented by this equation:[25]

$$\mu = \frac{\nu}{E} = \frac{\mathrm{q}}{6\pi\eta\mathrm{r}} \tag{3}$$

where q represents the net charge of the compound in solution, η is the viscosity of the solution, r is the hydrated radius of the compound, and ν is the velocity of the molecule. The friction coefficient, as defined by Stokes' Law, can be expressed as (f) where $f = 6\pi\eta r\nu$ and is dependent on the size and shape of the ion.[26]

Considering that neutral compounds and both positive and negatively charged compounds all need to migrate in the same direction for detection, another force must act upon the matrix and must be defined. This force that promotes the mobility of all the compounds in a single direction is the electroosmotic flow (EOF). The EOF is what causes anionic and neutral species to migrate towards the cathode in normal polarity. Thus, both forces work together to make it possible to separate all the compounds within the sample while maintaining a net migration along a single direction within the capillary.

The bulk flow characteristic of the EOF is induced and maintained by the charge on the sidewalls of the fused silica capillary.

The free silanol groups that make up the interior surface of the fused silica capillary hold a negative charge at a pH greater than three and promote the formation of an electrical double layer. This electrical double layer consists of the net negative charges on the capillary surface combined with free cations distributed in the BGE and is described by the zeta potential. Simply stated, the ions/hydrated ions (Na^+, K^+…) in the BGE are attracted to the negatively charged walls of the silica capillary, and this layering of charged surfaces leads to the formation of an electrical double layer.

The electrical double layer consists of an Inner Helmholtz layer, and an Outer Helmholtz layer. The effective mobility of the EOF is dependent on this outer layer and can be changed by altering the buffer ionic strength, or its pH, which controls the degree of ionization.[27] Higher ionic strength buffers shrink the electrical double layer, thus leading to a lower zeta potential and therefore a lower magnitude of flow and longer migration times.

The magnitude of the EOF is defined by the zeta potential which is the potential established by the surface charge of the capillary wall and the ionized buffer solution.[28] Increasing the zeta potential will increase the EOF ensuring that all analytes migrate towards the cathode as well as increasing the speed of the separation. However, it can cause problems with the resolution of the analytes. While a lower EOF may improve the overall resolution of the separation, it can lead to band broadening of slow migrating analytes, thus increasing the peak width and decreasing the separation efficiency.[26]

EOF can be expressed as

$$\mu_{EOF} = \varepsilon\zeta/4\pi\eta \quad (4)$$

where ε is the dielectric constant, ζ is the zeta potential, and η is the viscosity of the buffer. The equation

$$\mu_a = \mu_e + \mu_{EOF} \quad (5)$$

describes the calculation for the apparent electrophoretic mobility $\mu_a$of the analyte where μ_{EOF} is the electroomostic flow, and μ_e is the electrophoretic mobility of the analyte.[27]

CE has many advantages over more traditionally used separation methods such as high performance liquid chromatography (HPLC). Instead of having to use columns and solvent gradients to perform a separation that requires large volumes of solvents (liters) and sample (μL), CE is performed in a fused silica capillary with micron scale inner diameters (20-150 um) and relatively short lengths (50-200 cm) and requires milliliters of solvent.[25] The narrow bore capillaries require little BGE volume; thus, the total volume of reagents is considerably less than that used by HPLC, and with that there is also a corresponding reduction in sample volume (nL-pL) needed for sample analysis.

This reduction makes CE an ideal separation method for coupling to microdialysis for sample analysis. With CE, only nanoliter sample volumes are injected into the capillary for analysis. This makes it possible to use very low perfusion flow rates at the

microdialysis probe, which, as discussed earlier, increases the relative recovery at the probe. In addition, the relatively high surface to volume ratio of the capillaries limits the effects of Joule heating resulting from the high voltage applied across the capillary.[30]

By coupling microdialysis to capillary electrophoresis, one can obtain the perfect marriage of fast analysis time and the ability to manipulate small sample volumes for highly efficient separations, as illustrated in Figure 1.5.[8,29] With direct coupling of MD sampling with CE, microdialysis samples can be continuously manipulated and injected into the capillary electrophoresis system without inducing error due to sample handling. The on-line coupling of microdialysis to capillary electrophoresis has been previously reported by the Lunte groups and by the Kennedy group for the detection of amino acid neurotransmitters in the brain and the metabolism of nicotine.[31-35]

1.3 Microchip electrophoresis (MCE)

In 1990 Manz *et al*. first described the concept behind the development of a miniaturized total chemical analysis system.[36] This was partially in response to the trends and need for smaller inner diameter capillaries for separations with shorter analysis times in the fields of chromatography and electrophoresis. Since then these systems have proven to be effective in offering fast and highly efficient separations in a miniaturized device.[37] Early applications of microchip electrophoresis devices used glass substrates; this is the substrate primarily used in this thesis. Much like conventional capillary electrophoresis, which uses fused-silica capillaries, micro-fabricated devices have micron scale channels etched into the substrate.

The fundamental ideas and principles driving electrophoresis remain the same in

both capillary and microfluidic formats. The term microfluidics best describes the handling and control of the fluids and its control in a micro-scale environment. This is the same principle of scale which Harrison *et al*. described in 1992 in the first paper on a microchip-based capillary electrophoresis (MCE) system.[38] Electrophoresis can be performed more efficiently in a micro-scale device than with conventional capillaries because it can be accomplished faster over a shorter capillary distance. First, the sample plug can be of a significantly smaller volume than a conventional capillary electrophoresis due to increased control allowed by the device. In addition, heat dispersion is achieved in microfluidic devices more easily than in capillary devices [39] due to larger surface area to volume ratios and a larger mass of material such as glass and other polymers acting as a heat sink for the device. This allows higher field strengths to be applied across the shorter separation channel.[40] MCE also requires less sample and reagent consumption due to the relatively small size of the system as well.[37]

Chip material is a large consideration taken into account; this is because chip rigidity and ability to function under operating conditions is largely influenced by the chip material chosen for construction of the device. Glass materials such as quartz, borosilicate, and soda lime have been commonly used due to their similarity to fused silica capillaries.[41,42] Less expensive alternate materials with easier fabrication methods, such as polydimethylsiloxane (PDMS), poly(methylmethacrylate) (PMMA), and polyethylene terephthalate (PET) have also been explored.[43,44]

1.4 Microdialysis coupled to microchip electrophoresis (MD-MCE)

Over the past decade microchip electrophoresis has developed into an attractive platform for analysis of microdialysis samples.[42] Integrating microdialysis to microfluidics allows for relatively easy fluid manipulation using either electrokinetic manipulation or hydrodynamic forces.[13] No sample handling is required because all these steps can be integrated into the device. This ability to integrate these steps into the microfluidic device allows for greater accuracy and precision because no sample is lost due to manual manipulation of the sample. Microfluidics allows for even faster separation and sample analysis times than conventional CE, which helps to increases temporal resolution leading to an analytical system that can truly perform near-real time sample analysis on a complex sample matrix. Microfluidics also allows for the manipulation of extremely small sample volumes (ranging from nL to pL), which are amenable to the smaller volumes produced by microdialysis. This makes microchip electrophoresis an ideal analytical separation method for the direct analysis of microdialysis samples. Coupling these two methods, very fast analysis times in near-real time are not only possible but have the added benefit of more efficient separations at higher field strengths. It is also possible to integrate sample preparation and derivatization steps into the microfluidic device.

The cost of development and fabrication for these systems are relatively low since these devices can easily and quickly be mass-produced in a multitude of relatively inexpensive materials. Due to the relative ease of mass production and the use of photolithographic techniques, microfluidic devices can rapidly be prototyped and custom designed for specific applications and needs. Thus a single device can be designed easily

and relatively inexpensively for specific applications. These specially designed microfluidic devices can be optimized for many different types of detection methods.

The coupling of MD flow to the microfluidic device is the most important requirement for any MD-MCE device in that the on-line coupling of the microdialysis probe to the microfluidic device must be able to accommodate the continuous flow from the microdialysate without disturbing the electrophoretic separation. Another requirement of functionally coupling microdialysis to a microfluidic device is that the device must be able to deliver a discrete plug of the microdialysate into the separation channel at picoliter sized volumes. Many methods have been used in order to couple microdialysis to microchip based electrophoretic separations. Both pneumatic injection valves and flow-gated interfaces have been used.[45-47] The injection procedure for the devices employed in this thesis are modeled after a flow-through injection scheme pioneered by Chen's group and illustrated in Figure 1.6.[48] This design used a large flow-through channel for the microdialysate that was split with part of the sample hydrodynamically pumped toward the separation channel. A gated injection scheme is used to inject the sample into a separation channel of the microfluidic device, as shown in Figure 1.6 and is described below.

In the devices described and fabricated throughout this dissertation, a syringe pump was used to deliver the dialysate through the enlarged flow channel at the top of the device. This flow generates a hydrodynamic pressure inside the microfluidic channels. A gate is then established by applying a voltage to one of the fluid wells on the device and placing ground leads in the two other fluid wells. An electric field is thereby established between the high voltage lead and the respective ground leads. This electric

field prevents the sample from prematurely entering into the separation channel and going to the detector. In order to introduce a discreet sample plug into the separation channel, a high voltage is floated introducing the dialysate into the separation channel. The gate is reestablished after a specified amount of time, usually 0.3 to 1 second, by reapplying the high voltage. The injection time defines the sample plug size that is introduced into the separation channel. The S. M. Lunte group has previously reported on this method in depth.[42,49,50] The further integration of other on-chip functions, (e.g., embedded electrodes and micro-mixers) has lead to the development of the miniaturized near real time separation-based sensors described in this dissertation. A wide variety of papers have been published integrating microdialysis to MCE using laser-induced fluorescence.[45,46,49,51-53] Recently a paper published by the S. M. Lunte group described a device using microdialysis sampling with on-chip sample derivatization using LIF detection for the detection of amino acid neurotransmitters.[54]

1.5 Microchip electrophoresis coupled to electrochemical detection (MCE-EC)

Many reports have been published using microfluidic devices with electrochemical detection.[55-59] The first reports of microfluidic electrophoresis devices with integrated platinum electrodes as amperometric detectors were by the Mathies group.[60] Baldwin later expanded on this design to incorporate high voltage leads and ground leads printed onto the substrate used to drive the separation and fluid dynamics (Figure 1.6-D).[61]

Several reports have described devices using a carbon fiber working electrode placed in a polydimethylsiloxane (PDMS) reversibly bonded device.[59,62] Other

similarly styled devices utilize an electrode deposited on a glass slide, either using a screen printed carbon paste electrode or pyrolyzed photoresist. In these cases, a PDMS layer containing the microfluidic channels is aligned over the electrode to create a PDMS glass hybrid device.[63,64] These are the most widely used and reported methods for achieving electrochemical detection on a microfluidic device (Figure 1.7-A).[37,58,65,66]

In 1999, Wang *et al*. described a device with a screen printed working electrode where the sample flowed via EOF to the end of the separation channel and onto a thick film amperometric detector off-chip (Figure 1.7-B).[67] The screen-printed carbon electrode was mounted perpendicularly at the end of the separation channel of the microfluidic device off-channel. The plate with the printed electrode was held approximately 50 μm away from the end of the capillary channel. This allowed for the replacement of the electrode and alleviated the need to fabricate a new device every time an electrode failed, which helped create a system of exchangeable detectors and microfluidic devices.

More recently, the Martin group has developed a method of fabricating electrodes for MCE in a commercially available epoxy. Multiple types of electrode materials can be embedded within the epoxy, which is heated and sealed around the electrode material. To perform electrophoresis, simple PDMS devices containing channels can be reversibly sealed over the epoxy substrate with the electrode. The resulting electrodes and epoxy can be polished and the electrode regenerated multiple times.[68]

Recent publications have reported the use of simple replaceable working electrodes for in-channel amperometric detection placed inside the end of the separation

channel of the microfluidic device (Figure 1.7-E).[67,69,70] These devices use a fixed electrode holder at the outlet of the separation channel modeled after devices similar to those previously described by Wang *et al*. (Figure 1.7-D).[67] The devices using this detection model rely on 3-D micromanipulators to hold a carbon fiber electrode directly inside the end of the separation channel. While this can decrease overall analysis cost with the introduction of a replaceable electrode, it usually requires a supplementary detection cell along with the use of a three-dimensional micromanipulator, thereby increasing the complexity of the analytical system.

Many different types of electrode materials have been used with microchip electrophoresis. Carbon-based electrode materials such as carbon fiber, carbon paste, carbon ink, or pyrolyzed photoresist electrodes can be used.[63,64,71] Metal electrodes made from gold, platinum, and palladium, have also been reported in the literature.[68,72,73]

Multiple electrode configurations are also available. Each of these configurations are designed to isolate the electrochemical detector from the separation voltage. The end-channel alignment is the most prevalent method in which the electrode is placed 5–20 μm from the end of the separation channel. This allows for the voltage to dissipate before reaching the working electrode. However, this approach can result in lower separation efficiencies due to band broadening.[59] To increase the separation efficiency and decrease the effects of band broadening a decoupler can be used. A decoupler is a metal band placed directly in the separation channel. The decoupler grounds the separation voltage before reaching the working electrode. This allows the working electrode to also be placed inside the separation channel.[72] The configuration used throughout the

course of this dissertation is in-channel alignment. In this configuration an electrically isolated potentiostat is used with the working electrode placed 5–20 μm inside the separation channel. An electrically isolated potentiostat prevents the voltage required for the electrophoretic separation from interfering with potentiostat's function of maintaining the required potential at the working electrode. The potentiostat produces a potential from a battery and is not connected to ground, with no path to ground the potentiostat is electrically isolated and is not exposed to the electric field produced by the separation voltage. However, the working electrodes potential is influenced by the separation field and must be compensated for with the applied potential to the electrode.[74]

1.6 Microdialysis sampling with microchip capillary electrophoresis with electrochemical detection (MD-MCE-EC)

Systems using microdialysis-microchip electrophoresis with electrochemical detection have been rarely reported in the literature due to their complexity and difficulty of fabrication.[42] The work presented in this thesis primarily focuses on the development of a microdialysis microchip electrophoresis device using electrochemical detection for on-animal sensing. Many issues arise when designing an MD-MCE-EC device. The first consideration is how to couple microdialysis sampling directly to the microfluidic device. Then, sample introduction into the separation channel must be considered. Multiple approaches have been used for sample introduction including pinched injections, gated injections, segmented flow, and pneumatic valves. The S. Martin group has made some of the most significant contributions to the development of MD-MCE-EC devices.[47,51,62] They have reported MD-MCE-EC devices using

polydimethylsiloxane (PDMS) with carbon ink electrodes screen-printed on to a glass substrate.[51] This device used multiple integrated pneumatically actuated valves for sample introduction, and was employed for monitoring catecholamine release from PC 12 cells in culture.

1.7 Importance of nitric oxide and excitatory amino acids

Nitroglycerin was first synthesized by Ascanio Sobrero in 1946, and the procedure for nitrating glycerol was later adopted by his student, Alfred Nobel, for the manufacturing of dynamite.[75] It was in Nobel's dynamite factories that the antianginal effects of nitroglycerin were first noticed. Workers would often complain of persistent headaches during working hours and, most notably, the workers who suffered from chest pains (angina pectoris) and other ischemic heart conditions would experience some relief from their symptoms during their time around the substance.[76]

Physicians were quick to notice these effects and attributed them to vasodilation produced upon exposure to nitroglycerin. However, the exact mechanism by which vasodilation occurs due to nitroglycerin administration is still largely unknown. Nitroglycerin itself does not have any effect on vasodilation.[77] It is believed that vasodilation is caused by nitric oxide (NO), which is generated from nitroglycerin in the vascular smooth muscle. The proposed mechanism for the production of NO from nitroglycerin activation is via an intracellular enzymatic process where glutathione-S-transferase converts nitroglycerin into a functional vasodilator.[78] In 1998 the Nobel Prize in Physiology or Medicine was jointly awarded to Robert F. Furchgott, Louis J. Ignarro and Ferid Murad "for their discoveries concerning nitric oxide as a signaling

molecule in the cardiovascular system".[79]

Since then, nitric oxide has been recognized as an important signaling molecule involved in many physiological functions. It plays a key role in vascular protection. Nitric oxide has been well cited for its effects as a vasodilator as well as its anti-inflammatory, antithrombotic, and antiproliferative effects.[80-82] Nitric oxide has also been shown to contribute to reperfusion injury during an ischemic event.[83] During ischemia, nitric oxide can react with superoxide to produce the damaging oxidant peroxynitrite. In other disease states it has been shown that NO production is decreased in endothelial dysfunction. This reduced production of NO is caused by a decrease in L-arginine availability.[74]

Nitric oxide is also a multifunctional secondary messenger implicated in numerous physiological functions ranging from immune response, potentiation of synaptic transmission, dilation of blood vessels, and muscle relaxation. NO is relatively unstable and readily oxidizes to nitrite in the presence of oxygen, thus nitrite has become a key marker for measuring NO *in-vivo*.[81] For the studies described in this dissertation NO is produced by the metabolism of nitroglycerin, and monitored via the concentration of nitrite.

Excitatory amino acids such as glutamate and aspartate as well as inhibitory amino acids such as GABA occur at relatively high concentrations in the brain.[84] The concentrations of these amino acids are tightly controlled in the extracellular space. It has been previously shown that excess amounts of glutamate in the extracellular space caused by long term stimulation of post synaptic glutamate receptors, leads to excitotoxicity and potential neuronal damage.[85] Under ischemic conditions, it has

been found that high concentrations of glutamate are released into the extracellular space as a result of energy disruption caused by reduced oxygen levels. This form of excitotoxicity can eventually cause damage to mitochondria due to an influx of Ca^{+2} ions, which activate multiple enzymes within the cells including those responsible for activating apoptosis.[86]

1.8 Goal of dissertation/ chapter outline

The goal proposed and outlined in this dissertation is to develop a miniaturized separation-based sensor using microdialysis coupled to a microchip electrophoresis with amperometric detection for on-animal sensing. The system should be self-contained and consist of an on-line interface to couple microdialysis to microchip electrophoresis, high voltage power supplies, and an electrically isolated potentiostat. The instrument should also be controlled and data collected remotely using Bluetooth® or telemetry and a laptop PC. The system was optimized for the detection of nitrite produced during the subdermal delivery of nitroglycerin. This device is designed for the continuous monitoring of drug metabolism and neurotransmitters on a *freely roaming* animal. The complete system was fitted into a small backpack type system that could be remotely controlled and monitored for near real-time analysis. The microchip used for the on-animal separation-based sensor was fabricated using glass with platinum electrodes embedded into the substrate for electrochemical detection.

A brief summary of the chapters in this dissertation and their content follows.

Chapter 1: Introduction to the principles of microdialysis sampling and microchip electrophoresis

This chapter describes the background information on microdialysis sampling and electrophoresis in both the microfluidic and capillary format. The history of microdialysis and the rationale behind the coupling of microdialysis to electrophoretic separation-based analytical systems is discussed.

Chapter 2: Development and optimization of an all glass microdialysis microchip electrophoresis device with integrated amperometric detection

In this chapter, the development of an all-glass separation-based sensor using microdialysis coupled to microchip electrophoresis with amperometric detection is described. Details of the microdialysis sampling system coupled to a flow-gated interface for sample delivery fabricated into the microchip electrophoresis system are discussed. Fabrication of the MD-MCE-EC device along with the development of the in-channel configuration of an embedded Pt electrode is described in detail. The electronic system using a wireless isolated potentiostat for in-channel electrochemical detection in an all-glass microfluidic device is also described. Both normal and reversed polarity separations were performed with this device. The system was evaluated *in vitro* for the continuous monitoring of the production of hydrogen peroxide from the reaction of glucose oxidase with glucose.

Chapter 3: Development and optimization of an all-glass microdialysis microchip electrophoresis device for on-animal detection

This chapter describes the first report of a miniaturized MD-MCE-EC system for on-animal sensing via telemetry control. A linear microdialysis probe placed subcutaneously was used to monitor nitrite production via the administration of nitroglycerin. This system was tested on both sheep and rats. The system used in this study was controlled completely via telemetry for continuous analysis of samples collected from the microdialysis probe. Control studies were performed by collecting microdialysis samples off-line and analyzing them by conventional LC-EC system.

Chapter 4: Development and optimization of an all-glass microdialysis microchip electrophoresis device for dual detection using fluorescence and amperometric detection (MD-MCE-EC-LIF) with on-chip derivatization

The optimization of naphthalene 2.3-dicarboxaldehyde derivatized amino acids separation using and laser-induced fluorescence detection along with electrochemical detection is described. The separation was optimized on an all-glass microfluidic device and derivatization of the amino acids was accomplished on chip in a "micro-mixer." The initial optimization of the amino acid separation was conducted using off-chip sample derivatization. The optimized separation conditions were then evaluated in conjunction with the on-chip micro-mixer for the sample derivatization. The microfluidic device was able to separate and detect a mixture of seven amino acids via LIF. In a separate study,

the combined MCE-LIF-EC chip was used to simultaneously detect NDA-derivatized amino acids and hydrogen peroxide.

Chapter 5: Conclusions and future directions

An overview of the dissertation project and the overall conclusions are presented. Suggestions for future work toward a fully integrated and automated, portable, miniaturized, separation-based analytical system are made. The suggested work includes the addition of multiple simultaneous detection methods, along with transitioning the device from an on-animal based sensor to a bed-side point-of-care analytical system for humans. In addition, further development of high sensitivity electrodes and their fabrication is discussed.

1.6 References

[1] Bito, L., Davson, H., Levin, E., Murray, M. & Snider, N. The concentrations of free amino acids and other electrolytes in cerebrospinal fluid, in vivo dialysate of brain, and blood plasma of the dog. *Journal of Neurochemistry* **13,** 1057–1067 (1966).

[2] Delgado, J. M., DeFeudis, F. V., Roth, R. H., Ryugo, D. K. & Mitruka, B. M. Dialytrode for long term intracerebral perfusion in awake monkeys. *Arch Int Pharmacodyn Ther* **198,** 9–21 (1972).

[3] Ungerstedt, U. & Pycock, C. Functional correlates of dopamine neurotransmission. *Bull Schweiz Akad Med Wiss* **30,** 44–55 (1974).

[4] Mason, P. A. & Bhaskaran, D. In vivo microdialysis. *Kopf Carrier* **20**, 2-4 (1988).

[5] Shippenberg, T. S. & Thompson, A. C. Overview of Microdialysis. *Current Protocols in Neuroscience* **7**, 1-7 (John Wiley & Sons, Inc., 2001).

[6] CMA Microdialysis AB. *microdialysis.com* at <http://www.microdialysis.com/us/about-cma/about-cma>

[7] Cooley, J. C., Ducey, M.W., Regel, A.R., Nandi, P. Lunte, S.M., Lunte, C.E. in *Microdialysis in Drug Development* **4,** 35–66 (Springer New York, 2012).

[8] Nandi, P. & Lunte, S. M. Recent trends in microdialysis sampling integrated with conventional and microanalytical systems for monitoring biological events: a review. *Anal. Chim. Acta* **651,** 1–14 (2009).

[9] Van der Zeyden, M., Oldenziel, W. H., Rea, K., Cremers, T. I. & Westerink, B. H. Microdialysis of GABA and glutamate: analysis, interpretation and comparison with microsensors. *Pharmacol. Biochem. Behav.* **90,** 135–147 (2008).

[10] Watson, C. J., Venton, B. J. & Kennedy, R. T. In vivo measurements of neurotransmitters by microdialysis sampling. *Anal. Chem.* **78,** 1391–1399 (2006).

[11] Ben Hc Westerink & Cremers, T. I. F. H. *Handbook of Microdialysis, Volume 16: Methods, Applications and Perspectives (Handbook of Behavioral Neuroscience)*. 1–712 (Academic Press, 2007).

[12] Zhou, S. Y., Zuo, H., Stobaugh, J. F., Lunte, C. E. & Lunte, S. M. Continuous in vivo monitoring of amino acid neurotransmitters by microdialysis sampling with on-line derivatization and capillary electrophoresis separation. *Anal. Chem.* **67,** 594–599 (1995).

[13] Nandi, P., Kuhnline, C. D. & Lunte, S. M. Analytical considerations for microdialysis sampling. *Applications of Microdialysis in Pharmaceutical Science,* 39-92 (2011).

[14] Torto, N. A Review of Microdialysis Sampling Systems. *J. Chromatography* **70,** 1305–1309 (2009).

[15] Cremers, T., De Vries, M.G., Huinink, D. K., Van Loon, J.P., Hart, M., Ebert, B., Westerink, B.H.C., De Lange, E. C. M. Quantitative Microdialysis using modified ultraslow microdialysis: Direct rapid and reliable determination of free brain concentrations with the MetaQuant technique, *Journal od Neuroscience Methods* **178 (2),** 249-254 (2009).

[16] Song, Y. & Lunte, C. E. Comparison of calibration by delivery versus no net flux for quantitative in vivo microdialysis sampling. *Anal. Chim. Acta,* 251-262 (1999).

[17] Sood, P., Cole, S., Fraier, D. & Young, A. M. J. Evaluation of metaquant microdialysis for measurement of absolute concentrations of amphetamine and

dopamine in brain: A viable method for assessing pharmacokinetic profile of drugs in the brain. *Journal of Neuroscience Methods* **185,** 39–44 (2009).

[18] Cremers, T. I. F. H. *et al.* Quantitative microdialysis using modified ultraslow microdialysis: Direct rapid and reliable determination of free brain concentrations with the MetaQuant technique. *Journal of Neuroscience Methods* **178,** 249–254 (2009).

[19] Telting-Diaz, M., Scott, D. O. & Lunte, C. E. Intravenous microdialysis sampling in awake, freely-moving rats. *Anal. Chem.* **64,** 806–810 (1992).

[20] Huff, J., Heppert, K. & Davies, M. The Microdialysis Shunt Probe: Profile of Analytes in Rats with Erratic Bile Flow or Rapid Changes in Analyte Concentration in Bile. *Current Separations* 18:3, 85-90 (1999).

[21] Heppert, K. E. & Davies, M. I. Using a microdialysis shunt probe to monitor phenolphthalein glucuronide in rats with intact and diverted bile flow. *Anal. Chim. Acta* **379,** 359–366 (1999).

[22] Plock, N. & Kloft, C. Microdialysis—theoretical background and recent implementation in applied life-sciences. *European Journal of Pharmaceutical Sciences* **25,** 1–24 (2005).

[23] Jorgenson, J. W. & Lukacs, K. D. Zone electrophoresis in open-tubular glass capillaries. *Anal. Chem.* **53,** 1298–1302 (1981).

[24] Weinberger, R. Practical Capillary Electrophoresis (2nd Ed.) Weinberger Robert: Librairie Lavoisier. , 25-208 (1993).

[25] Xu, Y. Tutorial: Capillary Electrophoresis. *Chem. Educator* **1,** 1–14 (1996).

[26] Landers, J. P. Introduction to capillary electrophoresis. *Handbook of Capillary*

Electrophoresis, Second Edition., 4-48 (1997).

[27] Giddings, J. C. Unified separation science. Wiley, New York, 10-78 (1991).

[28] Kirby, B. J. & Hasselbrink, E. F. Zeta potential of microfluidic substrates: 1. Theory, experimental techniques, and effects on separations. *Electrophoresis* **25,** 187–202 (2004).

[29] Guihen, E. & O'Connor, W. T. Capillary and microchip electrophoresis in microdialysis: Recent applications. *Electrophoresis* **31,** 55–64 (2010).

[30] Evenhuis, C. J. & Haddad, P. R. Joule heating effects and the experimental determination of temperature during CE. *Electrophoresis* **30,** 897–909 (2009).

[31] Kennedy, R. T., Thompson, J. E. & Vickroy, T. W. In vivo monitoring of amino acids by direct sampling of brain extracellular fluid at ultralow flow rates and capillary electrophoresis. *Journal of Neuroscience Methods* **114,** 39–49 (2002).

[32] Lada, M. W. & Kennedy, R. T. Quantitative in Vivo Monitoring of Primary Amines in Rat Caudate Nucleus Using Microdialysis Coupled by a Flow-Gated Interface to Capillary Electrophoresis with Laser-Induced Fluorescence Detection. *Anal. Chem.* **68,** 2790–2797 (1996).

[33] Lada, M. W., Vickroy, T. W. & Kennedy, R. T. High Temporal Resolution Monitoring of Glutamate and Aspartate in Vivo Using Microdialysis On-Line with Capillary Electrophoresis with Laser-Induced Fluorescence Detection. *Anal. Chem.* **69,** 4560–4565 (1997).

[34] Hogan, B. L., Lunte, S. M., Stobaugh, J. F. & Lunte, C. E. Online coupling of in vivo microdialysis sampling with capillary electrophoresis. *Anal. Chem.* **66,** 596–602 (1994).

[35] Zhou, J., Heckert, D. M., Zuo, H., Lunte, C. E. & Lunte, S. M. On-line coupling of in vivo microdialysis with capillary electrophoresis/electrochemistry. *Anal. Chim. Acta* **379,** 307–317 (1999).

[36] Manz, A., Graber, N. & Widmer, H. M. Miniaturized total chemical analysis systems: A novel concept for chemical sensing. *Sensors and Actuators B: Chemical* **1,** 244–248 (1990).

[37] Lacher, N.A., Garrison, K. E., Martin, R. S. & Lunte, S. M. Microchip capillary electrophoresis/ electrochemistry, Wiley Online Library. *Electrophoresis,* 2526-36 (2001).

[38] Harrison, D. J., Manz, A., Fan, Z., Luedi, H. & Widmer, H. M. Capillary electrophoresis and sample injection systems integrated on a planar glass chip. *Anal. Chem.* **64,** 1926–1932 (1992).

[39] Rashid, M., Dou, Y. H., Auger, V. & Ali, Z. Recent developments in polymer microfluidic devices with capillary electrophoresis and electrochemical detection. *Micro Nanosyst.* **2**, 1-29 (2010).

[40] Wu, D., Qin, J. & Lin, B. Electrophoretic separations on microfluidic chips. *Journal of Chromatography A* **1184,** 542–559 (2008).

[41] Crain, M. M., Keynton R.S., Walsh, K.M. Roussel, T.J., Baldwin, R.P., Naber, J.F., Jackson, D.J. Fabrication of a glass capillary electrophoresis microchip with integrated electrodes. *Methods Mol. Biol.* **339,** 13–26 (2006).

[42] Scott, D. E., Grigsby, R. J. & Lunte, S. M. Microdialysis sampling coupled to microchip electrophoresis with integrated amperometric detection on an all-glass substrate. *ChemPysChem* **14,** 2288–2294 (2013).

[43] Coltro, W. K. T., Lunte, S. M. & Carrilho, E. Comparison of the analytical performance of electrophoresis microchannels fabricated in PDMS, glass, and polyester-toner. *Electrophoresis* **29,** 4928–4937 (2008).

[44] Viellard, J., Mazurezy, K.R., Morin, C., Hannes, B., Chevolot, Y., Desbene, P.L., Krawczyk, S. Application of microfluidic chip with integrated optics for electrophoretic separations of proteins☆. *Journal of Chromatography B* **845,** 218–225 (2007).

[45] Li, M. W., Huynh, B. H., Hulvey, M. K., Lunte, S. M. & Martin, R. S. Design and Characterization of Poly(dimethylsiloxane)-Based Valves for Interfacing Continuous-Flow Sampling to Microchip Electrophoresis - Analytical Chemistry (ACS Publications). *Anal. Chem.* **78,** 1042–1051 (2006).

[46] Huynh, B. H., Fogarty, B. A., Martin, R. S. & Lunte, S. M. On-Line Coupling of Microdialysis Sampling with Microchip-Based Capillary Electrophoresis. *Anal. Chem.* **76,** 6440–6447 (2004).

[47] Mecker, L. C. & Martin, R. S. Coupling Microdialysis Sampling to Microchip Electrophoresis in a Reversibly Sealed Device. *Journal of the Association for Laboratory Automation* **12,** 296–302 (2007).

[48] Lin, C.-C., Chen, C.-C., Lin, C.-E. & Chen, S.-H. Microchip electrophoresis with hydrodynamic injection and waste-removing function for quantitative analysis. *Journal of Chromatography A* **1051,** 69–74 (2004).

[49] Huynh, B. H., Fogarty, B. A., Nandi, P. & Lunte, S. M. A microchip electrophoresis device with on-line microdialysis sampling and on-chip sample derivatization by naphthalene 2, 3-dicarboxaldehyde/2-mercaptoethanol. *Journal*

of pharmaceutical and Biomedical Analysis **42,** 529–534 (2006).

[50] Nandi, P., Desai, D. P. & Lunte, S. M. Development of a PDMS-based microchip electrophoresis device for continuous online in vivo monitoring of microdialysis samples. *Electrophoresis* **31,** 1414–1422 (2010).

[51] Mecker, L. C. & Martin, R. S. Integration of microdialysis sampling and microchip electrophoresis with electrochemical detection. *Anal. Chem.* **80,** 9257–9264 (2008).

[52] Sandlin, Z. D., Shou, M., Shackman, J. G. & Kennedy, R. T. Microfluidic Electrophoresis Chip Coupled to Microdialysis for in Vivo Monitoring of Amino Acid Neurotransmitters. *Anal. Chem.* **77,** 7702–7708 (2005).

[53] Cellar, N. A., Burns, S. T., Meiners, J.-C., Chen, H. & Kennedy, R. T. Microfluidic Chip for Low-Flow Push-Pull Perfusion Sampling in Vivo with On-Line Analysis of Amino Acids. *Anal. Chem.* **77,** 7067–7073 (2005).

[54] Nandi, P., Scott, D. E., Desai, D. & Lunte, S. M. Development and optimization of an integrated PDMS based-microdialysis microchip electrophoresis device with on-chip derivatization for continuous monitoring of primary amines. *Electrophoresis* **6**, 895-902 (2013).

[55] Vandaveer, W. R., Pasas-Farmer, S. A., Fischer, D. J., Frankenfeld, C. N. & Lunte, S. M. Recent developments in electrochemical detection for microchip capillary electrophoresis. *Electrophoresis* **25,** 3528–3549 (2004).

[56] Mark, J. J. P., Scholz, R. & Matysik, F.-M. Electrochemical methods in conjunction with capillary and microchip electrophoresis. *Journal of Chromatography A* **1267,** 45–64 (2012).

[57] Wang, J. Electrochemical detection for microscale analytical systems: a review. *Talanta* **56,** 223–231 (2002).

[58] Xu, J.-J., Wang, A.-J. & Chen, H.-Y. Electrochemical detection modes for microchip capillary electrophoresis. *TrAC Trends in Analytical Chemistry* **26,** 125–132 (2007).

[59] Fischer, D. J., Hulvey, M. K., Regel, A. R. & Lunte, S. M. Amperometric detection in microchip electrophoresis devices: Effect of electrode material and alignment on analytical performance. *Electrophoresis* **30,** 3324–3333 (2009).

[60] Woolley, A. T., Lao, K., Glazer, A. N. & Mathies, R. A. Capillary electrophoresis chips with integrated electrochemical detection. *Anal. Chem.* **70,** 684–688 (1998).

[61] Baldwin, R. P. *et al.* Fully integrated on-chip electrochemical detection for capillary electrophoresis in a microfabricated device. *Anal. Chem.* **74,** 3690–3697 (2002).

[62] Martin, R. S., Ratzlaff, K. L., Huynh, B. H. & Lunte, S. M. In-channel electrochemical detection for microchip capillary electrophoresis using an electrically isolated potentiostat. *Anal. Chem.* **74,** 1136–1143 (2002).

[63] Fischer, D. J., Vandaveer, W. R., Grigsby, R. J. & Lunte, S. M. Pyrolyzed photoresist carbon electrodes for microchip electrophoresis with dual-electrode amperometric detection. *Electroanalysis* **17,** 1153–1159 (2005).

[64] Martin, R. S. *et al.* Carbon paste-based electrochemical detectors for microchip capillary electrophoresis/electrochemistry. *Analyst* **126,** 277–280 (2001).

[65] Du, Y. & Wang, E. Capillary electrophoresis and microchip capillary electrophoresis with electrochemical and electrochemiluminescence detection. *J.*

Sep. Sci. **30,** 875–890 (2007).

[66] Wang, J. Electrochemical Detection for Capillary Electrophoresis Microchips: A Review. *Electroanalysis* **17,** 1133–1140 (2005).

[67] Wang, J., Tian, B. & Sahlin, E. Micromachined electrophoresis chips with thick-film electrochemical detectors. *Anal. Chem.* **71,** 5436–5440 (1999).

[68] Selimovic, A., Johnson, A. S., Kiss, I. Z. & Martin, R. S. Use of epoxy-embedded electrodes to integrate electrochemical detection with microchip-based analysis systems. *Electrophoresis* **32,** 822–831 (2011).

[69] Zeng, Y., Chen, H., Pang, D.-W., Wang, Z.-L. & Cheng, J.-K. Microchip capillary electrophoresis with electrochemical detection. *Anal. Chem.* **74,** 2441–2445 (2002).

[70] Chen, G., Bao, H. & Yang, P. Fabrication and performance of a three-dimensionally adjustable device for the amperometric detection of microchip capillary electrophoresis. *Electrophoresis* **26,** 4632–4640 (2005).

[71] Regel, A. & Lunte, S. Integration of a graphite/poly(methyl-methacrylate) composite electrode into a poly(methylmethacrylate) substrate for electrochemical detection in microchips. *Electrophoresis* **34,** 2101–2106 (2013).

[72] Lacher, N. A., Lunte, S. M. & Martin, R. S. Development of a Microfabricated Palladium Decoupler/Electrochemical Detector for Microchip Capillary Electrophoresis Using a Hybrid Glass/Poly(dimethylsiloxane) Device. *Anal. Chem.* **76,** 2482–2491 (2004).

[73] Manica, D. P., Mitsumori, Y. & Ewing, A. G. Characterization of Electrode Fouling and Surface Regeneration for a Platinum Electrode on an Electrophoresis

Microchip. *Anal. Chem.* **75,** 4572–4577 (2003).

[74] Gunasekara, D. B., Hulvey, M. K. & Lunte, S. M. In-channel amperometric detection for microchip electrophoresis using a wireless isolated potentiostat. *Electrophoresis* **32,** 832–837 (2011).

[75] Tfelt-Hansen, P. C. & Tfelt-Hansen, J. Nitroglycerin headache and nitroglycerin-induced primary headaches from 1846 and onwards: a historical overview and an update. *Headache* **49,** 445–456 (2009).

[76] Ignarro, L. J. After 130 years, the molecular mechanism of action of nitroglycerin is revealed. *Proc. Natl. Acad. Sci. U.S.A.* **99,** 7816–7817 (2002).

[77] Hill, K. E., Hunt, R. W., Jr., Jones, R., Hoover, R. L. & Burk, R. F. Metabolism of nitroglycerin by smooth muscle cells. *Biochemical Pharmacology* **43,** 561–566 (1992).

[78] Kurz, M.A. Boyer, T.D., Whalen, R., Peterson, T.E., Harrison, D.G. Nitroglycerin metabolism in vascular tissue: role of glutathione S-transferases and relationship between NO. and NO2- formation. *Biochem J* **292**, 545-550 (1993).

[79] Hansson, G. K., Jörnvall, H. & Lindahl, S. G. *The Nobel Prize 1998 in physiology or medicine. Nitrogen oxide as a signal molecule in the cardiovascular system. Ugeskr. Laeg.* **160,** 7571–7578 (1998).

[80] Rochette, L. *et al.* Nitric oxide synthase inhibition and oxidative stress in cardiovascular diseases: Possible therapeutic targets? *Pharmacol. Ther.* **140,** 239–257 (2013).

[81] Pacher, P., Beckman, J. S. & Liaudet, L. Nitric Oxide and Peroxynitrite in Health and Disease. *Physiological Reviews* **87,** 315–424 (2007).

[82] Clough, G. F. Role of nitric oxide in the regulation of microvascular perfusion in human skin in vivo. *J. Physiol. (Lond.)* **516 (Pt 2),** 549–557 (1999).

[83] Rao, A. M., Dogan, A., Hatcher, J. F. & Dempsey, R. J. Fluorometric assay of nitrite and nitrate in brain tissue after traumatic brain injury and cerebral ischemia. *Brain Research* **793,** 265–270 (1998).

[84] Hyland, N. P. & Cryan, J. F. A gut feeling about GABA: Focus on GABA(B) Receptors. *Front. Pharmacol.* **1,** 1-9 (2010).

[85] Tao, R. & Auerbach, S. B. Regulation of serotonin release by GABA and excitatory amino acids. *Journal of Psychopharmacology* **14,** 100–113 (2000).

[86] Timmerman, W. & Westerink, B. H. Brain microdialysis of GABA and glutamate: what does it signify? *Synapse* **27,** 242–261 (1997).

[87] Cabaleiro, N., la Calle, de, I., Bendicho, C. & Lavilla, I. Current trends in liquid–liquid and solid–liquid extraction for cosmetic analysis: a review. *Anal. Methods* **5,** 323-340 (2012).

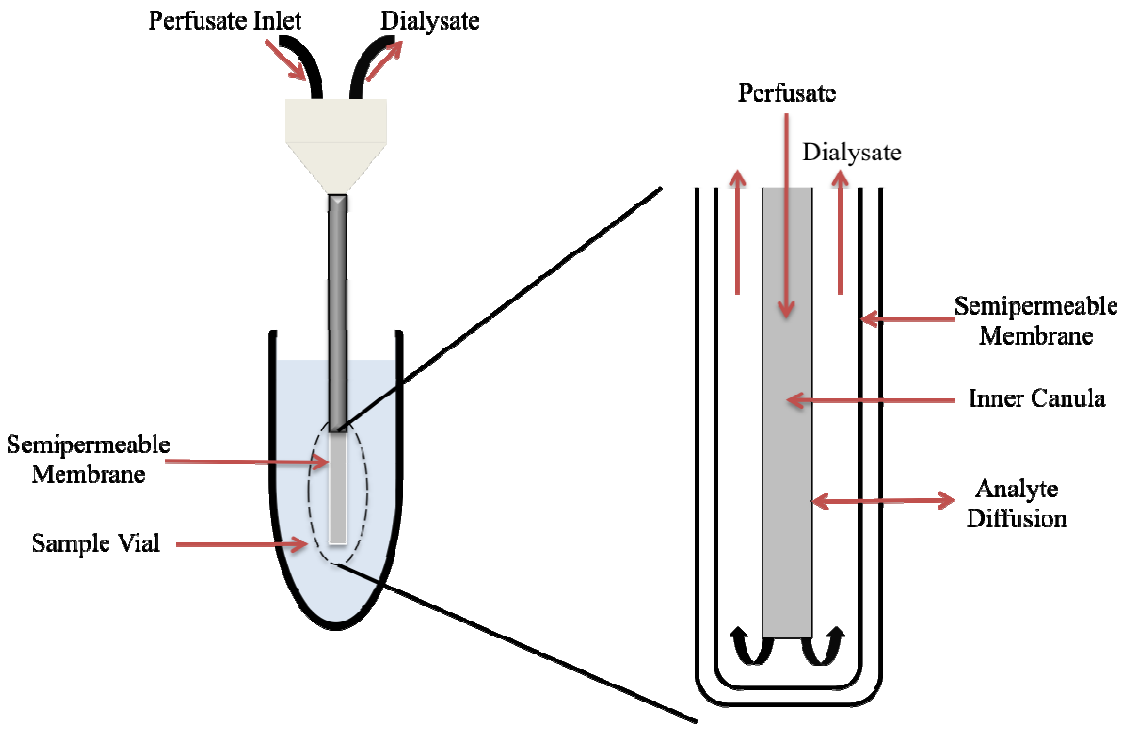

Figure 1.1. Microdialysis probe sampling diagram across the probe membrane. Image adapted from [87]

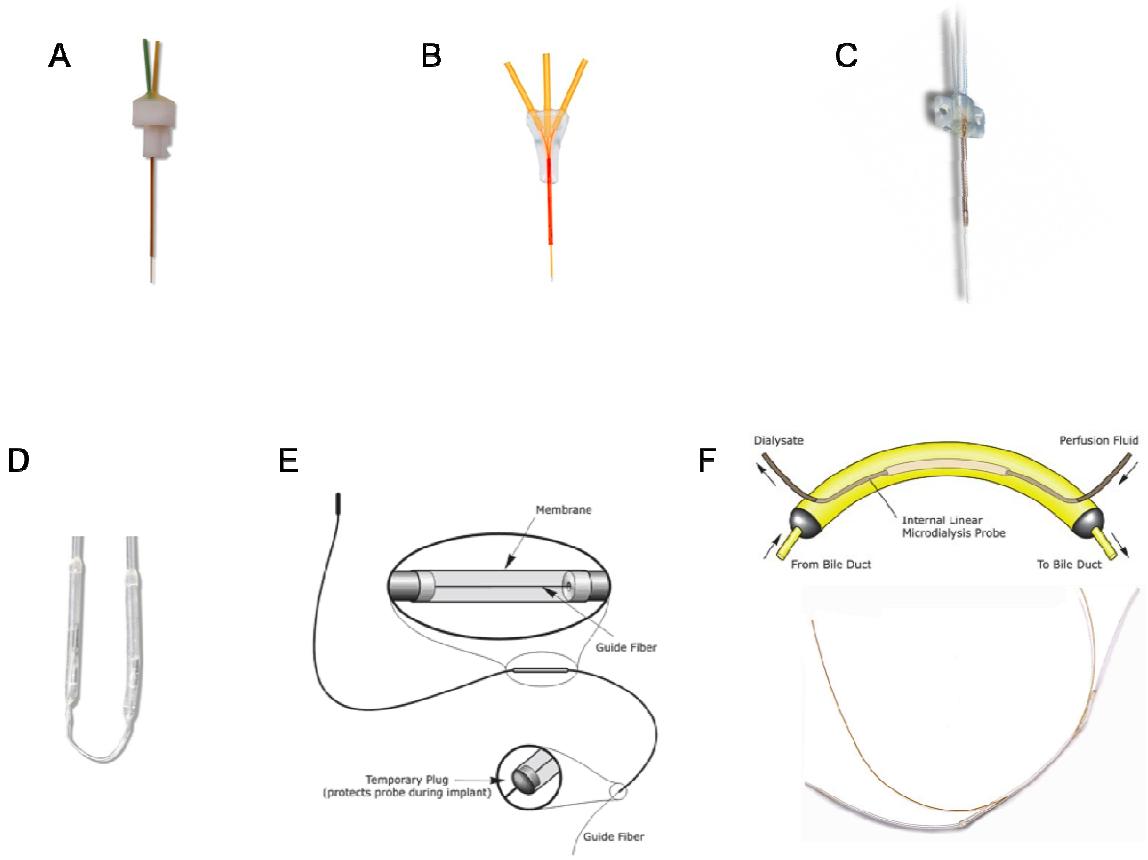

Figure 1.2. Microdialysis probes (A) Concentric probe for brain. (B) Metaquant probe for high recovery rates and makeup flow. (C) Flexible probe for intravenous use. (D) Loop Probe (E) Linear probe for tissue sampling (F) Shunt probe for bile duct sampling.

Note: This figure was adapted from [8] and images are reproduced with permission from BASi inc,[A,C,D,E,F] and Brains On-Line[B]

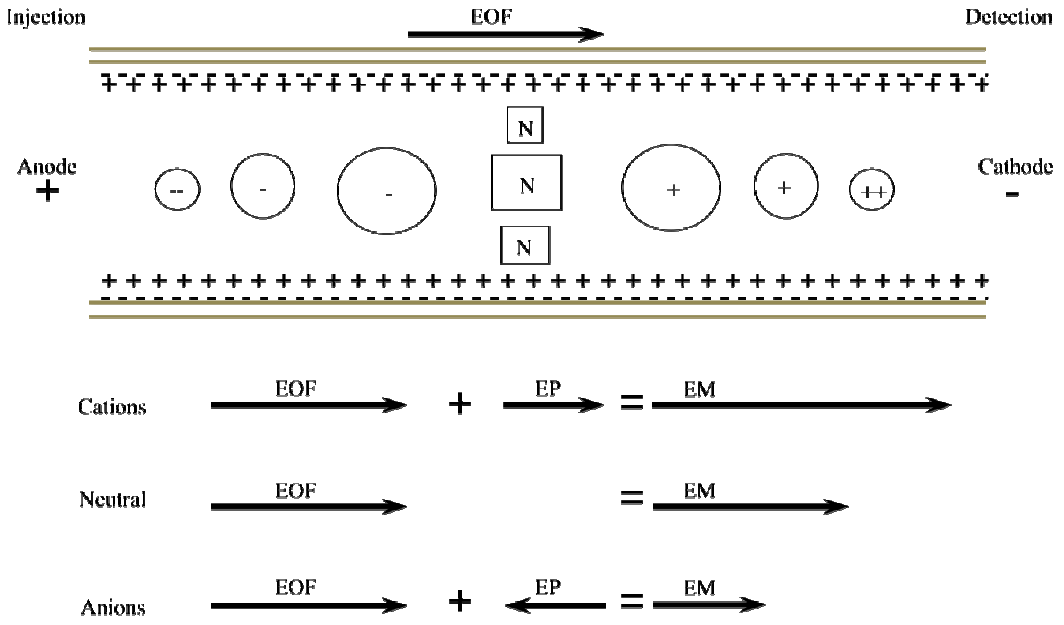

Figure 1.3. Electrophoretic and electroosmotic flow within a capillary. Electrical double layer is formed by the net negative charge of the capillary wall attracting positive ions from buffer. Analytes in solution separate based on electrophoretic mobility and electroosmotic flow.

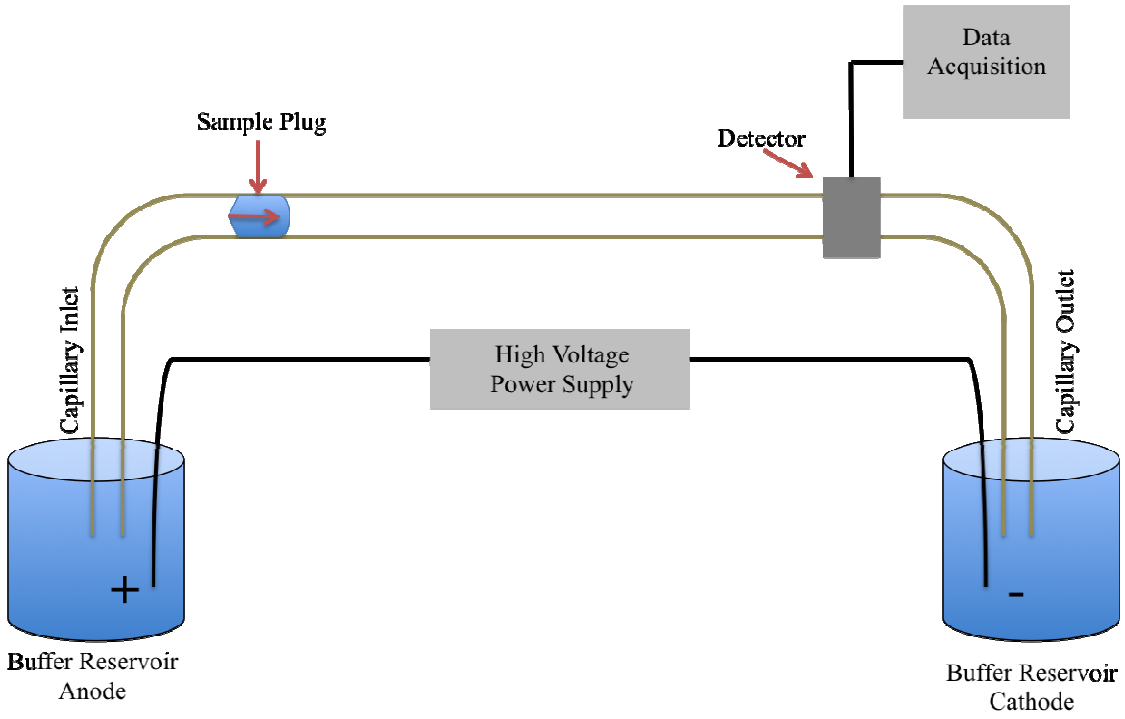

Figure 1.4. Simple diagram for capillary electrophoresis experimental set up.

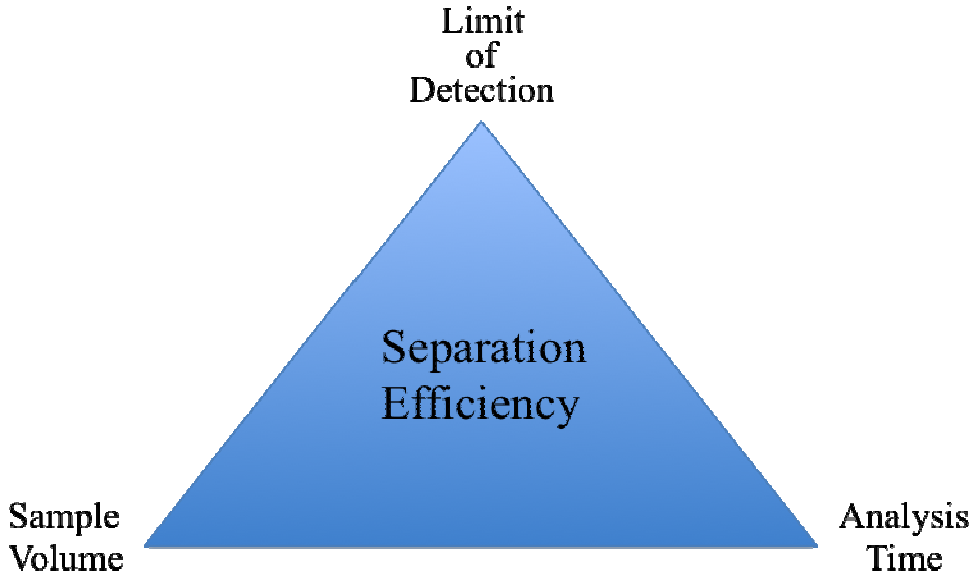

Figure 1.5. Diagram illustrating the relationship between sample volume, analysis time, and limit of detection for separation efficiency in capillary electrophoresis

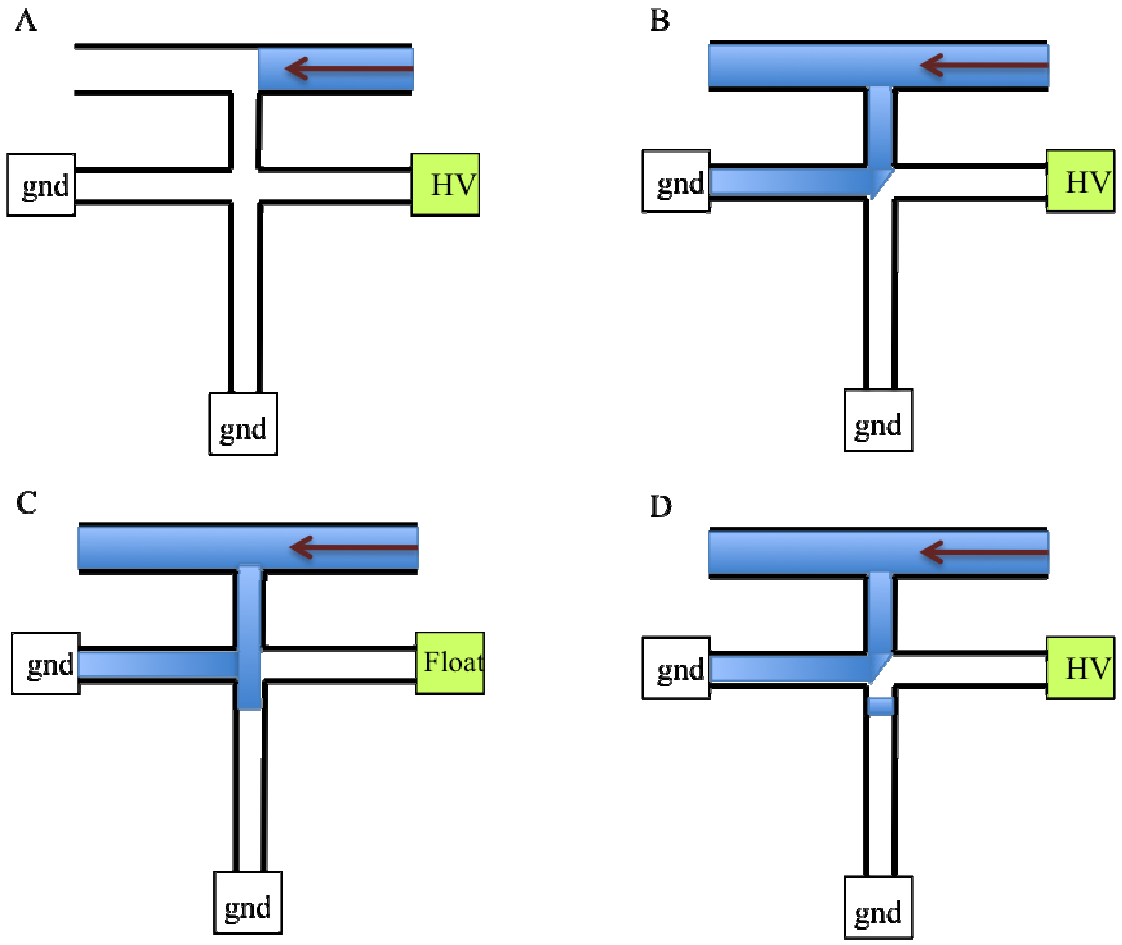

Figure 1.6. Illustration shows a gated injection with the use of a hydrodynamic flow: A) shows the sampling channel filling with the dialysate. B) shows established gate with the injection T completely filled. C) shows the high voltage being floated, and the dialysate entering the separation channel due to the hydrodynamic force. D) shows the gate being reestablished with the reapplication of the high voltage and the sample plug being completely injected into the separation channel.

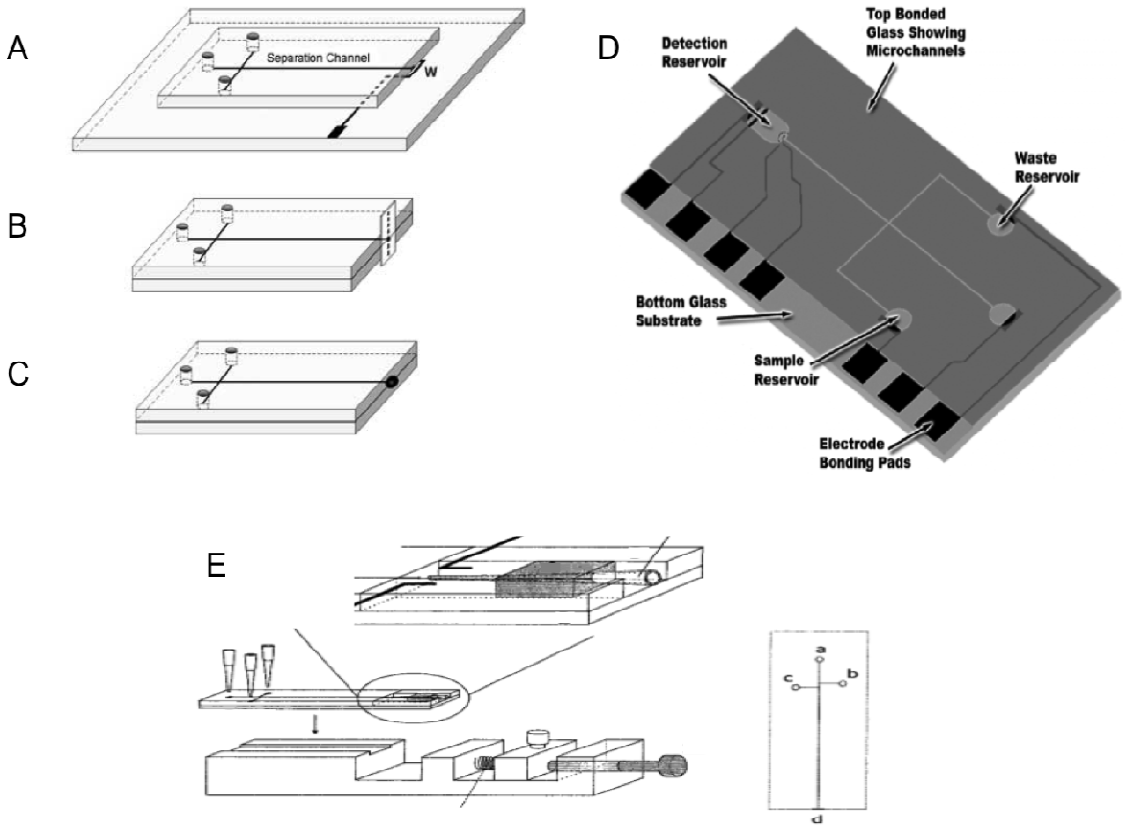

Figure 1.7. Electrochemical detector configurations for CE microchips based on different working electrode arrangements are shown in the following illustrations: A) 2 plates used with electrode printed end channel off capillary; B) flow off capillary placed onto an interchangeable perpendicular plate; C) flow through with the detector placed directly at the channel exit; D) capillary electrophoresis system developed using patterned electrodes required for operation for CE amperometric electrodes for EC; and E) capillary electrophoresis chip with integrated electrochemical detection cell using a plexiglass electrode holder and precision screws for 3D manipulation of electrode into the end of the capillary channel.

Note: Figure adapted from [66] Image A, B, C, reproduced with permission from [66], D reproduced with permission from [41], E reproduced with permission from [69]

Chapter 2

Microdialysis Sampling Coupled to Microchip Electrophoresis with Integrated Amperometric Detection on an All Glass Substrate

Scott, D.E., Grigsby, R. J. & Lunte, S.M. Microdialysis sampling coupled to microchip electrophoresis with integrated amperometric detection on an all-glass substrate. Chemphyschem 14, 2288-2294 (20130).

2.1. Introduction

A goal of our research group is to develop a separation-based sensor that can be placed on-animal for continuous monitoring of drug metabolism and neurotransmitters in freely roaming animals.[16] Since the entire system (chip and associated electronics) must be able to fit on the back of a large laboratory animal, using pneumatically actuated valves is not feasible. For these reasons, we have developed an all-glass microfluidic device with flow-gated injection for MD-MCE-EC. In this case, the injection process can be remotely controlled using a telemetry-enabled power supply mounted to a miniaturized portable device. An all-glass microfluidic device was chosen over one made of PDMS because it can withstand higher pressures without delamination. Additionally, the electroosmotic flow in glass MCE devices is more reproducible and stable over long periods of time.[17] There have been few reports in the literature concerning the fabrication of an all-glass chip with integrated electrochemical detection for microchip electrophoresis.[18-22] The main deterrent in producing such devices is the ability to completely seal the two pieces of glass in the vicinity of the electrode, especially in the cases where the electrode (or decoupler) is placed in the channel.

In this chapter, we describe the fabrication and evaluation of an all-glass MD-MCE chip with integrated electrochemical detection. Electrochemical detection is accomplished in an in-channel configuration using an electrically isolated wireless potentiostat.[23] The device is evaluated for the *in vitro* monitoring of hydrogen peroxide generated by glucose oxidase, as well as for the separation and detection of biological analytes in both positive and negative polarity mode.

2.2. Materials and Methods

2.2.1. Reagents and Materials

Tetradecyltrimethyl ammonium bromide (TTAB), sodium nitrite, sodium chloride, ascorbic acid, and glucose were purchased from Sigma-Aldrich (St. Louis, MO). Boric acid, 49% hydrofluoric acid, hydrochloric acid, hydrogen peroxide, nitric acid, methanol, isopropyl alcohol and acetone were purchased from Fisher Scientific (Pittsburgh, PA). Glucose oxidase was purchased from BBI Enzymes (Madison, WI). Solutions were prepared in deionized water (18 MΩ) using a Millipore A10 system (Billerica, MA). Chrome and AZ1518 photoresist-coated soda-lime glass blanks were obtained from Nanofilm (Westlake Village, CA). AZ® 300 MIF developer was purchased from Capitol Scientific, Inc. (Austin, TX). Chrome etchant (CR-7S) was purchased from Cyantek Corp. (Freemont, CA). Platinum (Pt) and titanium (Ti) sputtering targets were purchased from the Kurt J. Lesker Company (Jefferson Hills, PA). Colloidal silver was purchased from Ted Pella, Inc. (Redding, CA). PEEK tubing was purchased from IDEX Health & Science (Oak Harbor, WA). DL-1 loop microdialysis probes were purchased from BAS, Inc. (West Lafayette, IN).

2.2.2. Microchip Fabrication

The all-glass microdialysis-microchip electrophoresis device with embedded platinum working and counter electrodes was fabricated in-house. The chip configuration is shown in Figure 2.1. The microfluidic channels and integrated electrode designs were drawn using AutoCAD software (Autodesk, San Rafael, CA) to produce a

negative tone mask transparency (Infinite Graphics, Inc., Minneapolis, MN). The printed masks were overlaid on 4" × 4"× 0.060" chrome and AZ1518 photoresist coated soda-lime glass blanks. The plates were photolithographically patterned using an I-line UV flood source with an exposure dose of 86 mJ cm^{-2} (ABM, Inc., Scotts Valley, CA), developed in AZ® 300 MIF for 30 seconds and baked at 100 °C for 10 minutes using a hot plate. Once the photoresist is developed and hardened, the exposed chrome layer is etched using chrome etchant.

Fluid wells were drilled in the plate containing the microfluidic channels using a 1.55 mm diamond drill bit (TrueBite, Inc., Vestal, NY) mounted in a Dremel® drill press. The microfluidic wells and access holes were drilled before the glass was etched. This allows the etching process to smooth the splintering and roughness of the access holes caused during the drilling process, as well as to remove any debris from the drilling process. The plates were then etched at a rate of 5 µm min^{-1} in a 20:14:66 solution (49% hydrofluoric acid: concentrated nitric acid: water) to a depth of 15 microns for the microfluidic channels.[24] Etch depths were verified using an Alpha-Step 200 stylus profilometer (Tencor, Milpitas, CA). The patterned and etched glass blanks were then cut into individual chips using a tungsten carbide cutting wheel, resulting in four chips per plate. Following a thorough water rinse, the etched plates were placed in an acetone bath to dissolve the layer of AZ® 1518 photoresist. The remaining chromium was then removed from each piece using CR-7S etchant.

To produce the embedded platinum electrodes, recesses in a separate glass plate for electrode deposition were patterned and developed using the same photolithographic methods as described above. However, in this case, the patterned glass plates were

etched in 10:1 buffered oxide etchant (JT Baker, Austin, TX) with an etch rate of 0.35 μm min^{-1}, to produce a trench with a depth of approximately 500 nm. Following a thorough water rinse, the plate was dried on a hotplate at 100 °C for 10 minutes. It was then exposed to oxygen plasma (March Plasmod, Concord, CA) for 1 minute in order to promote adhesion of the metal to the etched glass surface.[25] Immediately following the oxygen plasma treatment, the glass plate was placed directly into the vacuum chamber of an AXXIS DC magnetron sputtering system (Kurt J. Lesker Co.) and pumped down to a base pressure of 5.0×10^{-7} Torr. Using argon as the process gas, a 40 nm adhesion layer of titanium was deposited, followed by a 460 nm layer of platinum metal. All deposition was done at a pressure of 2.4×10^{-3} Torr, with applied powers of 220 W and 200 W, respectively. The excess metal around the electrodes was lifted off in an acetone bath. The remaining chromium layer was removed from each piece using the aforementioned CR-7S etchant. This process resulted in glass plates with embedded Pt electrodes, as can be seen in Figure 2.1.

To complete the fabrication of the microfluidic device, the two halves were thoroughly scrubbed with an Aconox™ soaked sponge, and rinsed with DI water.[26] After drying with nitrogen, the two halves were then exposed to an oxygen plasma for 2 min. After plasma treatment, the two halves were brought together under a stream of deionized pure water, and then visually inspected for the presence of air bubbles between the glass plates. If bubbles were present, the plates were pried apart and the previous step repeated until none were present. The plates were then more-precisely aligned under a microscope so that the front of the working electrode was positioned no more than five microns into the end of the separation channel. Four assembled chips were then placed

between two ceramic tiles in a programmable muffle furnace (750 Series, Fisher Scientific) for thermal bonding, with a 300 g weight being placed over each chip (11.6 g cm^{-2}). The temperature ramping protocol that follows was adapted from previous publications.[7] The temperature was ramped from 25 °C to 540 °C at 3 °C min^{-1}, then ramped to 630 °C at a rate of 4 °C min^{-1}. The temperature was held at 630 °C for 3 hours, cooled at 3 °C min^{-1} to 540 °C, and then cooled at 1.5 °C min^{-1} to the annealing temperature of 510 °C and held there for 30 minutes. Following the annealing process, the furnace was cooled to 460 °C at 0.5 °C min^{-1} to minimize the induction of stress after annealing. After the kiln temperature was below the strain point of the glass, it was cooled to room temperature at 5 °C min^{-1}.

Additionally, for some of the devices used in this study, a calcium-assisted bonding step, as described by Chiu *et al.*, was used in conjunction with full thermal bonding.[27] For the calcium-assisted bonding step, the substrate surfaces were washed with a 5% Alconox™ solution by using a fiber wipe to gently scrub each plate with the solution. The substrates were then washed again in a 5% Alconox/5% calcium acetate solution and then the etched sides of each plate were gently rubbed together for approximately 2 min. This wash step with 5% Alconox/5% calcium acetate solution was repeated three times. The plates of glass were rinsed with water while the electrodes and the microfluidic channels were roughly aligned by hand. The chip was then visually inspected to ensure that no air bubbles were present between the glass plates. The plates were then more precisely aligned under a microscope so that the front of the working electrode was positioned no more than five microns into the end of the separation channel. The assembled chip was then clamped using binder clips to ensure that the

electrode alignment did not shift during processing. The clamped chip was then placed in a low temperature oven (Lindberg/Blue-M, SPX Thermal Product Solutions, Riverside, MI) at 65 °C for one hour after which time the temperature was increased to 110 °C for a minimum of 2 hours. Longer curing times of up to 96 hours for the calcium-assisted bonding promote a significantly higher success rate for full thermal bonding of the substrates. The assembled chip was then inspected for proper electrode alignment and for areas of nonspecific binding identified by Newton rings. In the case of electrode misalignment or the formation of Newton rings, the chip can easily be pried apart and reassembled by repeating the procedure above until all requirements are met. This process, while more time intensive, allows for the elimination of weights used in the thermal bonding process.

After the glass plates were bonded together, bonded port connectors and fittings were attached to the chip using LS EPOXY two-part adhesive (Labsmith, Livermore, CA) over one of the access holes for the microdialysis sampling channel. Copper wires were also connected to the platinum counter and working electrodes through the access holes using colloidal silver.

2.3. Evaluation On-line

2.3.1. Direct infusion method

Direct infusion experiments were accomplished using a CMA 107 syringe pump (N. Chelmsford, MA) connected to the chip using 15cm of 1/32 × 0.005 PEEK tubing. The syringe was filled with either 50 mM boric acid buffer at pH 9.2, or 10 mM boric

acid buffer containing 2 mM TTAB at pH 9.2, depending on the experiment. The experimental setup is shown in Figure 2.2A.

2.3.2. Microdialysis sampling

Microdialysis sampling was accomplished using a BASi loop microdialysis probe with a 1 cm membrane and 30 kDa molecular weight cut-off. Each side of the 1 cm semipermeable membrane has 16 cm of fluorinated ethylene propylene (FEP) tubing, which can be cut to desired lengths. The probe was placed in an open 2 mL sample vial, which was used as a reaction well. The reaction well was then placed in a sample holder and secured to a stage (Figure 2.2B). The FEP tubing from the probe was connected to the syringe pump; all 16 cm of the attached tubing was used in this case. To connect the probe to the chip, 6 cm of the 1/32 × 0.005 FEP tubing was removed and replaced with 5 cm of PEEK tubing with similar dimensions using tubing connectors. The probe was connected to the chip using 1/32 LabSmith connectors and fittings (LabSmith, Livermore, CA). This setup results in having 16 cm of tubing going from the syringe to the probe and 15 cm of tubing going from the probe to the chip.

Before each experiment, a conditioning procedure was performed on the chip that consisted of a rinse with methanol for 5 minutes followed by deionized water for 5 minutes. The chip was then rinsed with 0.1 N HCl for 5 minutes, followed by deionized pure water for 5 minutes. The final conditioning step consisted of a 10-minute rinse with 0.1 N NaOH followed by an additional 10-minute rinse with the run buffer. Following the conditioning procedure, the chip was secured to a stage. A high voltage lead was placed into the buffer reservoir of the chip, and ground leads were placed into the buffer

waste and sample waste reservoirs. The voltage applied to the buffer reservoir was set at ± 1600 V (positive/reverse polarity). Using Kirchoff's rules for calculating field strength, as described by Seiler *et al*., a field strength of 254 V cm^{-1} for the 2.5 cm separation channel was calculated.[28] Prior to each injection, the charging current of the working electrode was allowed to dissipate, producing a stable baseline. The microdialysis flow rate was 1.0 μL min^{-1}. The injection time was set at 1 second. Analysis took between 40 and 60 seconds, depending on the analyte of interest.

2.3.3. Detection

A Pinnacle model 9051 electrically isolated wireless potentiostat (Pinnacle Technology, Lawrence, KS) was employed for detection in a two-electrode format at a 13 Hz sampling rate. Physical contact between the electrode and the potentiostat was accomplished using colloidal silver and copper wire. The 9051 single-channel isolated potentiostat maintains a set voltage bias of up to 4 V between the working and counter electrodes, and wirelessly transmits up to 2 digitized signals directly to a Bluetooth® module connected to a PC at a sample rate of 1 Mbit sec^{-1}. The Bluetooth® module directly imports the data to the PC with support from Serenia software suites.

The electrochemical cell consisted of platinum working (15 □m) and counter electrodes (300 □m) deposited into a 500 nm channel etched into the glass surface. The working electrode was aligned directly at the edge of the separation channel using in-channel alignment, with the electrode being no more than 5 □m inside the separation channel. Using the 9051 electrically isolated potentiostat makes it possible to place the working electrode directly in the separation channel without destroying the potentiostat.

For in-channel alignment, the separation potential creates a positive bias shift in reverse polarity separations, and a negative bias shift in positive polarity separations. The bias applied to the electrode depends on its exact alignment in the separation channel, with compensation for the bias shift adjusted according to the mode of separation.[23]

2.4. Results and discussion

2.4.1. Device fabrication

The aim for the microchip fabrication processes was to develop a simple and reproducible method for integrating a metal electrode into an all-glass chip with a good success rate. Previous reports by Crain *et al.* describe a fabrication process for an all-glass microfluidic device using multiple acid-based cleaning steps and a final RCA base cleaning step.[29] Our group was able to eliminate the use of these potentially dangerous cleaning steps while maintaining a high success rate. This was achieved in three ways. First, by drilling the access holes prior to channel etching, small particles that remained from the drilling step were dissolved away in the hydrofluoric acid used to make the channels. Secondly, it was found that simply scrubbing the glass with soap and water prior to device assembly was sufficient to remove organic and particulate contamination from the surface. Lastly, by implementing a calcium-assisted bonding step as described by Allen *et al.*,[27] bonding success was guaranteed before the assembled pieces were subjected to the irreversible, high-temperature thermal bonding process.

In the all-glass MCE-EC device described by the Baldwin group, the end-channel configuration, in which the electrode was placed just outside the separation channel in the

detection reservoir, was used. To help mitigate some of the effects of band broadening induced by the end-channel alignment, a curved working and counter electrode design was used.[19-21,29] In this work, in-channel alignment was used to eliminate the effects of band broadening that can be generated due to the end-channel alignment of the electrodes.

Some publications have reported the use of simple replaceable working electrodes for amperometric detection in microchip electrophoresis. This approach uses a fixed electrode holder at the outlet of the separation channel.[30-32] While this can decrease the overall production cost of the chip, it requires a supplementary detection cell along with the use of a three-dimensional micromanipulator, thus increasing the complexity of the analytical system. The use of micromanipulators also reduces the ability to miniaturize the system, while minimizing the potential for making this a truly portable device. Conversely, our chip design implements an integrated counter electrode, thus simplifying fabrication and experimental setup.

2.4.2. Evaluation of chip by direct infusion

The microfluidic device used in these studies employs a flow-through gated injection scheme. The approach was adapted from Lin *et al*.,[33] who used it in a direct injection scheme with fluorescence detection; it has been previously described by our group for microdialysis sampling.[7,12,14] In our system, a syringe pump was used to deliver the dialysate through the enlarged flow channel at the top of the device. This flow generates a hydrodynamic pressure inside the microfluidic channels. A gate is established by applying an electric field between the high voltage lead and the respective

ground leads at the waste reservoirs (Figure 2.1). This prevents the sample from prematurely entering to the separation channel. In order to introduce a discrete sample plug into the separation channel, the high voltage is floated, introducing the pressure-driven perfusate into the separation channel. The gate is then reestablished after a specified amount of time by reapplying the high voltage. Thus, injection time and flow rate define the sample plug size that is introduced into the separation channel.

2.4.3. Reverse polarity separations

The system was first evaluated in reverse polarity for the continuous monitoring of hydrogen peroxide and nitrite with direct infusion of the analyte. Using 10 mM boric acid containing 2 mM TTAB at pH 9.2 as a run buffer, 1 mM standard solutions of both nitrite and hydrogen peroxide were perfused into the chip at a flow rate of 1 μL min^{-1} (Figure 2.2A). The electrophoretic separation was accomplished in 20 seconds (Figure 2.3). Ten sequential injections resulted in an average peak heights of 4.7 nA for nitrite and 4.4 nA for hydrogen peroxide, with RSD values of 7.4% and 10.8%, respectively (n = 10). This separation demonstrated the ability to perform fast sampling and separations on chip, along with the ability of the system to perform these separations over repeated injections with a reasonably low relative standard deviation.

In a separate experiment, a 1 mM standard solution of nitrite, ascorbic acid, and hydrogen peroxide in 10 mM boric acid and 2 mM TTAB at pH 9.2 was perfused through the chip at a flow rate of 1 μL min^{-1} (Figure 2.4). This experiment was run to evaluate the ability of the chip to perform separations of multiple analytes with baseline resolution. The separation of the three analytes was accomplished in 20 seconds with an

average peak height of 4.1 nA for nitrite, 8.2 nA for ascorbic acid, and 1.8 nA for H_2O_2, with RSD values of 7.5%, 6.52% and 4.3%, respectively (n = 10).

2.4.4. Positive polarity separation

The system was then evaluated in positive polarity with a 50 mM boric acid buffer at pH 9.2. A standard solution of 1 mM hydrogen peroxide was used with direct infusion to test the system's versatility (Figure 2.5). For this experiment, the separation time was set for 45 seconds, with an average peak height of 3.9 nA and an RSD value of 8.27% (n=10). Positive polarity along with simple boric acid buffer was used for these MD experiments to eliminate the use of a surfactant, which could interfere with the recovery of analyte at the probe and inhibit enzyme activity.

2.4.5. Microdialysis-microchip electrophoresis with electrochemical detection

The system was evaluated for MD sampling. These experiments were conducted using positive polarity with the experimental setup shown in Figure 2.2B. A BASi loop probe was specifically chosen for its flexibility, size (1.2 mm OD at thickest point), and biocompatibility; it will also be employed for future on-animal experiments using dermal sampling. The total length of tubing from the probe to the chip was 15 cm and the flow rate of the pump was 1 µL/min. Figure 2.6 shows the response obtained when 100 µL aliquots of 10 mM hydrogen peroxide standard were serially added at five minute intervals via micropipette to the sample vial that contained the microdialysis probe immersed in 50 mM boric acid buffer. The lag time, defined as the period of time it takes for the analyte of interest to be transferred from the probe to the device for sample

injection and subsequent detection, was 5 minutes. The rise time was also measured; this is defined as the period of time which is required for the probe to achieve 90% of the response to the change in concentration.[34] In this case, the rise time was less than the separation time (60 seconds), leading to an overall temporal resolution of one minute for these studies.

2.4.6. Monitoring enzymatic generation of H_2O_2 by MD-MCE-ED

To demonstrate the ability of this system to continuously monitor an enzymatic reaction, the generation of hydrogen peroxide from glucose oxidase was measured. Glucose oxidase readily catalyzes glucose to gluconic acid, with simultaneous production of hydrogen peroxide. The BASi loop microdialysis probe was placed in a vial containing 50 mg of glucose oxidase (360 U mg^{-1}) in 1 mL of 50 mM boric acid buffer at pH 9.2. A large excess of enzyme was used due to its low activity at pH 9.2. The probe was perfused with 50 mM boric acid buffer at a flow rate of 1 μL min^{-1}. A baseline for the sample prior to the addition of glucose was measured for 30 minutes, resulting in no visible amperometric peak for peroxide (Fig. 7). 100 μL aliquots of 1 mM glucose were then added to the vial of glucose oxidase using passive mixing; a steady increase in hydrogen peroxide was observed. Figure 2.7 shows the electropherogram obtained for hydrogen peroxide as a function of time following the addition of glucose to the reaction vial.

2.5. Conclusions

In this chapter, an on-line microdialysis-microchip electrophoresis system using integrated in-channel electrochemical detection with a platinum electrode is described. The device can be employed in either positive or negative polarity. The lag time, response time, and temporal resolution for the device were determined using hydrogen peroxide as a model analyte. Finally, the device was evaluated for continuous monitoring of hydrogen peroxide generated by glucose oxidase in the presence of glucose. The ultimate goal is to use this chip in conjunction with a portable analysis system for the continuous monitoring of drugs and neurotransmitters in awake, freely roaming animals.

2.5. References

[1] Hogan, B. L., Lunte, S. M., Stobaugh, J. F. & Lunte, C. E. Online coupling of in vivo microdialysis sampling with capillary electrophoresis. *Anal. Chem.* **66,** 596–602 (1994).

[2] Lada, M. W., Vickroy, T. W. & Kennedy, R. T. High Temporal Resolution Monitoring of Glutamate and Aspartate in Vivo Using Microdialysis On-Line with Capillary Electrophoresis with Laser-Induced Fluorescence Detection. *Anal. Chem.* **69,** 4560–4565 (1997).

[3] Schultz, K. N. & Kennedy, R. T. Time-resolved microdialysis for in vivo neurochemical measurements and other applications. *Annu Rev Anal Chem* **1,** 627–661 (2008).

[4] Nandi, P. & Lunte, S. M. Recent trends in microdialysis sampling integrated with conventional and microanalytical systems for monitoring biological events: a review. *Anal. Chim. Acta* **651,** 1–14 (2009).

[5] Guihen, E. & O'Connor, W. T. Capillary and microchip electrophoresis in microdialysis: Recent applications. *Electrophoresis* **31,** 55–64 (2010).

[6] Nandi, P., Kuhnline, C. D. & Lunte, S. M. Analytical considerations for microdialysis sampling. *Applications of Microdialysis in Pharmaceutical Science*, 39-92 (2011).

[7] Huynh, B. H., Fogarty, B. A., Martin, R. S. & Lunte, S. M. On-Line Coupling of Microdialysis Sampling with Microchip-Based Capillary Electrophoresis. *Anal. Chem.* **76,** 6440–6447 (2004).

[8] Sandlin, Z. D., Shou, M., Shackman, J. G. & Kennedy, R. T. Microfluidic

Electrophoresis Chip Coupled to Microdialysis for in Vivo Monitoring of Amino Acid Neurotransmitters. *Anal. Chem.* **77,** 7702–7708 (2005).

[9] Wang, M., Roman, G. T., Schultz, K., Jennings, C. & Kennedy, R. T. Improved Temporal Resolution for in Vivo Microdialysis by Using Segmented Flow. *Anal. Chem*. **80,** 5607–5615 (2008).

[10] Nandi, P., Desai, D. P. & Lunte, S. M. Development of a PDMS-based microchip electrophoresis device for continuous online in vivo monitoring of microdialysis samples. *Electrophoresis* **31,** 1414–1422 (2010).

[11] Mecker, L. C. & Martin, R. S. Coupling Microdialysis Sampling to Microchip Electrophoresis in a Reversibly Sealed Device. *Journal of the Association for Laboratory Automation* **12,** 296–302 (2007).

[12] Huynh, B. H., Fogarty, B. A., Nandi, P. & Lunte, S. M. A microchip electrophoresis device with on-line microdialysis sampling and on-chip sample derivatization by naphthalene 2, 3-dicarboxaldehyde/2-mercaptoethanol for amino acid and peptide analysis. *Journal of Pharmaceutical and Biomedical Analysis* **42,** 529–534 (2006).

[13] Wang, M., Roman, G. T., Perry, M. L. & Kennedy, R. T. Microfluidic chip for high efficiency electrophoretic analysis of segmented flow from a microdialysis Probe and in vivo chemical monitoring. *Anal. Chem.* **81,** 9072–9078 (2009).

[14] Nandi, P., Scott, D. E., Desai, D. & Lunte, S. M. Development and optimization of an integrated PDMS based-microdialysis microchip electrophoresis device with on-chip derivatization for continuous monitoring of primary amines. *Electrophoresis* **34**, *895-902* (2013).

[15] Mecker, L. C. & Martin, R. S. Integration of microdialysis sampling and microchip electrophoresis with electrochemical detection. *Anal. Chem.* **80,** 9257–9264 (2008).

[16] Lunte, S. M., Scott, D.E. Grigsby, R., Gunesekara, D., Saylor, R., Regal, A., Naylor, E., Gabbert, S., Jonson, D., Janle, E. Progress regarding the development of an on-animal separation based sensor for monitoring drugs and neurotransmitters in freely roaming animals. *Monitoring Molecules in Neuroscience* 1–3 (2012).

[17] Coltro, W. K. T., Lunte, S. M. & Carrilho, E. Comparison of the analytical performance of electrophoresis microchannels fabricated in PDMS, glass, and polyester-toner. *Electrophoresis* **29,** 4928–4937 (2008).

[18] Baldwin, R. P., Roussel, T.J., Crain, M.M., Bathlagunta, R., Jackson, D.J., Gullapalli, J., Conklin, J.A., Pai, R., Naber, J.F., Walsh, K.M., Keyton, R.S. Fully integrated on-chip electrochemical detection for capillary electrophoresis in a microfabricated device. *Anal. Chem.* **74,** 3690–3697 (2002).

[19] Keynton, R. S., Roussel, T.J., Crain, M.M., Jackson, D.J., Franco, D.B., Naber, J.F., Walsh, K.M., Baldwin, R.P. Design and development of microfabricated capillary electrophoresis devices with electrochemical detection. *Anal. Chim. Acta* **507,** 95–105 (2004).

[20] Jackson, D. J., Naber, J.F., Roussel, T.J., Crain, M.M., Walsh, K.M., Keyton, R.S., Baldwin, R.P. Portable High-Voltage Power Supply and Electrochemical Detection Circuits for Microchip Capillary Electrophoresis. *Anal. Chem.* **75,** 3643–3649 (2003).

[21] Pai, R. S., Walsh, K.M., Crain, M.M., Roussel, T.J., Jackson, D.J., Baldwin, R.P., Keyton, R.S., Naber, J.F. Fully Integrated Three-Dimensional Electrodes for Electrochemical Detection in Microchips: Fabrication, Characterization, and Applications. *Anal. Chem.* **81,** 4762–4769 (2009).

[22] Berthold, A., Laugere, F., Schellevis, H., DeBoer, C.R. Laros, M., Guijt, R.M., Sarro, P.M., Vallekoop, M.J. Fabrication of a glass-implemented microcapillary electrophoresis device with integrated contactless conductivity detection. *Electrophoresis* **23,** 3511–3519 (2002).

[23] Gunasekara, D. B., Hulvey, M. K. & Lunte, S. M. In-channel amperometric detection for microchip electrophoresis using a wireless isolated potentiostat. *Electrophoresis* **32,** 832–837 (2011).

[24] Fan, Z. H. & Harrison, D. J. Micromachining of capillary electrophoresis injectors and separators on glass chips and evaluation of flow at capillary intersections. *Anal. Chem.* **66,** 177–184 (1994).

[25] Benjamin, P. & Weaver, C. The Adhesion of Evaporated Metal Films on Glass. *Proceedings of the Royal Society A: Mathematical, Physical and Engineering Sciences* **261,** 516–531 (1961).

[26] Mattox, D. M. Surface cleaning in thin film technology. *Thin Solid Films* **53,** 81–96 (1978).

[27] Allen, P. B. & Chiu, D. T. Calcium-assisted glass-to-glass bonding for fabrication of glass microfluidic devices. *Anal. Chem.* **80,** 7153–7157 (2008).

[28] Seiler, K., Fan, Z. H., Fluri, K. & Harrison, D. J. Electroosmotic Pumping and Valveless Control of Fluid Flow within a Manifold of Capillaries on a Glass Chip.

Anal. Chem. **66,** 3485–3491 (1994).

[29] Crain, M. M. *et al.* Fabrication of a glass capillary electrophoresis microchip with integrated electrodes. *Methods Mol. Biol.* **339,** 13–26 (2006).

[30] Zeng, Y., Chen, H., Pang, D.-W., Wang, Z.-L. & Cheng, J.-K. Microchip capillary electrophoresis with electrochemical detection. *Anal. Chem.* **74,** 2441–2445 (2002).

[31] Wang, J., Tian, B. & Sahlin, E. Micromachined electrophoresis chips with thick-film electrochemical detectors. *Anal. Chem.* **71,** 5436–5440 (1999).

[32] Chen, G., Bao, H. & Yang, P. Fabrication and performance of a three-dimensionally adjustable device for the amperometric detection of microchip capillary electrophoresis. *Electrophoresis* **26,** 4632–4640 (2005).

[33] Lin, Y. H., Lee, G. B., Li, C. W., Huang, G. R. & Chen, S. H. Flow-through sampling for electrophoresis-based microfluidic chips using hydrodynamic pumping. *Journal of Chromatography A* **937,** 115–125 (2001).

[34] Skoog, D. A., F. J. Holler, and S. R. Crouch. "Principles of Instrumental Analysis, Section I, Chapter 5, Thomson Brooks/Cole, Belmont, CA, 2007." *Brooks/Cole, Belmont, CA* 425-442 (2007).

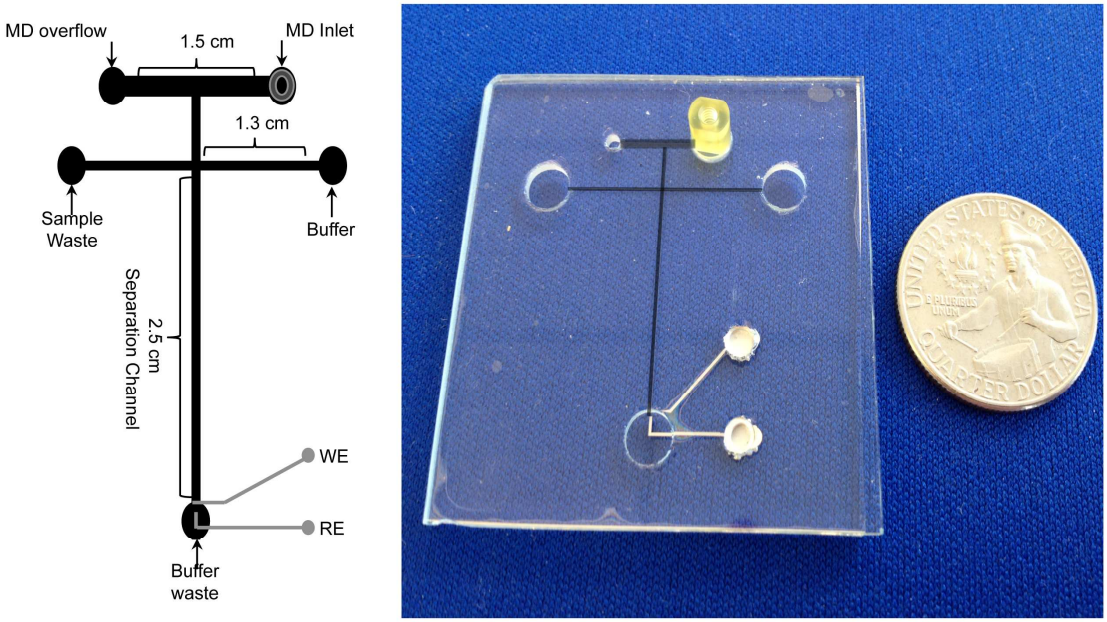

Figure 2.1: A schematic of the "double T" 2.5 cm microchip design and electrode placement for flow-through studies MD-MCE studies with channel dimensions. All microfludic channels were etched to 15 μm deep and 40 μm wide, except for the microdialysis inlet channel, which was 500 μm wide.

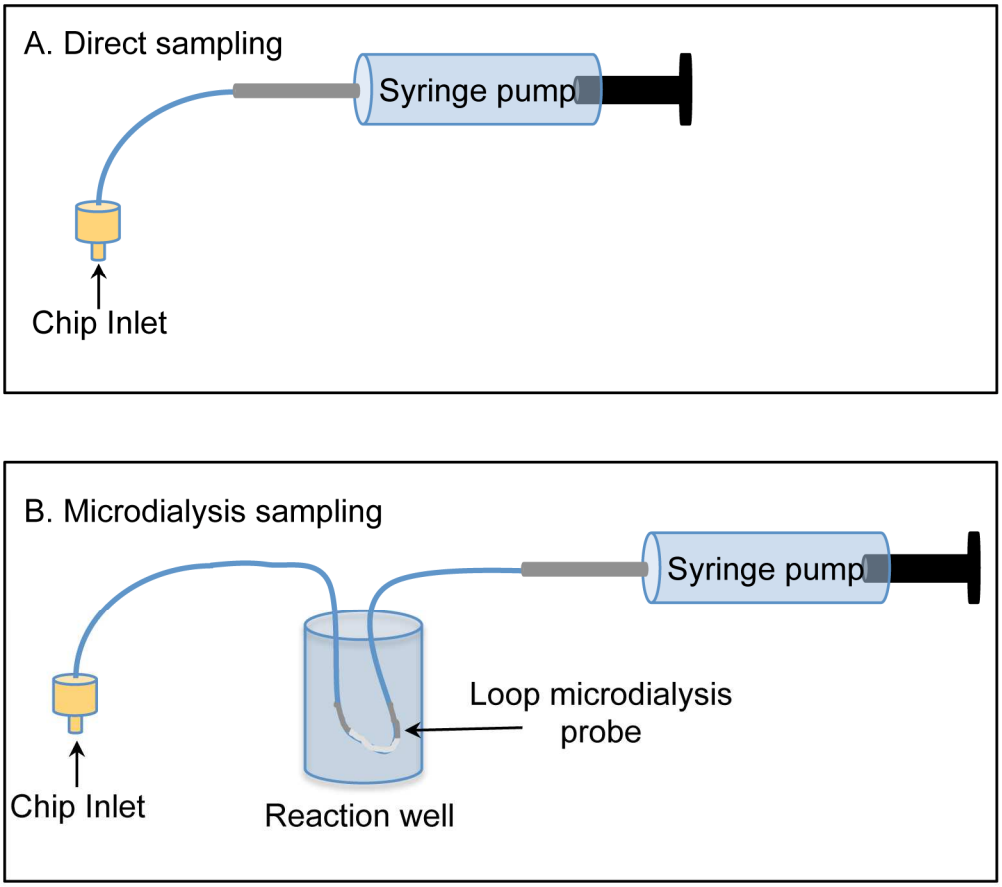

Figure 2.2: A) Experimental setup for the direct perfusion of analyte into the device. B) Experimental setup for the microdialysis sampling, which includes the loop microdialysis probe inside the reaction well.

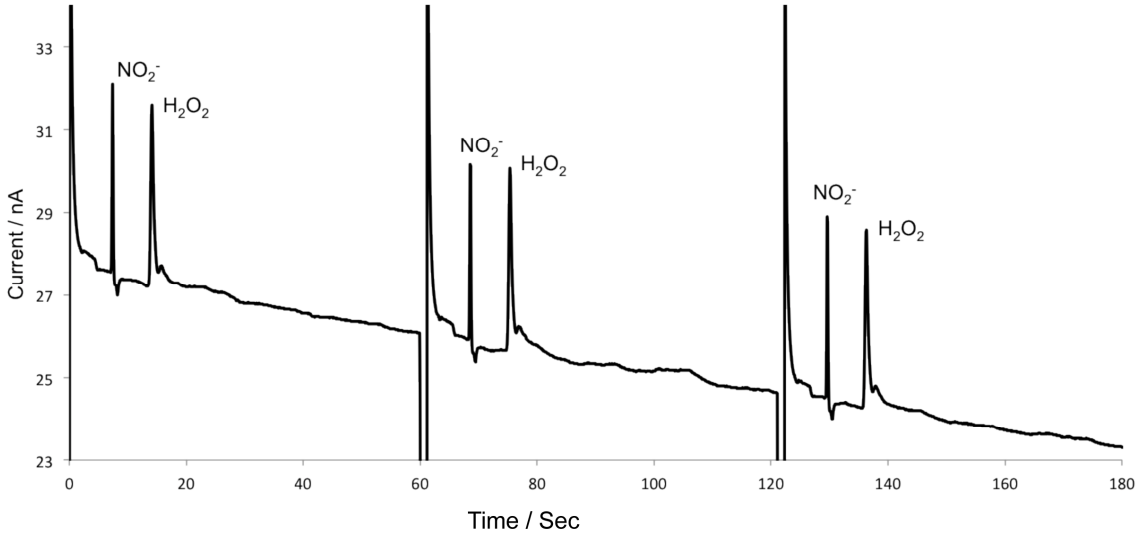

Figure 2.3: Separation of nitrite and hydrogen peroxide using direct infusion and reversed polarity. Perfusate buffer: 10 mM boric acid and 2 mM TTAB at pH 9.2, 1 mM nitrite and 1mM hydrogen peroxide, at a flow rate of 1 μL min^{-1}. Separation buffer: 10 mM boric acid and 2 mM TTAB at pH 9.2. The applied voltage was -1600 V, generating a field strength of 254 V cm^{-1}, with an injection time of 1 second. The working electrode was set to a 1.1 V bias to the Pt counter electrode.

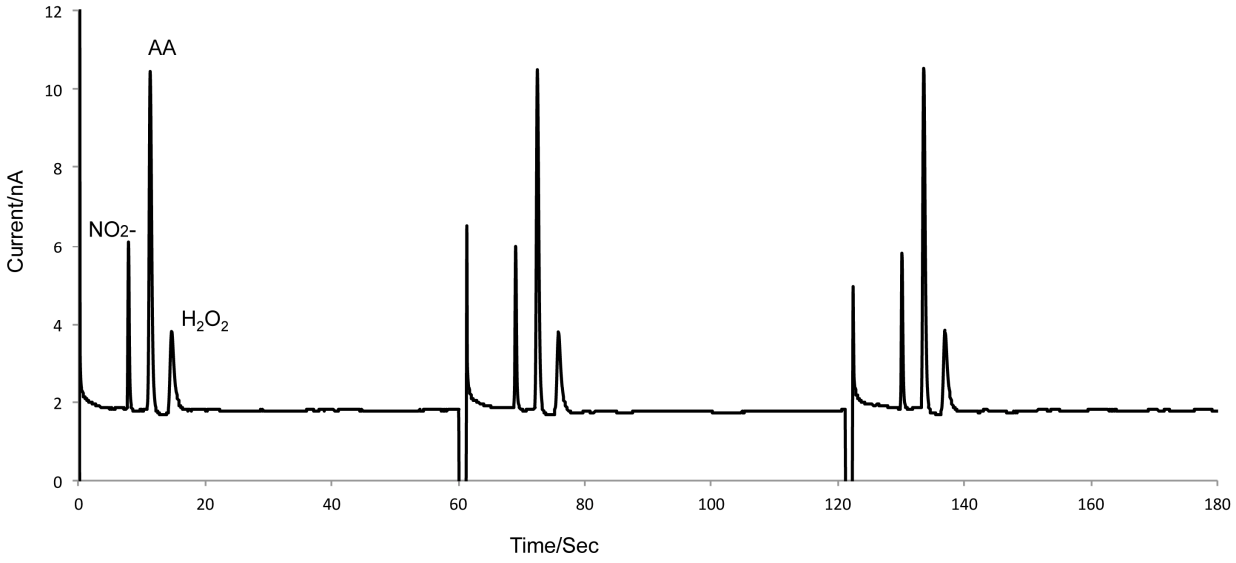

Figure 2.4: Separation of 1 mM nitrite, 1 mM ascorbic acid, and 1 mM hydrogen peroxide using direct infusion. Syringe pump buffer: 10 mM boric acid and 2 mM TTAB at pH 9.2, 1 mM nitrite, 1 mM ascorbic acid, and 1 mM hydrogen peroxide. All other conditions are identical to Figure 2.3.

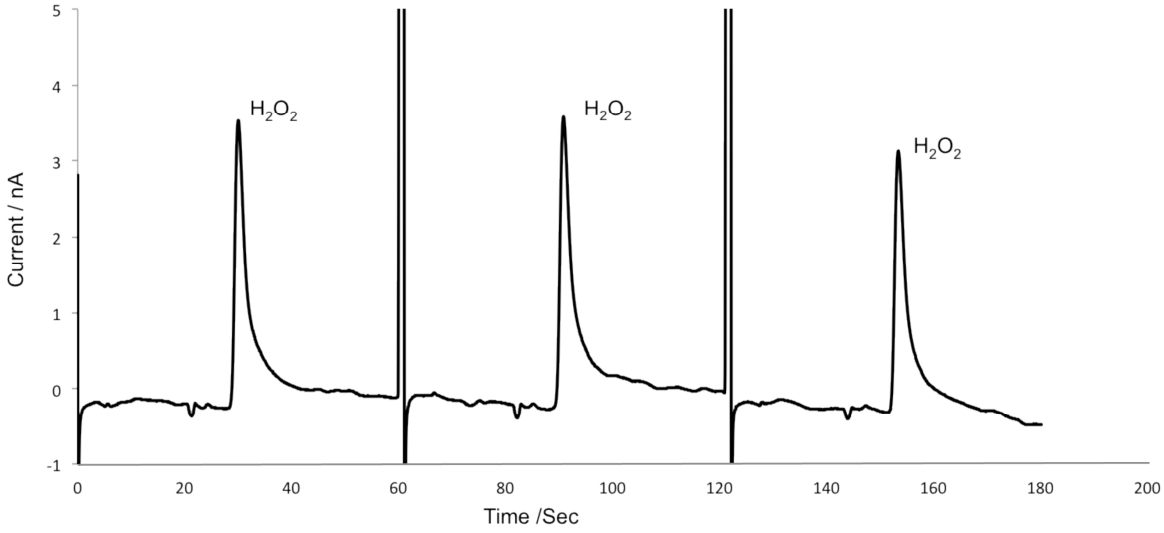

Figure 2.5: Detection of 1 mM hydrogen peroxide using direct infusion and normal polarity. Syringe pump buffer: 50 mM boric acid at pH 9.2. Separation buffer consisted of 50 mM boric acid at pH 9.2. The applied voltage was +1600 V. All other conditions are identical to Figure 2.3.

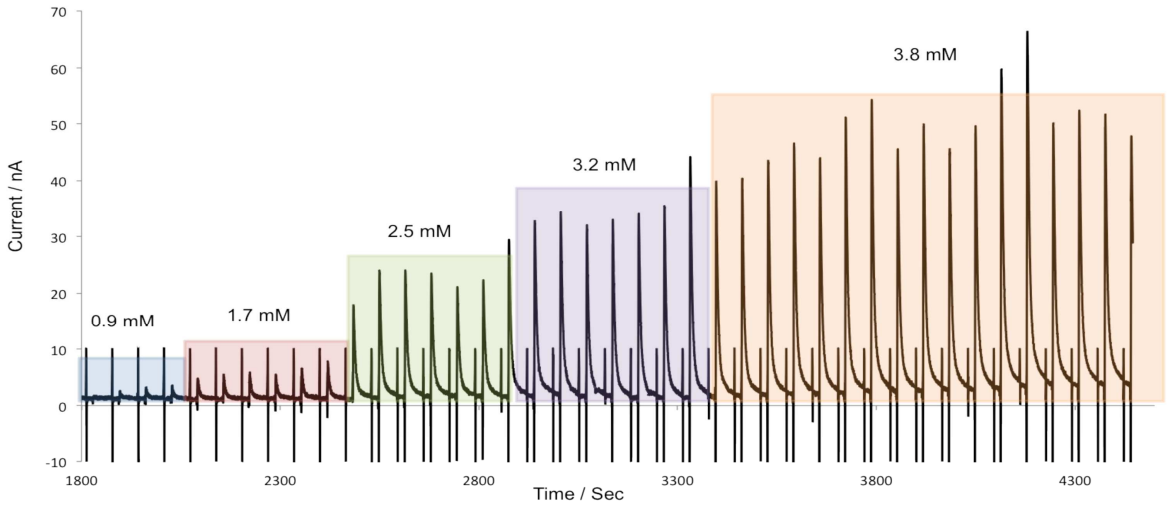

Figure 2.6: On-line microdialysis sampling with serial additions of hydrogen peroxide standard to the vial containing the microdialysis probe. Microdialysis perfusate: 50 mM boric acid at pH 9.2. The 2 mL vial contained 50 mM boric acid at pH 9.2. 100 µL of 10 mM hydrogen peroxide was serially added to the reaction well. Separation and detection conditions were identical to Figure 2.5. Syringe pump was set at a flow rate of 1 µL min^{-1} for microdialysis sampling.

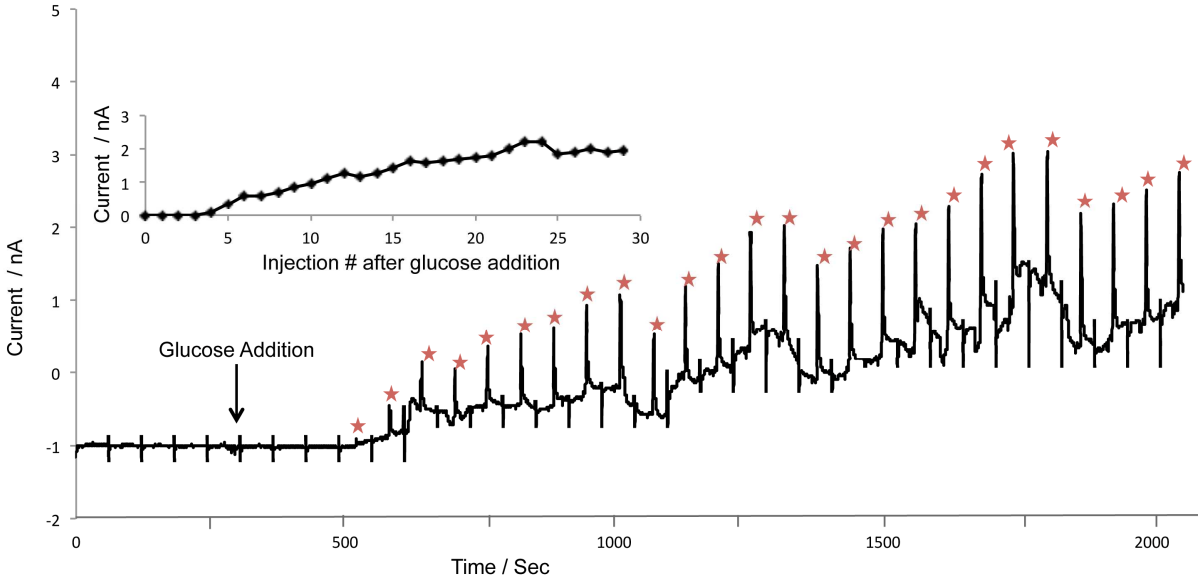

Figure 2.7: Enzymatic reaction-induced concentration change experiment with glucose oxidase to produce hydrogen peroxide. Syringe pump buffer: 50 mM boric acid at pH 9.2. The 2 mL reaction well contained 1 mL of 50 mM boric acid at pH 9.2 and 50 mg of glucose oxidase. 100 µL of 1 mM glucose was added to the reaction well to stimulate the production of hydrogen peroxide. All other conditions are identical to those in Figure 2.6.

Chapter 3

On-animal Separation Based Sensor for Monitoring Drug Metabolism in *Freely Roaming* Sheep

3.1. Introduction

Drugs are known to influence both physiology and behavior. Pharmaceutical compounds are constantly under development for behavioral disorders including ADHD, drug addiction and depression.[1-3] Some pharmaceuticals can also exhibit undesirable behavioral effects as has been seen by some of the drugs used to treat sleep deprivation.[4] Methods that can be employed for the simultaneous monitoring of drug metabolism and disposition along with neurotransmitter release and behavior are therefore important for drug development. *In vivo* voltammetry and analyte specific biosensors have been used extensively to monitor the release of neurotransmitters and changes in the concentrations of other endogenous molecules, such as glucose, in freely moving animals.[5,6] These techniques can provide information regarding the relative concentrations of specific substances in the brain, blood or other tissues with temporal resolution ranging from milliseconds to days. The primary disadvantage of these approaches is that they are generally only able to monitor one or two analytes at a time and are not generally useful in drug metabolism studies.

Microdialysis is a technique that has been used extensively to monitor the metabolism and disposition of drugs in a variety of tissues, as well as for monitoring neurotransmitter release in the brain.[7-10] The primary advantage of microdialysis over *in vivo* voltammery and biosensors is that it is a generic sampling method that collects molecules from the extracellular fluid of interest based on molecular weight. Therefore, it is possible to customize the analytical method that is used to analyze the microdialysis sample for the specific analyte(s) of interest. If a separation method is employed as part of the in the analytical method, several analytes, such as a drug and its metabolites or

amino acid neurotransmitters, can be monitored simultaneously. Depending on the volume requirements of the analytical method, it is also possible to analyze the same sample using multiple analytical methods. There are also many different types of probe configurations that have been specifically designed for sampling blood, brain and peripheral tissues. This makes it possible to monitor transport of molecules across the blood brain barrier, along with neurotransmitter release. An excellent example of this is the report by Davies *et al.* where they used multiple probes to monitor the transport and metabolism of Ritalin across the blood brain barrier along with brain dopamine concentrations.[11] Microdialysis sampling is routinely performed on awake freely moving animals and commercially available systems, such as the Raturn™, allow for simultaneous microdialysis sampling and behavior measurements in rats and mice. In the Davies study, the authors were able to correlate brain drug and catecholamine levels with the activity of the rat using a motion detector attached to the Raturn™. Although the rat was freely moving, it was not *freely roaming*.

A system that allows for a rat to be *freely roaming* during microdialysis sampling was reported by Cooper *et.al*.[12] In this approach, an osmotic pump implanted under the skin of the rat is used to deliver the perfusate through the probe at a flow rate of approximately 200 nanoliters per minute. On-rat collection was accomplished using a plastic vial that was attached to the outlet of the probe. With this system, it was possible for the rat to be outside the bowl and collect neurochemical data. However, the collection vial must be manually removed from the rat to obtain a sample for analysis. This limits the temporal resolution that can be obtained. Achieving high temporal resolution is important consideration when monitoring neurotransmitter release, which happens on the

order of seconds. Wang *et al*. reported on a method of off-line *in vivo* monitoring based on the collection of nanoliter microdialysate fractions using segmented flow to achieve a reported temporal resolution as low as 2 seconds.[13]

Capillary electrophoresis has been shown to be an ideal analytical method for the analysis of microdialysis samples due to its small sample volume requirements and fast separation times.[9,14] The pico- to nanoliter volume requirements of CE make it possible to monitor biochemical events with good temporal resolution. The on-line coupling of microdialysis to capillary electrophoresis was first reported in 1994 and provided the added advantage of eliminating manual manipulation of submicroliter samples, leading to better injection precision and the ability to perform near real time monitoring.[15] The use of capillary electrophoresis also made it possible to independently choose the separation mode and the detector that was most specific for the analytes of interest, leading to a "separation based sensor". These sensors have been used for a variety of applications including monitoring drug metabolism, neurotransmitter release and reactive oxygen species. One disadvantage of CE is that the systems are generally large and the animal must be connected to the microdialysis sampling analytical systems using long lengths of tubing.

The goal of this work was to develop an on-animal separation based sensor that could be used for the simultaneous monitoring drug metabolism and behavior in *freely roaming* animals. Microchip electrophoresis is a miniaturized version of CE that has considerable promise for on-animal measurements. The chips used for MCE generally require lower total voltages for the separation than those used for CE. This makes it possible to use miniaturized high voltage power supplies and detectors as part of the

system. Chips are also small and planar making them easier to integrate into a portable analysis system. Several approaches have been reported for coupling microdialysis to electrophoretic separations on chip. The first paper employed a flow-gated interface that was originally proposed by Chen's group to inject picoliter volumes from the micordialysate perfusate into the separation channel.[16] More recently pneumatic injection valves and droplets have been employed for this purpose.[16-18] The most common method of detection for MD-MCE includes on-chip derivatization with a fluorophore and laser-induced fluorescence detection.[16,17,19-23]

Electrochemical detection has been less frequently explored for MD-CE or MD-MCE. Zhou et.al. used MD-CE-EC to monitor the transdermal delivery and metabolism of nicotine.[24] The Martin group was the first to report the coupling of microdialysis to microchip electrophoresis with electrochemical detection and has made some of the most significant contributions to this field.[18,19,25] In one application, they used MD-MCE-EC in a PDMS chip to monitor catecholamine release from PC 12 cells in culture at a carbon working electrode. More recently, we reported an all glass chip containing an embedded platinum working electrode for MD-MCE-EC.[26] This chip employed a flow gated injection, which relies on precise timing of the application of potentials to different reservoirs. This injection mode is easier to miniaturize and control remotely than approaches that use valves or droplets to introduce the sample into the chip and therefore more suitable for on-animal experiments. An additional advantage of electrochemical detection for this application is that the electrodes and potentiostats can also be easily miniaturized.

Sheep have been used for many microdialysis studies, especially regarding maternal behavior and breeding.[27,28] In this paper, a miniaturized separation-based sensor using microdialysis coupled to microchip electrophoresis with amperometric detection for on-animal sensing is described. The system consists of an on-line interface to couple microdialysis to microchip electrophoresis, high voltage power supplies, and an electrically isolated potentiostat. The instrument is controlled and data are collected remotely using a Bluetooth interface and a laptop PC. The system was demonstrated with sheep as a model by monitoring nitrite production during subdermal delivery of nitroglycerin. The complete system is about the size of a lunchbox and was mounted on the back of the sheep during the drug metabolism studies, allowing measurements to be made in *freely roaming* animals.

3.2 Experimental Section

3.2.1 Materials and reagents

Calcium chloride, disodium phosphate heptahydrate, magnesium chloride, monosodium phosphate monohydrate, sodium chloride, sodium nitrite, tetrabutylammonium hydroxide (TBAOH), and potassium chloride were purchased from Sigma-Aldrich (St. Louis, MO). Acetone, hydrochloric acid, 49% hydrofluoric acid, hydrogen peroxide, isopropyl alcohol, methanol, nitric acid, and sulfuric acid were purchased from Fisher Scientific (Pittsburgh, PA). DEA-NONate was purchased from Cayman Chemical (Ann Arbor, MI). Ultrapure water was generated using a Millipore Synthesis (18 mOhm) A10 system (Kansas City, MO). Chrome and AZ1518 photoresist-

coated soda-lime glass blanks were obtained from Nanofilm (West Lake Village, CA). AZ® 300 MIF was purchased from Capitol Scientific, Inc. (Austin, TX). Chrome etchant CR-7S was purchased from Cyantek Corp. (Freemont, CA). Platinum (Pt) and titanium (Ti) sputtering targets were purchased from the Kurt J. Lesker Company (Jefferson Hills, PA). Colloidal silver (Ag) was purchased from Ted Pella, Inc. (Redding, CA). Nitroglycerin injectable USP (5mg/mL) was obtained from American Regent, Inc. (Shirley, NY). Lidocaine HCl 2% usp injectable was purchased from Bimeda (Oakbrook Terrace, Il)

3.2.2 Microchip fabrication

The all-glass microfluidic devices were fabricated with platinum embedded into the glass substrate as the working and counter electrodes, which were fabricated in-house at the Adams Institute clean room facilities as previously described in chapter 2.[26]

3.2.3 Instrumental set-up

The hardware for the portable analysis system consisted of an EMCO high voltage power supply (Model CA20N-5, EMCO High Voltage Corporation, Sutter Creek, CA), two external adjustable voltage (3-19V) Tekkeon laptop batteries (Model MP3450, Tekkeon Inc., Irvine, CA), and an electrically isolated potentiostat set at a data sampling rate of 30 Hz. Data collection and device control was accomplished using integrated telemetry via Bluetooth® module Mitsumi WML-C46AHR (Mitsumi, Tokyo, Japan) as shown in Figure 3.1. All data was collected and analyzed using a modified version of Sirenia® software suite (Pinnacle Technology, Lawrence, KS).

The top plate of an epoxy based photopolymer resin holder (Harvest Technologies, Belton, TX) secured the microfluidic device to the platform, which held the primary control board and high voltage power supply. A smaller board with a built-in Pinnacle isolated potentiostat (Figure 3.1(2)) and high voltage leads and ground leads (Figures 3.1(3) and 3.1(4)) was secured onto the top plate and placed into contact with the microfluidic device. The isolated potentiostat was telemetry controlled via Bluetooth® (Figure 3.1(6)), and the applied voltage to the working electrode ranged between 0.1 volts to 1.2 volts. The potential applied to the working electrode could be adjusted remotely during the course of the experiment. The potentiostat was coupled to the microfluidic device with spring-loaded gold contact pins (MILL-MAX, Oyster Bay, NY) connecting the potentiostat to the contact pads fabricated into the working and counter electrodes.

High voltage leads were built into the smaller board, where one lead applied the potential from the EMCO power supply (potential range between 200 and 1800 volts) and two ground leads for the system. Platinum wire was used to make electric contact between the built-in leads and the microfluidic device. The high voltage lead was placed into the buffer reservoir and held at a potential of -1600 V for reverse polarity experiments. The ground leads were placed in the buffer waste and the sample waste. The electrochemical detection cell was a two-electrode system, consisting of a 15 micron wide platinum working electrode placed in the in-channel configuration with an embedded platinum counter electrode.

3.2.4 Sampling, buffer, and injection parameters

All sampling for analyte analysis in the microfluidic device occurred by either direct infusion or microdialysis sampling.[26] For the direct infusion, one end of a 15 cm 1/32 x 0.005 FEP tubing was coupled to the chip using a 1/32 LabSmith port connector. The other was directly attached to the CMA 107 syringe pump (CMA, N. Chelmsford, MA) using tubing connectors. Microdialysis sampling was accomplished using a 30 kDa 1cm BASi loop microdialysis probe (West Lafayette, IN). Each side of the 1cm semipermeable membrane is attached to 16 cm of fluorinated ethylene propylene (FEP) tubing, which was cut to the desired length. The FEP tubing from the probe was connected to the CMA 107 syringe pump; all 16 cm of attached tubing was used from the other end. Approximately 5 cm of the 1/32 x 0.005 FEP tubing was removed and replaced with 5 cm of PEEK tubing with similar dimensions using tubing connectors in order to couple the probe to the chip. The probe was connected to the chip using 1/32 LabSmith connectors and fittings (LabSmith, Livermore, CA).

Before each experiment, a conditioning procedure was performed on the chip in order to produce a uniform charge on the channel side walls and help establish an electrical double layer as previously described.[26] Following the conditioning procedure, the chip was secured in the Pinnacle board chip holder (Pinnacle Technology, Lawrence, KS) as shown in Figure 3.1.

The CMA 107 syringe pump was set at a flow rate of 1 μL min^{-1}. Sample introduction and gating for this microfluidic design was performed as previously described.[23,26] The potential applied across the separation channel was set to -1600 V volts in order to establish a gate and overcome the hydrodynamics induced by the pump

pressure. The high voltage was floated for one second in order to achieve an injection time of one second. A 50 mM phosphate buffer run buffer was used in these studies with reverse polarity separation. Migration time for nitrite to elute took approximately 26 seconds. The separation was allowed to run for 1-2 minutes depending on the experimental design.

The buffer used for the electrophoresis experiments was a 50 mM phosphate buffer at pH 7.4. The buffer was made using 1.55 g L^{-1} monosodium phosphate and 10.38 g L^{-1} disodium phosphate and naturally buffers at pH 7.4. Different perfusates were investigated during the course of this study. The ruggedness experiments were conducted early on during the experimental process and used a 10 mM Borate buffer with 2 mM TTAB. A perfusate of 50 mM phosphate buffer at pH 7.4 was used for the reproducibility experiment along with the production of nitrite from DEA-NONOate. In all other experiments a perfusate of 50 mM phosphate buffer with 119 mM NaCl at pH 7.4 was used.

3.2.5 Ruggedness and reproducibility of the integrated separation based sensor

The ruggedness of the system and its ability to perform while in motion, akin to that of being a *freely roaming* animal, was evaluated. Two motion tests were performed. The first was a cart test in which the system was placed on a rolling cart in motion. The system was set up for the analysis of a 1 mM solution of nitrite and 1 mM peroxide in 10 mM borate with 2 mM TTAB at pH 9.2 as the perfusate. The perfusate was introduced into the microfluidic device using direct injection via a CMA 107 syringe pump at a flow rate of 1 μL min^{-1}. The separation buffer was 10 mM borate with 2mM TTAB at pH 9.2

and a voltage of -1600 volts was applied at the buffer reservoir for the separation. The platinum working electrode was held at 1.1 volt vs. a platinum counter electrode. The second motion test performed used a Stovall Belly Dancer™ Shaker, 220/240VAC (Greensboro, NC) with the system being shaken at various rates of rotation for a series of injections. System analysis was performed under the same conditions as stated previously for the cart test.

To evaluate how reproducible the response of the system was over an extended period of time, a 1 mM solution of nitrite in 50 mM phosphate buffer was used as the perfusate and introduced into the microfluidic device using direct injection via a CMA 107 syringe pump at a flow rate of 1 μL min^{-1} over a 24 hour period. A sample injection was performed every two minutes during the course of the experiment. The separation buffer was 50 mM phosphate at pH 7.4 and a voltage of -1600 volts was applied at the buffer reservoir for the separation. The platinum working electrode was held at 1.1 volt vs. a platinum counter electrode. The buffer in the buffer reservoir, buffer waste, and sample waste were manually replenished using a micropipette every two hours in order to prevent ion depletion from affecting the separation.

3.2.6 *In vitro* evaluation of on-line microdialysis-microchip electrophoresis with electrochemical detection using DEA-NONOate

The production of nitrite from DEA-NONOate was performed using a BASi 1 cm loop microdialysis probe secured inside a two mL reaction vial containing one mL of 50 mM phosphate buffer at pH 10 along with 100 μL of 48 mM DEA-NONOate. The microdialysis perfusate consisted of 50 mM phosphate buffer at pH 7.4. The flow rate

was 1 μL per minute. The solution in the reaction well was prepared at pH 10. To initiate the reaction, the pH in the reaction well was carefully lowered to pH of 7.4 using 0.05M HCl. The separation buffer was 50 mM phosphate at pH 7.4 and a voltage of -1600 volts was applied at the buffer reservoir for the separation. Finally, the platinum working electrode was held at 1.1 volt vs. a platinum counter electrode.

3.2.7 On-line MD-MCE-EC rat studies

Male Sprague-Dawley rats weighing between 300~350 grams were used for these experiments. The rat was induced into a light plane of anesthesia using an isoflurane chamber before being given a ketamine-xylazine-acepromazine cocktail (KXA) via intraperitoneal injection. The animal was prepped by shaving and cleaning a three inch by one inch area on the left dorsal side of the rat midline between the anterior and posterior of the animal. Two 1 cm BASi loop microdialysis probes with a polyacrylonitrile membrane with a 30 kDa molecular weight cutoff (BASinc, West Lafayette, IN) were implanted subcutaneously parallel to each other. One probe was used for direct analysis on with the MD-MCE-EC system with the second probe used for sample collection for off-line analysis on a conventional LC-EC system. The rat was placed on a nose cone to maintain the plane of anesthesia by inhalation of isoflurane using a vaporizer. The nitroglycerin solutions used for these and other animal studies were prepared from a 5 mg/mL stock solution of the drug formulated in an ethanol (30%) and polyethylene glycol (30%) solution (American Regent, Inc., Shirley, NY).

A one hour baseline microdialysis perfusion was performed by using a solution consisting of 50 mM phosphate buffer with 119 mM at pH 7.4 pumped through the probe

at a flow rate of 1 μL per minute. After baseline monitoring, the subcutaneous delivery of nitroglycerin commenced immediately followed by for a two hour sampling period. This was accomplished by switching syringes from the separation buffer to a solution of 50 mM phosphate buffer and 119 mM NaCl containing 4.8 mg mL^{-1} of nitroglycerin. In order to estimate the concentration of nitrite being produced, the system was calibrated off-line using direct perfusion before the animal experiments commenced using standard solutions of nitrite ranging from 2.5 μM to 25 μM prepared in 50 mM phosphate buffer with 119 mM NaCl at pH 7.4.

3.2.8 *In-vivo* analysis in sheep

Female domesticated sheep, donated to the Purdue University College of Veterinary Medicine, were secured in a small calf cart for ease of probe implantation and in order to properly secure the ruffwear "double back" harness (Ruffwear Inc., Bend, OR) and mount the complete analysis system on the animal. The 1 cm BASi loop microdialysis probe implant site was prepped by shaving and cleaning an area on the left dorsal side of the sheep before the harness and system was secured to the animal. Once the system was secured on the animal, the implant site was sterilized and a local anesthetic of Lidocaine HCl 2% usp injection (Bimeda, Oakbrook Terrace, Il) was administered. Two half-inch incisions were made into the skin approximately 3 cm apart, and two separate microdialysis probes were implanted parallel to one another through the incision points. As described above for the rat experiments, one probe was used for on-line analysis and the other was used for sample collection for off-line analysis by LCEC. A one-hour baseline perfusion was first performed using 50 mM phosphate with 119 mM

NaCl at pH 7.4 at a flow rate of 1 μL per minute. Following base line monitoring, the perfusate was changed to a solution containing 4.8 mg mL^{-1} of intravenous nitroglycerin solution for two hours. The perfusion of nitroglycerin was started by switching syringes to a solution of 50 mM phosphate buffer and 119 mM NaCl with 4.8 mg mL^{-1} of nitroglycerin. Dialysate samples were collected every 10 minutes and immediately placed in a -80 freezer. All large animal surgeries were overseen by Dr. Elsa Janle and carried out with help from Crystal Haggen and Pamela Lachick at the Purdue University College of Veterinary Medicine Large Animal Hospital.

3.2.9 Off-line analysis of nitrite using liquid chromatography/electrochemistry

Liquid chromatographic analysis of the off-line samples was accomplished using a Shimadzu® LC-20AD pump operating at a flow rate of 0.4 mL min^{-1}. A Phenomenex® Synergi Hydro-RP 4 μm 80Å 2x150 mm C-18 column was employed and the mobile phase consisted of 1 mM TBAOH and 15 mM H_2SO_4 at a pH of 4.0 for the separation of nitrite. A two microliter Rheodyne® 7725i injection valve was used (IDEX Health & Science, Oak Harbor, WA). Detection was accomplished using a Bioanalytical Sytems Inc. Amperometric Detector Model LC-4C (BASi, West Layfette, IN) with a glassy carbon electrode at an applied potential of +1.025 V vs. a Ag/AgCl reference electrode (BASi West Layfette, IN). A calibration curve from 2.5 μM to 25 μM was obtained prior to analysis for quantitation. This method was developed in the C. Lunte lab by Sean D. Willis and all data, using this method, was obtain thanks to his hard work.

3.3 Results and discussion

The microfluidic devices used in these studies were constructed from soda lime glass using conventional photolithographic procedures.[26] Soda lime glass is softer than the more commonly used borosilicate or quartz glass substrates. It is easily etched and can be bonded at lower temperatures and for shorter durations. Due to the glass being easier to etch, the relatively shallow depth of the electrode patterns (500 nm) were easier to obtain. Bonding at lower temperatures also allows for the electrode to go through the thermal bonding process without destroying the integrity of the electrode material. The chip contained a double T interface that has been has been previously described for coupling microdialysis samples to the microchip electrophoresis system.[23,26] Figure 2.1, as shown in chapter 2, shows the overall chip design including the dimensions and electrode placement. The two electrode electrochemical detection cell consisted of a 15 micron wide platinum working electrode placed in the in-channel configuration with a 100 micron embedded platinum counter electrode.

The chips used in these studies employed gated injection to introduce sample into the separation channel. This type of injection procedure was adapted from Chen *et al*., and has been used with other chip designs previously described by our group.[23,26,30] To briefly explain, a syringe pump was used to deliver the dialysate at 1 μL min^{-1} through the 500 μm wide flow channel at the top of the device. To prevent the sample from prematurely entering into the separation channel, a gate was established by applying a voltage at the buffer reservoir to the buffer and sample waste reservoirs. In these experiments, a voltage of -1600 V was used, which generated enough EOF to overcome the hydrodynamic force being applied by the syringe pump. Injection of the

microdialysis sample into the separation channel was accomplished by floating the high voltage for one second. This temporarily eliminated the EOF and allowed the hydrodynamic pressure to become the dominant force inside the microfluidic device and introduces a discreet plug of sample into the separation channel. The gate is then reestablished by reapplying the high voltage at the buffer reservoir. The injection time defined the sample plug size that is introduced into the separation channel.

The device was tested for ruggedness in anticipation of the environment that the system would encounter when deployed on a *freely roaming* animal. One of the largest concerns for the system was its ability to continually perform while the animal was in motion. A cart test, as seen in Figure 3.2, was performed to evaluate the system under random and vigorous motion to ensure that movement did not interfere with the electrophoretic separation and detection. The cart was pushed at random speeds and decelerated, both over time and immediately, to assess how this type of movement would impact the function of the system. Figure 3.2 shows some increase in noise due to movement and various aberrations. Excessive noise can be attributed to bumping the cart vigorously into hard surfaces and the rapid deceleration due to forced impact with vertical support structures

A more rhythmic motion was also tested to simulate noise caused by locomotion. In an effort to simulate this, a Stovall Belly Dancer™ Shaker was used at various rates of rotation. Figure 3.3 shows a slight increase in base line noise of approximately ±0.6 nA due to the simulation locomotion. However, this increase did not disrupt the electrophoretic separation or the detection of target analytes.

The overall reproducibility of the MD-MCE-EC chip and the gated injection process was evaluated by running the system in the direct infusion mode continuously for 24-hours. The migration times and peak heights for a 1 mM concentration of nitrite were monitored over a 24-hour period with a sample plug injected every two minutes, resulting in 720 consecutive injections of a 1 mM nitrite standard giving a RSD for the peak height of approximately 9.6 percent for the entire 24-hour period.

3.3.1 On-line MD-MCE-EC of nitrite generation by DEA-NONOate

In an effort to test the systems ability to monitor the generation of nitrite production *in-vivo,* and *in-vitro* experiment was performed. This was accomplished through monitoring nitrite production from the acid catalyzed decomposition of DEA-NONOate. At pH values below eight, DEA-NONOate rapidly releases nitric oxide by spontaneous disassociation, which readily oxidizes to the more stable oxidation product, nitrite, in the presence of oxygen.[31] Release was accomplished by lowering the pH from 10 to 7.4 of a vial containing DEA-nanoate and following the production of nitrite as a function of time (Figure 3.4). The series of electropherograms shown started at four minutes after the pH was lowered to 7.4. There was no visible peak for nitrite during the initiation of the reaction. The peak intensity then rapidly increased from a 0.4 nA peak for the first injection as shown in Figure 3.4 to a 1.7 nA peak for the last injection at the nine minute mark. After this time the concentration of nitrite within the sample stabilized and no increase in peak intensity was seen. Figure 3.4 shows the electropherograms for all subsequent injections with the nitrite peak being highlighted.

3.3.2 Optimization of buffer system for *in vivo* analysis

In vivo experiments must be conducted using a perfusate that is compatible with the tissue being sampled to maintain tissue integrity. Therefore the perfusate was modified to minimize disturbance of the native electrolyte levels for the subcutaneous sampling experiments. The subcutaneous sampling perfusate buffer or "pseudo saline" consisted of a 50 mM phosphate buffer with 119 mM NaCl and the separation buffer consisted of 50 mM phosphate buffer at pH 7.4. The perfusate solution could not be used as the run buffer because the additional NaCl increased the conductivity of the buffer leading to extremely high currents and joule heating.

The double t design used for these studies allowed for the use of contrasting conductivity buffers without adversely affecting the gate or injection. In fact, in this application, we found that the addition of NaCl to the perfusate was actually beneficial and produced isotachophoretic stacking of the nitrite to occur, leading to an improvement in the LOD for this analyte. The chloride ions in the perfusate acted as the leading electrolyte while the phosphate ions in the run buffer act as the terminating electrolyte.[32] Figure 3.5 shows the effects of the perfusate composition on the separation and the corresponding peak height for nitrite. The electropherogram for nitrite using a 50 mM phosphate buffer for the perfusate and 50 mM phosphate buffer for the separation is shown in Figure 3.5a. By adding 119 mM NaCl to the perfusate, to create a pseudo saline solution, and keeping the separation buffer the same, a distinctive dip in the baseline (Figure 3.5c) due to the NaCl can be seen. The addition of NaCl also caused an increase in signal intensity for nitrite as shown in Figure 3.5b.

3.3.3 *In-vivo* studies off-animal with rats

Nitroglycerin is a pro-drug that undergoes complex metabolic biotransformation, predominantly in the smooth muscle intracellular space. The exact mechanism by which vasodilation occurs due to nitroglycerin administration is still largely unknown. It is believed that vasodilation is caused by nitric oxide (NO), which is generated from nitroglycerin in the presence of glutathione-S-transferase.[33] Nitric oxide is converted to nitrite in the presence of oxygen *in vivo* and is often used as an indicator of NO production.[34] Intravenous nitroglycerin is readily available in 5 mg mL^{-1} solutions.

For the *in vivo* microdialysis experiments, two-loop microdialysis probes were implanted subcutaneously into the epidermal tissue. One probe was coupled directly into the MD-MCE-EC system and the other probe was used for sample collection for later analysis by LC-EC. The probes were placed parallel to each other approximately 1-5 cm apart in an effort to reduce error from variability in the implant sites. This method allowed for a direct comparison of nitrite production in the animal without having to compensate for the error induced from animal to animal variability. Baseline collection was performed for one hour before the drug was administered in order to stimulate nitrite production for the following two hours.

To be sure the system would work for *in vivo* measurements, the system was first evaluated off-animal with rats. The results are shown in Figure 3.6. The first 60 minutes of the plot correspond to baseline levels of nitrite obtained using a perfusate of 50 mM phosphate buffer with 119 mM NaCl. After one hour, the composition of the perfusate was changed to 4.8 mg mL^{-1} nitroglycerin with 50 mM phosphate buffer, and 119 mM NaCl causing the appearance of nitrite. Figure 3.6b is the electropherogram showing part

of the data from a series of injections with the nitrite peak being highlighted. Figure 3.7a shows the production of nitrite over time following the delivery of nitroglycerin through the microdialysis probe. Figure 3.7b highlights an area from the blank obtained during the first 60 minutes obtained using the background perfusate. While Figure 3.7c shows an electropherogram obtained after one hour of delivery of nitroglycerin through the probe.

A comparison of the results obtained using the on-line system and off-line analysis (using LC-EC) for one of the rats are shown in Figure 3.8. Since the off-line analysis gives the average concentration of nitrite over the 10 minute sampling period, this data is depicted as a bar graph. In contrast, the on-line system gives a single point measurement every two minutes so this data is represented as points on the graph. It can be seen by Figure 3.8 that there is an increase in lag time for the on-line system compared to the off-line due to the additional tubing length required to couple the microdialysis probe implanted in the rat to the microfluidic device. A calibration curve was made using direct infusion of nitrite from the syringe pump. The calibration curve was made using five concentrations ranging between 2.5 μM to 50 μM giving and R^2 value of 0.98. The recovery of the microdialysis probe was determined using LC-EC give a relative recovery of 78 percent.

3.3.4 On-animal experiments using sheep

Sheep are the ideal model for the study of miniaturized MD-MCE-EC system (Figure 3.9) because of their size, general docile personality and the fact that they have been used previously for behavioral studies using microdialysis.[27,28] It is also a

species that recovers well from general anesthesia and surgery. In these experiments, the complete on-line microdialysis-microchip electrophoresis system was attached to a harness that secures the system to the sheep. The working system including all electronics and the microdialysis pump were secured within the box that attached to the harness. Two laptop batteries were used to run the system and were easily secured underneath the box to straps sewn into the harness. Figure 3.9 depicts a complete and running telemetry system with data being collected via Bluetooth®. Duplicate experiments matching those completed on the rat model were performed on the sheep. The only noticeable difference in the experimental design for the sheep animal model was that the sheep was awake and not anesthetized during the course of the experiment. Although the sheep were not completely *freely roaming* throughout the experiments, later data was collected while the sheep were *freely roaming* and in contact with other sheep.

Figure 3.10a shows the peak height for nitrite for each injection made during the experiment using the MD-MCE-EC. Figure 3.10b shows a highlighted area of the electropherogram from multiple injections with the nitrite peak being highlighted. As with the rat studies, the results obtained on-animal using the MD-MCE-EC system were compared to those obtained using another probe on the animal and off-line analysis (Figure 3.11). Using LC-EC, nitrite concentrations were measured starting at the ten minute mark of the base line perfusion. An increase in nitrite levels was seen after nitroglycerin perfusion had started at the 60 minute with a peak concentration intensity at approximately 100 minutes. After the peak nitrite response was observed, a slight decrease occurred for the remainder of the experiment.

The identity of nitrite was confirmed off-line by spiking collected sample with a nitrite standard and testing it using LC-EC. In these experiments, the concentration of nitrite peaked at approximately 17 μM, taking recovery into account (Figure 3.11). An increase in nitrite concentration within the first vial collection from the start of nitroglycerin perfusion was expected. A significant lag time of 50 minutes prior to an increase in response was observed with the MD-MCE-EC system. This lag time was calculated using the distance between the microdialysis probe and the system as well as the dimensions of tubing required. A lag time of five minutes prior to an increase in response was observed with the LC-EC system. This lag time was calculated using the distance between the microdialysis probe and the collection vial as well as the dimensions of tubing required.

The comparison between the MD-MCE-EC system with the LC-EC in Figure 3.11 demonstrates the on-line capabilities of the system. Using the MD-MCE-EC system decreased analysis time and allowed for the interpretation of the data in near real-time. The sample was directly collected via microdialysis and analysed in near real time all while they system was tethered to the back of the animal and all data was wirelessly streamed to a PC interface for immediate interpretation. The system was able to collect and analyze data from *in vivo* monitoring every two minutes with immediately interpretable data. In comparison, in the LC-EC system 10 μL samples were collected via microdialysis and stored for later collection. At a flow rate of 1 μL min^{-1} flow rates, this produced one sample for analysis every ten minutes. The data shown in Figure 3.11 for the LC-EC system is therefore an average concentration for the entire ten-minute

sampling time, where as the MD-MCE-EC system produces a data point every two minutes.

The device as shown in Figure 3.9 was tested on an untethered and unrestrained freely moving sheep. During these evaluations the sheep was allowed to interact in a pen with two other sheep while communication with the device was being maintained via blue tooth. The functionality of the device was monitored for a short duration in which the animal was *freely roaming*. Communication was maintained with the device and the system could be manipulated via telemetry while the animal was unrestrained. Only the system functionality and the ability to maintain communication via telemetry was tested during this time due to experimental concerns for the functionality and well-being of the prototype hardware.

3.4 Conclusion

In this work, the development of a miniaturized on-animal separation-based sensor using microdialysis sampling and electrochemical detection on a microfluidic platform is described. The complete system utilized a miniaturized high voltage power supply and potentiostat. The microfluidic microchip could be integrated into the device, and the whole system was controlled wirelessly. In these studies the overall functionality of the device was tested in an effort to demonstrate it's capability as an on-animal-based sensor. The ultimate goal is to apply this methodology to monitor neurotransmitters of *freely roaming* sheep and correlate concentration with behavior.

3.5 References:

[1] Heal, D. J., Smith, S. L., Gosden, J. & Nutt, D. J. Amphetamine, past and present--a pharmacological and clinical perspective. *J. Psychopharmacol. (Oxford)* **27,** 479–496 (2013).

[2] Heidbreder, C. Rationale in support of the use of selective dopamine D receptor antagonists for the pharmacotherapeutic management of substance use disorders. *Naunyn Schmiedebergs Arch. Pharmacol.* **386,** 167–176 (2013).

[3] Uppal, A., Singh, A., Gahtori, P., Ghosh, S. K. & Ahmad, M. Z. Antidepressants: current strategies and future opportunities. *Curr. Pharm. Des.* **16,** 4243–4253 (2010).

[4] Gunja, N. In the Zzz zone: the effects of Z-drugs on human performance and driving. *J Med Toxicol* **9,** 163–171 (2013).

[5] Wilson, G. S. & Johnson, M. A. In-vivo electrochemistry: what can we learn about living systems? *Chem. Rev.* **108,** 2462–2481 (2008).

[6] Takmakov, P., McKinney, C. J., Carelli, R. M. & Wightman, R. M. Instrumentation for fast-scan cyclic voltammetry combined with electrophysiology for behavioral experiments in freely moving animals. *Rev Sci Instrum* **82,** 074302 (2011).

[7] Cooley, J. C., Ducey, M.W., Regel, A.R., Nandi, P. Lunte, S.M., Lunte, C.E. in *Microdialysis in Drug Development* **4,** 35–66 (Springer New York, 2012).

[8] Nandi, P., Kuhnline, C. D. & Lunte, S. M. Analytical considerations for microdalysis sampling - *Applications of Microdialysis in Pharmaceutical Science* 39-92 (2011).

[9] Nandi, P. & Lunte, S. M. Recent trends in microdialysis sampling integrated with conventional and microanalytical systems for monitoring biological events: a review. *Anal. Chim. Acta* **651,** 1–14 (2009).

[10] Kennedy, R. T. Emerging trends in in vivo neurochemical monitoring by microdialysis. *Current Opinion in Chemical Biology* **17,** 860–867 (2013).

[11] Huff, J. K. & Davies, M. I. Microdialysis monitoring of methylphenidate in blood and brain correlated with changes in dopamine and rat activity. *Journal of Pharmaceutical and Biomedical Analysis* **29,** 767–777 (2002).

[12] Cooper, J. D., Heppert, K. E., Davies, M. I. & Lunte, S. M. Evaluation of an osmotic pump for microdialysis sampling in an awake and untethered rat. *Journal of Neuroscience Methods* **160,** 269–275 (2007).

[13] Wang, M., Slaney, T., Mabrouk, O. & Kennedy, R. T. Collection of nanoliter microdialysate fractions in plugs for off-line in vivo chemical monitoring with up to 2s temporal resolution. *Journal of Neuroscience Methods* **190,** 39–48 (2010).

[14] Bowser, M. T. & Kennedy, R. T. In vivomonitoring of amine neurotransmitters using microdialysis with on-line capillary electrophoresis. *Electrophoresis* **22,** 3668–3676 (2001).

[15] Hogan, B. L., Lunte, S. M., Stobaugh, J. F. & Lunte, C. E. Online coupling of in vivo microdialysis sampling with capillary electrophoresis. *Anal. Chem.* **66,** 596–602 (1994).

[16] Huynh, B. H., Fogarty, B. A., Martin, R. S. & Lunte, S. M. On-Line Coupling of Microdialysis Sampling with Microchip-Based Capillary Electrophoresis. *Anal. Chem.* **76,** 6440–6447 (2004).

[17] Li, M. W., Huynh, B. H., Hulvey, M. K., Lunte, S. M. & Martin, R. S. Design and Characterization of Poly(dimethylsiloxane)-Based Valves for Interfacing Continuous-Flow Sampling to Microchip Electrophoresis. *Anal. Chem.* **78,** 1042–1051 (2006).

[18] Mecker, L. C. & Martin, R. S. Coupling Microdialysis Sampling to Microchip Electrophoresis in a Reversibly Sealed Device. *Journal of the Association for Laboratory Automation* **12,** 296–302 (2007).

[19] Mecker, L. C. & Martin, R. S. Integration of microdialysis sampling and microchip electrophoresis with electrochemical detection. *Anal. Chem.* **80,** 9257–9264 (2008).

[20] Huynh, B. H., Fogarty, B. A., Nandi, P. & Lunte, S. M. A microchip electrophoresis device with on-line microdialysis sampling and on-chip sample derivatization by naphthalene 2, 3-dicarboxaldehyde/2-mercaptoethanol *Journal of Pharmaceutical and Biomedical Analysis* **42,** 529–534 (2006).

[21] Sandlin, Z. D., Shou, M., Shackman, J. G. & Kennedy, R. T. Microfluidic Electrophoresis Chip Coupled to Microdialysis for in Vivo Monitoring of Amino Acid Neurotransmitters. *Anal. Chem.* **77,** 7702–7708 (2005).

[22] Cellar, N. A., Burns, S. T., Meiners, J.-C., Chen, H. & Kennedy, R. T. Microfluidic chip for low-flow push-pull perfusion sampling in vivo with on-Line analysis of amino acids. *Anal. Chem.* **77,** 7067–7073 (2005).

[23] Nandi, P., Scott, D. E., Desai, D. & Lunte, S. M. Development and optimization of an integrated PDMS based-microdialysis microchip electrophoresis device with

on-chip derivatization for continuous monitoring of primary amines. *Electrophoresis* **6**, 895-902 (2013).

[24] Zhou, J., Heckert, D. M., Zuo, H., Lunte, C. E. & Lunte, S. M. On-line coupling of in vivo microdialysis with capillary electrophoresis/electrochemistry. *Anal. Chim. Acta* **379,** 307–317 (1999).

[25] Martin, R. S., Ratzlaff, K. L., Huynh, B. H. & Lunte, S. M. In-Channel Electrochemical Detection for Microchip Capillary Electrophoresis Using an Electrically Isolated Potentiostat. *Anal. Chem.* **74,** 1136–1143 (2002).

[26] Scott, D. E., Grigsby, R. J. & Lunte, S. M. Microdialysis sampling coupled to microchip electrophoresis with integrated amperometric detection on an all-glass substrate. *Chemphyschem* **14,** 2288–2294 (2013).

[27] Westerink, B. H. C. Brain microdialysis and its application for the study of animal behaviour. *Behav. Brain Res.* **70,** 103–124 (1995).

[28] Kendrick, K. M. Microdialysis in large unrestrained animals : neuroendocrine and behavioural studies of acetylcholine, amino acid, monoamine and neuropeptide release in the sheep. *Techniques in the behavioral and neural sciences* **7,** 327–348 (1991).

[29] Allen, P. B. & Chiu, D. T. Calcium-assisted glass-to-glass bonding for fabrication of glass microfluidic devices. *Anal. Chem.* **80,** 7153–7157 (2008).

[30] Lin, Y. H., Lee, G. B., Li, C. W., Huang, G. R. & Chen, S. H. Flow-through sampling for electrophoresis-based microfluidic chips using hydrodynamic pumping. *Journal of Chromatography A* **937,** 115–125 (2001).

[31] Mainz, E. R. *et al.* Monitoring intracellular nitric oxide production using microchip electrophoresis and laser-induced fluorescence detection. *Anal. Methods* **4,** 414 (2012).

[32] Weinberger, R. Practical Capillary Electrophoresis (2nd Ed.) Weinberger Robert: Librairie Lavoisier. 25-208 (1993).

[33] Kurz, M.A., Boyer, T.D., Whalen, R., Peterson, T.E., Harrison, D.G. Nitroglycerin metabolism in vascular tissue: role of glutathione S-transferases and relationship between NO and NO2- formation. *Biochem J* **292**, 545-550 (1993).

[34] Ignarro, L. J. After 130 years, the molecular mechanism of action of nitroglycerin is revealed. *Proc. Natl. Acad. Sci. U.S.A.* **99,** 7816–7817 (2002).

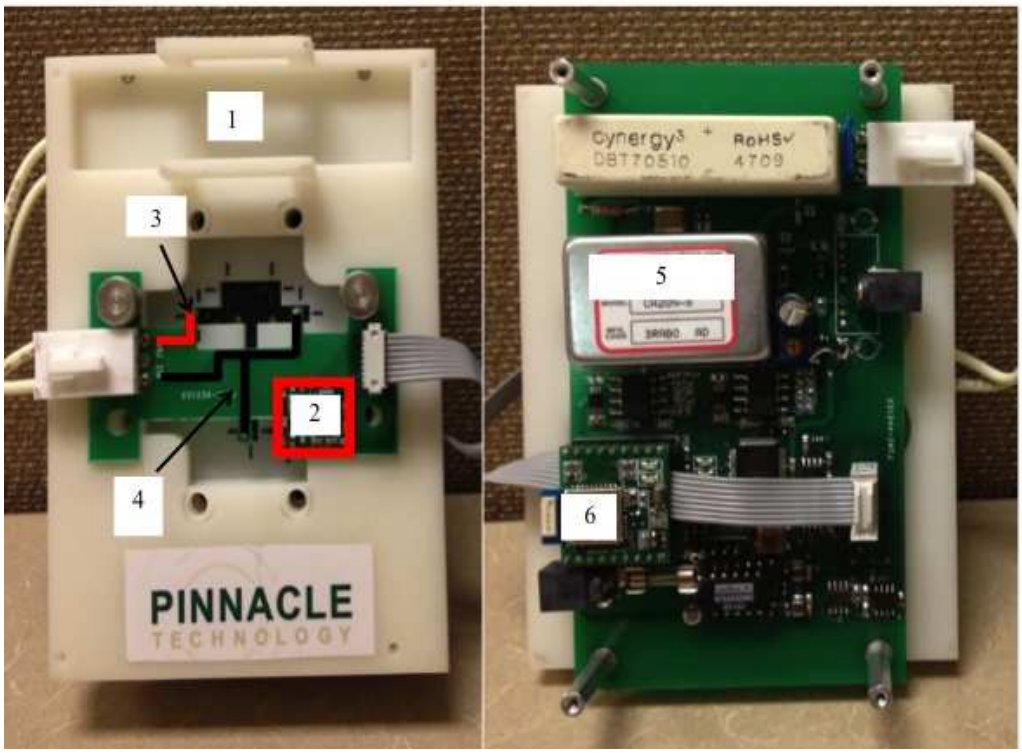

Figure 3.1. On-animal separation based sensor. The photo shows: (1) a holder for chip and microdialysis pump that also serves as a mount for all major electrical components, (2) electrically isolated potentiostat, (3) high voltage lead highlighted in red, (4) ground connectors highlighted in black, (5) high voltage power supply, and (6) Bluetooth® module

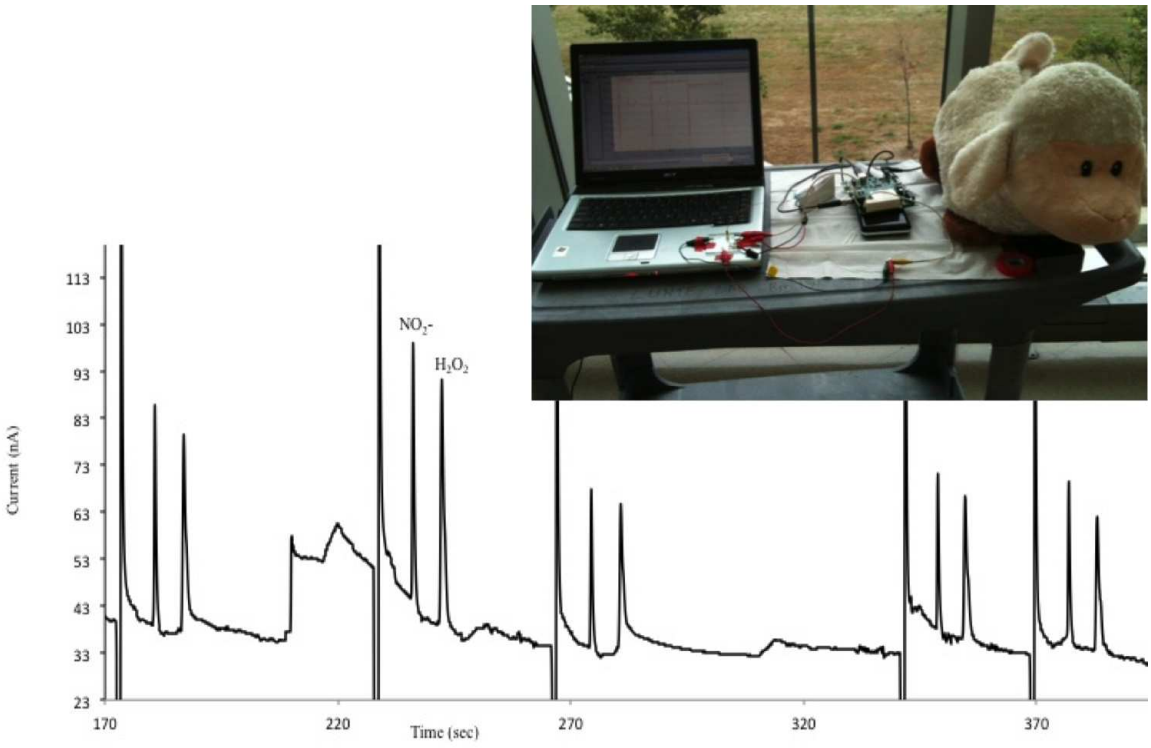

Figure 3.2. A "cart test" for the analysis on the effects of rapid and vigorous motion. Perfusate contained 1 mM nitrite with 1 mM peroxide in 10 mM boric acid buffer with 2 mM TTAB. Separation buffer: 10 mM boric acid with 2 mM TTAB. Separation voltage was -1600 V with a 1 second injection and the electrode bias set to 1.1 V with platinum reference. Pump flow rate was set at 1 μL min^{-1}.

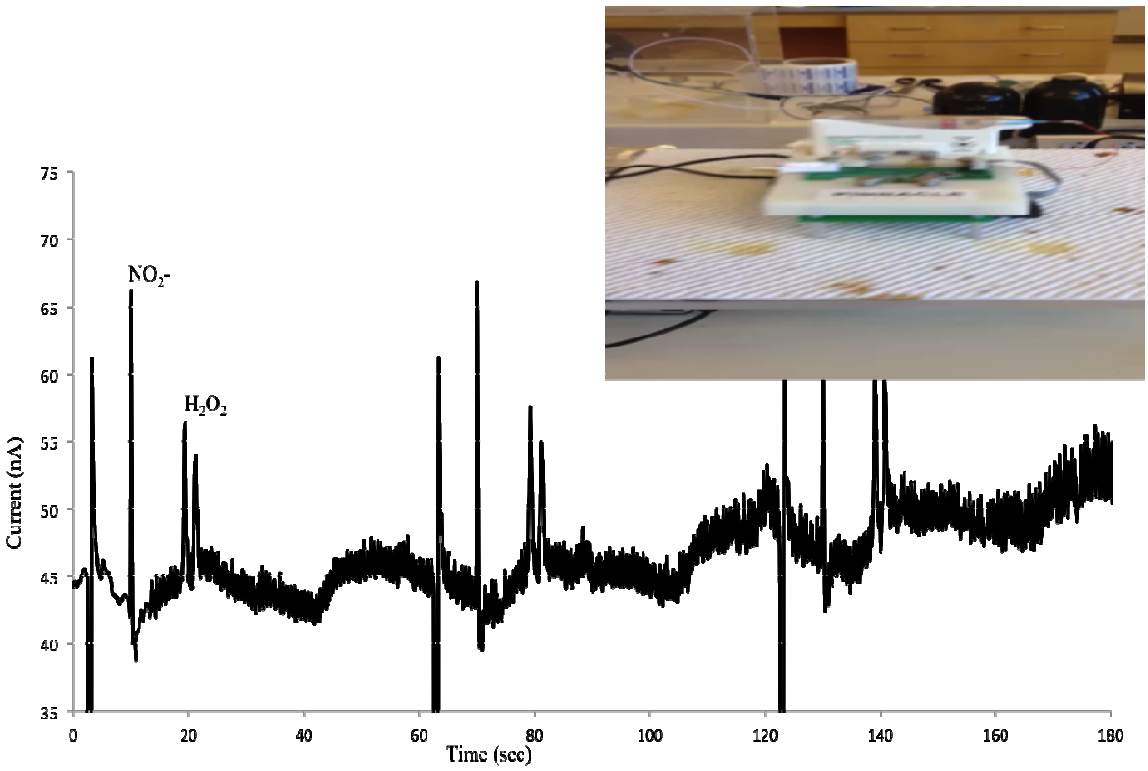

Figure 3.3. A Stovall Belly Dancer™ Shaker, 220/240VAC with the system being shaken at various rates of rotation for analysis of the effects on system performance due to motion. Operating conditions are identical to Figure 3.2

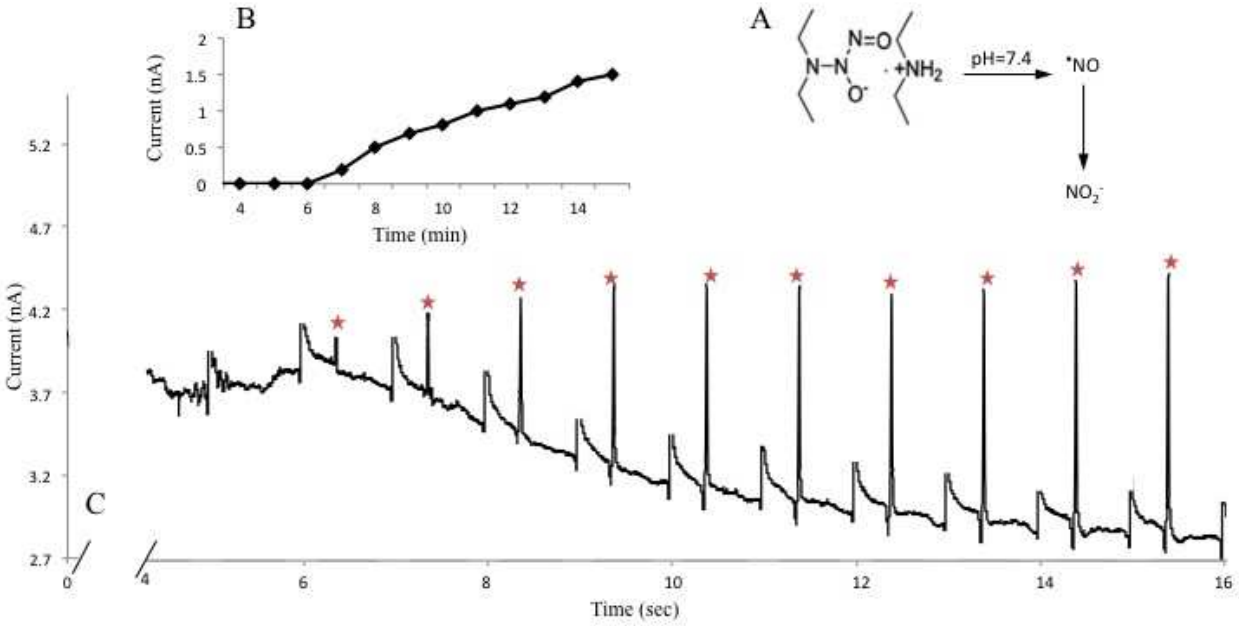

Figure 3.4. Monitoring nitrite production by DEA NONOate. A 2 mL reaction well containing the microdialysis probe contained 1 mL of 50 mM phosphate buffer at pH 10 and 100 uL of 48 mM DEA NONOate. HCl was added to the reaction well to reach pH 7.4 and stimulate nitrite production. Separation buffer and perfusate: 50 mM phosphate buffer at pH 7.4. Flow rate was 1 μL min^{-1}. (A) DEA NONOate reaction (B) Electropherogram of nitrite production over time t=0 is 4 minutes after start of reaction (C) Peak height vs. time for nitrite is shown using MD-MCE system.

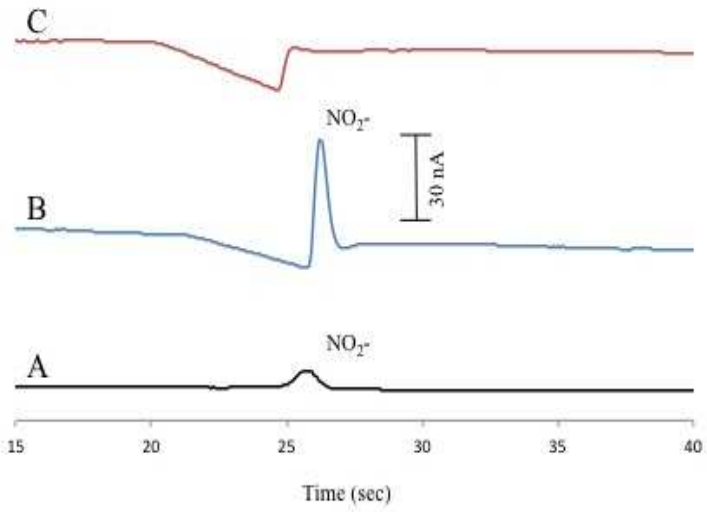

Figure 3.5. Effect of perfusate composition on response for 1 mM nitrite. (A) 50 mM phosphate buffer (B) 50 mM phosphate buffer containing 119 mM NaCl. (C) Blank using a perfusate of 50 mM phosphate buffer and 119 mM NaCl. Separation buffer: 50 mM phosphate at pH 7.4. Separation voltage was -1600 V with a 1 second injection and the electrode bias set to 1.1 V with platinum counter. Pump flow rate was set at 1 μL min^{-1}.

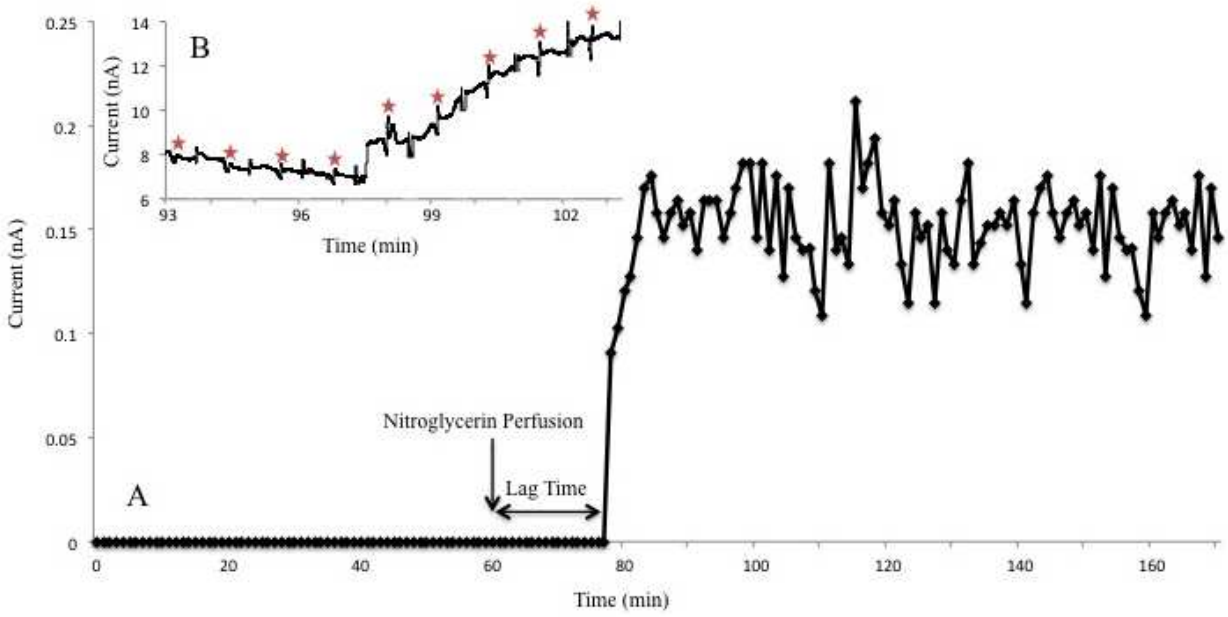

Figure 3.6. Production of nitrite in the rat from a subcutaneous perfusion of nitroglycerin through a loop microdialysis probe. (A) Peak height for nitrite for each injection made during the experiment. The first 60 minutes was from a perfusion of 50 mM phosphate buffer with 119 mM NaCl. After one hour 4.8 mg mL^{-1} nitroglycerin with 50 mM phosphate buffer and 119 mM NaCl was perfused through the microdialysis probe. (B) Data from multiple injections with the nitrite peak are shown highlighted. Operating conditions are identical to Figure 3.4.

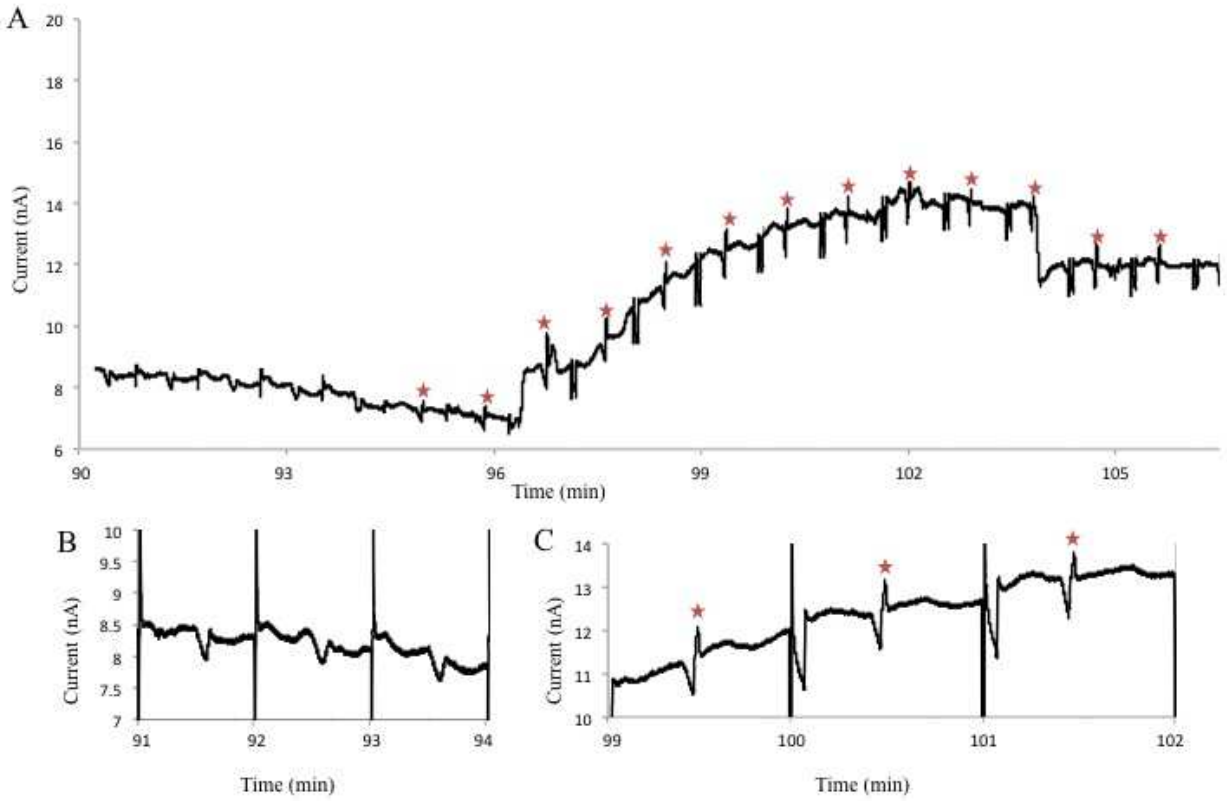

Figure 3.7. Subcutaneous nitrite production obtained from a microdialysis probe implanted in a rat with the delivery of nitroglycerin through the microdialysis probe. (a) Electropherograms acquired from MD-MCE-EC for production of nitrite over time (b) Blank obtained during the first 60 min obtained using a perfusate of of 50 mM phosphate buffer with 119 mM NaCl. (c) Continuous sampling obtained after one hour, perfusion of 4.8 mg mL^{-1} nitroglycerin with 50 mM phosphate buffer and 119 mM NaCl perfused through the microdialysis probe. Operating conditions are identical to Figure 3.4.

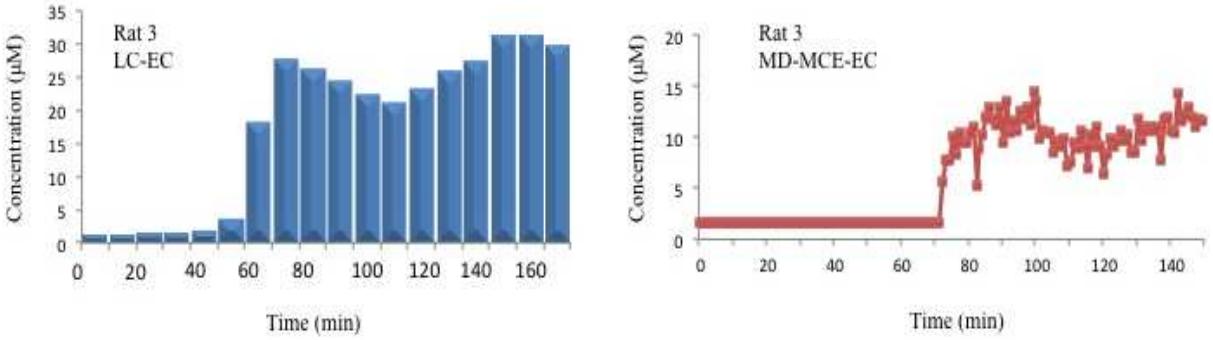

Figure 3.8. Production of nitrite in the rat, due to the subcutaneous perfusion of nitroglycerin through the microdialysis probe. Three separate rats were used and corresponding data is shown for one set of experiments. The bar graphs depict the data obtained via off-line sampling and LC-EC. Samples were collected every ten minutes from a microdialysis probe with a flow of 1 μL min^{-1}. The peak height for each sample collected is shown. The line graphs depict data obtained in near real-time using the MD-MCE-EC system. Increase in lag time for the MD-MCE-EC system is due to additional tubing length required for tubing connectors. The experimental conditions are identical to Figure 3.5. The operating conditions are identical to Figure 3.4.

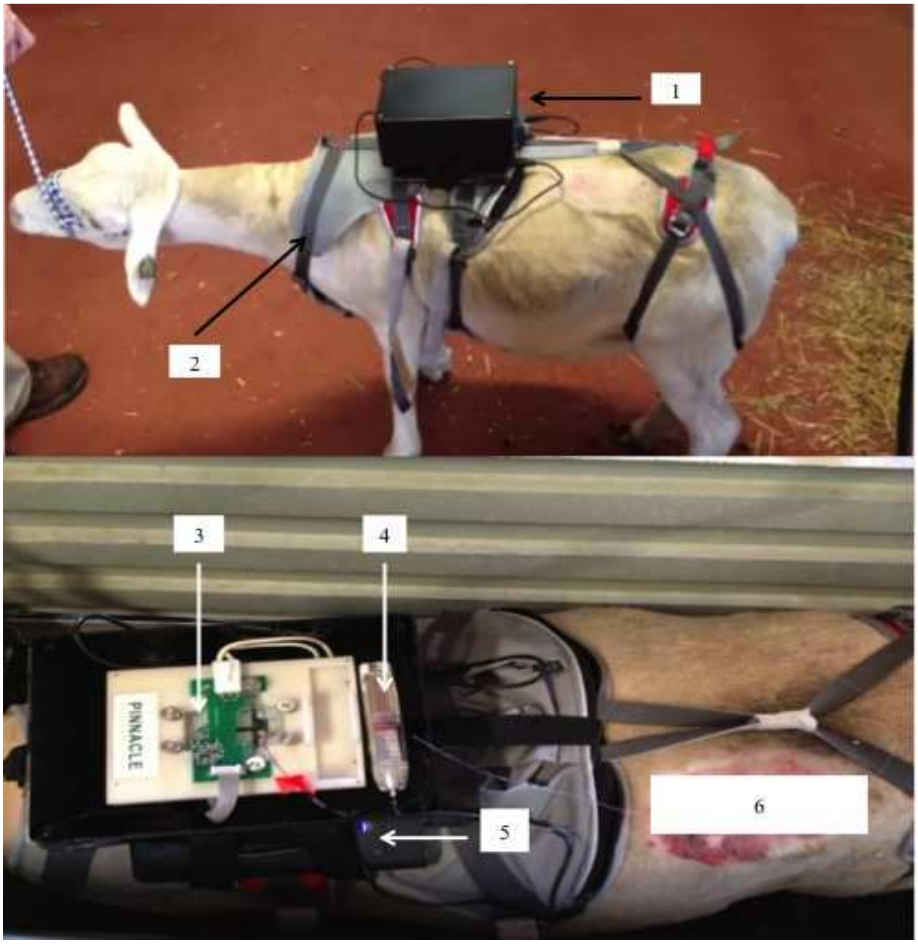

Figure 3.9. Miniaturized MD-MCE-EC system is labeled as follows: (1) Complete MD-MCE-EC system mounted on animal. (2) Harness secures system to the animal. (3) Sensor components secured within the box and attached to the harness. (4) Syringe pump secured to the chip holder. (5) Laptop batteries (6) Microdialysis probe implant site. This figure depicts a fully functioning and operational telemetry system with data being collected via Bluetooth®.

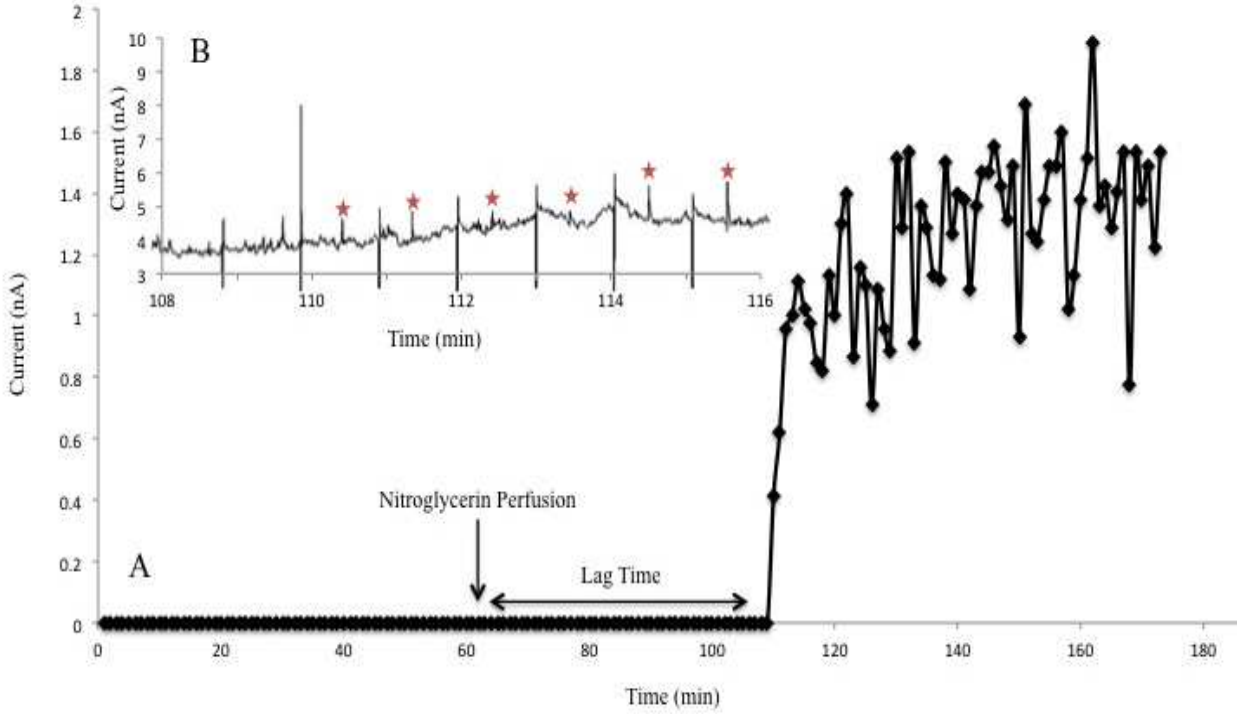

Figure 3.10. Production of nitrite in the sheep due to the subcutaneous perfusion of nitroglycerin through the microdialysis probe. (A) Peak height is shown as a function of time for nitrite during the experiment. The first 60 minutes is from a perfusion of 50 mM phosphate buffer with 119 mM NaCl. After one hour 4.8 mg mL^{-1} nitroglycerin with 50 mM phosphate buffer and 119 mM NaCl was perfused through the microdialysis probe. (B) Data from multiple injections with the nitrite peak is highlighted. Operating conditions are identical to Figure 3.4.

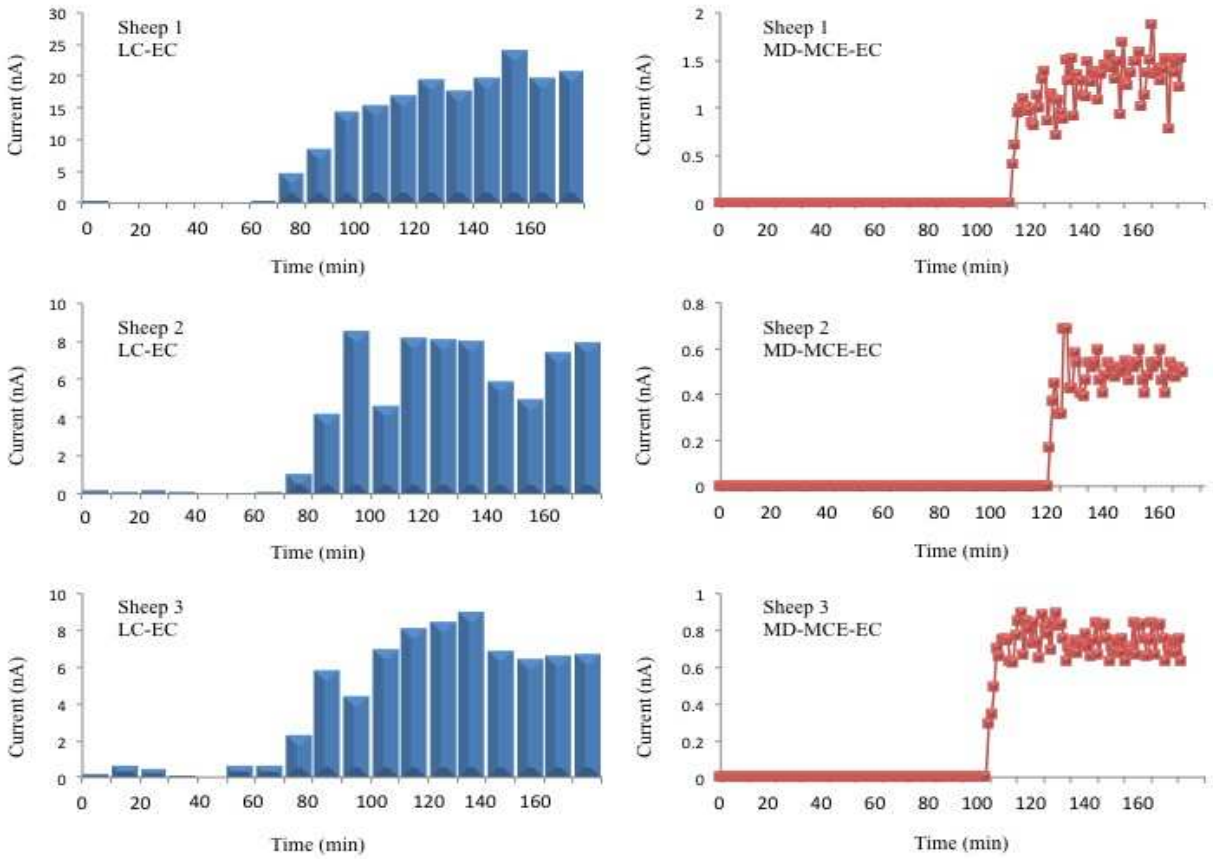

Figure 3.11. These graphs chart the production of nitrite in sheep due to the subcutaneous perfusion of nitroglycerin through the microdialysis probe. Three separate sheep were used and their corresponding data is shown. The bar graphs depict the data obtained via off-line sampling and LC-EC. Samples were collected every ten minutes from a microdialysis probe with a flow of 1 μL min^{-1}. The peak height for each sample collected is shown. The line graphs depict data obtained in near real-time using the MD-MCE-EC system. Increase in lag time for the MD-MCE-EC system is due to additional tubing length required for tubing connectors. The experimental conditions are identical to Figure 3.10. The operating conditions are identical to Figure 3.4.

Chapter 4

Development and Optimization of an All Glass Microdialysis Microchip Electrophoresis Device with On-Chip Derivatization and Simultaneous Fluorescence and Amperometric Detection (MD-MCE-EC-LIF)

4.1. Introduction

Lab-on-chip technologies have become popular over the past twenty years and have been adapted to almost all facets of analytical chemistry.[1] These devices emphasize integration and functionality.[2] Due to their flexibility, portability, rapid prototyping capability, and ability to integrate detection into the device, the lab-on-chip systems have become attractive platforms for DNA sequencing, single cell analysis, environmental sensors and point-of-care devices.[3-7] One of the most powerful assets of lab-on-chip technology is the ability to integrate multiple processes on a single device. The most common processes implemented on these devices includes sample handling, filtering, mixing, separation, and analysis.[8] This chapter describes the development of a microchip electrophoresis device using microdialysis sampling with on-chip sample derivatization and dual detection via electrochemical and laser-induced fluorescence.

Micro-mixers can be classified into two categories, passive and active.[9] The microfluidic devices described in this chapter used a passive micro-mixer, which means the mixer relies on the hydrodynamic flow to manipulate the fluid and the channel design to induce mixing.[10] Passive mixers are designed with channel geometries that increase the total surface area and break up the laminar flow of the fluid in order to induce turbulent flow by decreasing the path of diffusion in the mixing channel.[11] The micromixer used in this dissertation was adapted from a design previously reported by the Lunte research group and relies on mass transport to provide diffusion with turbulent flow.[12,9] The micromixer was specifically designed and optimized to continuously mix the reagents for the optimal derivatization time before entering into a separation channel. Pradyot Nandi previously did this optimization work for the micromixer and the

flow rates at which it was operated.

Detectors are chosen based on their selectivity for the target molecules of interest. Because of this, the choice of a detection method introduces limitations to the applications of the chip by excluding compounds from the detection scheme that do not exhibit the properties of interest.[13] The use of two orthogonal detection schemes can be used to improve analysis and characterization of complex sample matrixes.[14] This is especially true for *in vivo* microdialysis sampling, where the probe is implanted into complex environments and the uptake of multiple compounds possessing different chemical and physical properties is possible.[15] Laser-induced fluorescence (LIF) is the most widely used method of detection for microfluidic devices because of its high sensitivity.[14] Using fluorescent tags or derivatizing agents for specific labeling of analytes of interest is easily integrated into microfluidic devices and aids in making LIF a popular method of detection.

On-chip derivatization schemes for LIF detection have been commonly used for the detection of analytes in microdialysis-microchip electrophoresis systems.[16-18] Coupling MCE with combined LIF and EC detection has been previously reported by Lapos *et al*.[14] In the Lapos paper, several 4-chloro-7- nitrobenzofurazan (NBD) labeled amino acids and electrochemical active analytes including dopamine and catechol were detected. The detection signals for these analytes were generated simultaneously and the peaks for the analytes did not overlap in the two electropherograms produced.

In the research presented here, EC and LIF detection was also performed simultaneously. To the best of my knowledge, this is the first report of coupling

microdialysis sampling to MCE with LIF and EC detection with in-channel sample derivatization. The method is selective and has the potential to be sensitive, which makes it possible to detect multiple analytes in a microdialysis sample with different chemical and physical properties to be exploited for sample detection.

4.2. Materials and Methods

4.2.1. Reagents and Materials

Sodium dodecyl sulfate (SDS), arginine, glycine, GABA, glutamic acid, aspartic acid, and taurine were all purchased from Sigma-Aldrich (St. Louis, MO). Boric acid, 49% hydrofluoric acid, hydrochloric acid, hydrogen peroxide, nitric acid, methanol, isopropyl alcohol and acetone were received from Fisher Scientific (Pittsburgh, PA). Naphthalene 2,3 dicarboxaldehyde (NDA) was received from Molecular Probes (Eugene, OR). Solutions were prepared in deionized water (18 MΩ) using a Millipore A10 system (Billerica, MA) and filtered using 0.22 μm Cameo teflon syringe cartridges from Osmonics (Minnetonka, MN). Chrome and AZ1518 photoresist-coated borosilicate glass blanks were obtained from Telic Co. (Valencia, CA). AZ® 300 MIF developer was purchased from Capitol Scientific, Inc. (Austin, TX). Chrome etchant (CR-7S) was purchased from Cyantek Corp. (Freemont, CA). Platinum (Pt) and titanium (Ti) sputtering targets were purchased from the Kurt J. Lesker Company (Jefferson Hills, PA). Colloidal silver was purchased from Ted Pella, Inc. (Redding, CA). PEEK tubing was purchased from IDEX Health & Science (Oak Harbor, WA). DL-1 loop microdialysis probes were purchased from BAS, Inc. (West Lafayette, IN).

4.2.2. Microchip Fabrication

All microfluidic devices were fabricated in house using borosilicate glass from Telic Co. (Valencia, CA) and utilizing standard photolithographic techniques as previously described.[19] Two designs for the all-glass microchip electrophoresis device were used during the course of this study as described below (gated serpentine chip and flow-gated derivatization chip).

Separation optimization studies were carried out using the gated serpentine design with a 14 cm serpentine channel as shown in Figure 4.1–A. For the on-line derivatization and MCE with LIF and EC detection, an all-glass microdialysis-microchip electrophoresis device with on-chip mixer and a 14 cm serpentine separation channel modeled after a previously published design was used.[12] The embedded platinum working and reference electrode were integrated onto the microfluidic device as previously described in chapter two.[12] The chip configuration and schematic are shown in Figure 4.1-B.

The microfluidic channels, derivatization channels, and integrated electrode designs were drawn using AutoCAD software (Autodesk, San Rafael, CA). The borosilicate glass blanks were photolithographically patterned using an I-line UV flood source and developed in AZ® 300 MIF. Microfluidic buffer and waste wells as well as access holes for sample perfusion were drilled prior to etching using a diamond drill bit (TrueBite, Inc., Vestal, NY) mounted in a Dremel® drill press. The plates containing the channels were then etched at a rate of 1 µm min^{-1} using a 20:14:66 hydrofluoric acid (HF) solution (49% hydrofluoric acid: concentrated nitric acid: water). Producing

microfluidic channels that were 15 μm in depth. The etched plates were placed in an acetone bath to remove the remaining photoresist. The protective chromium mask was then removed using CR-7S etchant.

The embedded platinum electrodes were patterned and developed using the same photolithographic methods as previously described.[19] The patterned glass plates were etched with HF to produce a trench with a depth of approximately 500 nm. The glass plates were then exposed to oxygen plasma for five minutes (March Plasmod, Concord, CA) in an effort to promote proper surface chemistry for metal adhesion to the etched glass surface. Following the plasma treatment, the glass plates were placed into an AXXIS DC magnetron sputtering system (Kurt J. Lesker Co.) and pumped down to a base pressure of 5.0×10^{-7} Torr. A 40 nm adhesion layer of titanium was deposited first, followed by a 460 nm layer of platinum metal. This process resulted in a glass plate with embedded Pt electrodes, as can be seen in Figure 4.1-B.

All devices used in this study were bonded using calcium-assisted bonding as described by Chiu *et al.*, followed by full thermal bonding. For the calcium-assisted bonding step, the substrate surfaces were washed with a 5% Alconox™ solution. The substrates were then washed again in a 5% Alconox™ /5% calcium acetate solution and each plate was gently rubbed together for approximately 2 minutes. This wash step was repeated three times. The electrodes and the microfluidic channels were then roughly aligned by hand under running water and the chip was visually inspected to ensure that no air bubbles were present between the glass plates. The plates were then more precisely aligned under a microscope. The two glass plates were then clamped using binder clips and placed in a low temperature oven (Lindberg/Blue-M, SPX Thermal

Product Solutions, Riverside, MI) at 65 °C for one hour. After one hour the temperature was increased to 110 °C for a minimum of two hours and up to 96 hours in order to promote a significantly higher success rate for full thermal bonding.

To complete the bonding process for the microfluidic device, the assembled chip was placed on top of a ceramic tile in a programmable muffle furnace (750 Series, Fisher Scientific) for thermal bonding. Thermal bonding was accomplished using a temperature ramping protocol that was specifically designed to reduce stress and strain, while maintaining the optical integrity of the borosilicate glass. The furnace temperature was ramped from 25 °C to 300 °C at 1.5 °C min^{-1} and held at 300 °C temperature for two hours. The oven was then ramped to 610 °C at a rate of 1.5 °C min^{-1}. The temperature was held at 610 °C for eight hours and then cooled at 1.5 °C min^{-1} to 300 °C, to bring the glass temperature well below the strain point, then cooled at 5 °C min^{-1} to room temperature of 25 °C. The use of a slow ramp rate (1.5 °C min^{-1}) helped to minimize stress on the glass during the bonding process. Ramping the temperature too fast will induce strain on the glass and will fracture the chips. Increasing the temperature above 610 °C softens the glass too much; at this temperature the bottom plate can take on any patterns left on the ceramic tile, thus reducing the optical integrity of the device for LIF detection.

After the glass plates were bonded, port connectors and fittings were attached to the chip over one of the access holes for the microdialysis sampling channel using LS EPOXY two-part adhesive (Labsmith, Livermore, CA). Copper wires were also connected to the platinum reference and working electrodes through the access holes using colloidal silver.

4.3 Microchip electrophoresis experiments

4.3.1 Detection

4.3.1.1 LIF detection: The LIF detection system has been previously described[12] and consists of an inverted Nikon Ti-2000 series epi-fluorescent microscope (Nikon Instruments Inc., Melville, NY) equipped with a photo multiplier tube (PMT) (Hamamatsu, Bridgewater, NJ, USA) operated at 1.1 kV. Data was collected using LabVIEW software (National Instruments, Austin, TX) on a computer that was coupled to the PMT by means of a low noise current preamplifier and low pass filter model SR 570 (Stanford Research Systems, Sunnyvale, CA) and an NI USB–6229 analog to digital converter (National Instruments, Austin, TX).

The microfluidic device was positioned on the microscope stage. A 445 nm diode laser from Omicron (Rodgau, Germany) set to operate at 15 mW was used for excitation. A single mode light-guiding glass fiber was used to couple the laser into the microscope. The laser was focused at a point of the separation channel approximately 0.2 cm from the waste reservoir through a 40X objective. Filter cubes housing the appropriate excitation/emission filters and dichroic mirrors were installed inside the carousel. A custom-built filter cube, for analysis of cyanobenz[f]isoindole CBI labeled amines, was purchased from Chroma Technology Corp. (Bellows Falls, VT) (25 mm diameter z442/10X clean-up filter, 25 mm diameter 510hq/50m bandpass emission filter, and 25.5 × 36mm laser dichroic filter and transmit hq510/50m).

4.3.1.2 Amperometric detection: The electrochemical detection system consists of a platinum working (15 μm) and reference electrodes (300 μm) deposited into a 500 nm channel etched into the glass surface (as previously described in[19]). The working electrode was aligned directly at the edge of the separation channel using in-channel alignment, with the electrode being no more than 5 μm inside the separation channel. A Pinnacle model 9051 electrically isolated wireless potentiostat (Pinnacle Technology, Lawrence, KS) in a two-electrode format at a 13 Hz sampling rate was used for this study. Physical contact between the electrode and the potentiostat was accomplished using colloidal silver and copper wire. The 9051 single-channel isolated potentiostat maintains a set voltage bias of up to 4 V between the working and reference electrodes, and wirelessly transmits a digitized signal directly to a Bluetooth® module connected to a PC at a sample rate of 1 sample/sec. The Bluetooth® module directly imports the data to the PC with support from Serenia software suites.

4.3.2 Chip handling

All microfluidic devices were preconditioned by aspirating solutions of 0.1 N hydrochloric acid, deionized water, methanol, and 0.1 N sodium hydroxide through the device as previously described.[19] Following the conditioning procedure, the chip was secured to a stage. High voltage and ground leads were placed into the appropriate reservoirs. Prior to each injection, the charging current at the electrochemical detector was allowed to dissipate, producing a stable baseline. The injection time was set at 0.3 seconds for gated injections on the gated serpentine chip and at 1 second for microdialysis experiments using flow gated injects in this study.

4.3.3 Microdialysis sampling

Microdialysis sampling was accomplished using a BASi loop microdialysis probe with a 1 cm membrane and 30 kDa molecular weight cut-off. Each side of the 1 cm semipermeable membrane has 16 cm of fluorinated ethylene propylene (FEP) tubing that can be cut to desired lengths. The probe was placed in an open 2 mL sample vial, which was used as a sample well. The reaction well was then placed in a sample holder and secured to a stage. The FEP tubing from the probe was connected to the syringe pump; all 16 cm of the attached tubing was used in this case. To connect the probe to the chip, 6 cm of the 1/32 × 0.005 FEP tubing was removed and replaced with 5 cm of PEEK tubing with similar dimensions using tubing connectors. The probe was connected to the chip using 1/32 LabSmith connectors and fittings (LabSmith, Livermore, CA).

4.3.4 Separation optimization

The separation was optimized on the gated serpentine chip for Arg, Asp, GABA, Glu, Gly, Ser, and Tau all at concentrations of 2 μM in a 50 mM boric acid at pH 9.2 using a 14 cm separation channel. The amines were derivatized off-chip using a 40 fold excess, of NDA and CN^-. The separation of Arg, Asp, GABA, Glu, Gly, Ser, and Tau under optimized conditions using a 14 cm serpentine chip design with LIF is shown in Figure 4.4. The final separation buffer was 50 mM boric acid and 6.5 mM SDS at pH 9.2. The applied voltage was +10000 V and +6000 V, with an injection time of 1 second.

4.3.5 On-chip sample derivatization of amino acids

Sample derivatization was accomplished on chip using three CMA 102 syringe pumps connected to the chip using 1/32 × 0.005 PEEK tubing. A 10 μM amino acid solution was placed in one syringe and pumped into the mixing chamber at a flow rate of 0.5 μL min^{-1}. NDA was delivered into the mixing chamber via a second syringe pump at a concentration of 50 μM with a flow rate of 0.3 μL min^{-1}. NaCN was also delivered via a third syringe pump at a flow rate of 0.3 μL min^{-1} at a 50 μM concentration.

4.3.6 On-chip derivatization with dual LIF and EC detection:

The design included three ports for fluid delivery of the sample, NDA, and NaCN. All fluids were delivered with a CMA 102 syringe pump with the flow rates for the sample set at 0.5 μL min^{-1} at a 10 μM concentration, NDA was set at 0.3 μL min^{-1} for a 50 μM concentration, and NaCN was also delivered at 0.3 μL min^{-1} NaCN at a 50 μM concentration. The separation buffer was made of 50 mM boric acid and 6.5 mM SDS at pH 9.2. The applied voltage was +10000 V with a 1 second injection.

This dual detection experiment was repeated with a microdialysis probe used for sample recovery. The microdialysis probe was connected to the sample inlet port with the microdialysis membrane secured in a 2 mL sample well. The sample well contained a solution of Arg, Asp, GABA, Glu, Gly, Ser, and Tau all at a concentration of 10 μM along with 1 mM of hydrogen peroxide, in 50 mM boric acid and 6.5 mM SDS buffer.

4.3.7 Online derivatization with dual detection on a microdialysis microchip electrophoresis system

The optimal derivatization of the analytes was accomplished in pH 9.2 borate buffer with separation buffer consisting of 50 mM boric acid and 6.5 mM SDS at pH 9.2. All perfusates were delivered with a CMA 104 syringe pump, with the flow rates for the sample set at 0.5 μL min^{-1} at a 10 μM concentration. NDA was set at 0.3 μL min^{-1} for a 50 μM concentration, and NaCN was also delivered at 0.3 μL min^{-1} NaCN at a 50 μM concentration.

4.4 Results and Discussion

This microfluidic system was developed with the purpose of being a fully integrated system, in an effort to reduce contamination and error due to sample handling. The advantage of dual detection on a single microfluidic device is that it allows simultaneous analysis of species with different chemical and physical properties. The microfluidic device was fabricated with a combination of microdialysis, an on-line interface to microdialysis on chip sample derivatization and electrophoresis. The device utilizes the dual detection methods of LIF with electrochemical detection, thereby creating a powerful analytical tool capable of high efficiency separations with short analysis times and low consumption of sample and reagents.

In an effort to detect the biogenic amines that are important for complex neurochemical systems, LIF detection was used. An on-chip micromixer for sample derivatization was incorporated into the microfluidic device, in order to minimize sample

handling and create a near real-time analysis system, Naphthalene 2,3-carboxaldehyde/CN- was used as the derivatizing agent for the amino acids. This fluorogenic agent produces CBI derivatives that excite at 420 nm and emit at 490 nm. The derivatization chamber consisted of a single channel with a series of flow diverters to increase turbulent flow and aid in mixing.

It has been shown the NDA/CN- (CBI) products are more stable over time but take longer to occur then if using a thiol such as 2-mercaptoethanol (2ME) as the nucleophile.[20] The mixing chamber length was optimized for maximum yield and optimal derivatization time of NDA/CN- so that at a total flow rate of 1 μL min^{-1} the CBI derivative was allowed to mix for 15 minutes before it was injected into the separation chamber.

4.4.1 Separation optimization

The separation of the seven amino acids was optimized by Simon Pfeiffer to give a separation efficiency of approximately 30,000 plate numbers in regards to glycine. From Simon's optimization work, two different concentrations of SDS were shown to resolve all of the amino acids in the sample, but a concentration of 6.5 mM SDS was chosen because of its higher separation efficiency, and because it produced a more stable and reproducible separation overall. The derivatization of NDA/CN^- is optimal at around pH 9.2, for this reason different pH conditions were not explored during the separation optimization. However, different concentrations of borate buffer were explored during the optimization process. It was found that higher concentrations did allow for higher resolution separation due to the higher ionic strength but this also lead to irreproducibility

within the separation and cause the chip to foul more often due to bubble formation and irregularities in peak migration times. For this reason the SDS concentration was the parameter that was optimized and had the largest impact on the separation. Sodium dodecyl sulfate (SDS) is an anionic surfactant used as a buffer modifier for MEKC. SDS forms micelles and migrates towards the anode, which in this case reduced the complex of the CBI derivative and the micellar velocity compared to that of the bulk flow.[21]

The optimal separation was achieved for Arg, Asp, GABA, Glu, Gly, Ser, and Tau all at concentrations of 2 μM in a 50 mM boric acid at pH 9.2 using a 14 cm serpentine separation channel and at different concentrations of SDS. Off-chip derivatization of the amines was accomplished using a 40 fold excess, of NDA and CN^-. For quantitative analysis, all samples were injected 45 minutes after derivatization was initiated, to ensure that the reaction was complete. Figure 4.3 shows the effect of SDS concentration on the migration time of the target analytes. The critical micelle concentration (CMC) of SDS under these conditions was 3 mM. The separation of Arg, Asp, GABA, Glu, Gly, Ser, and Tau under optimized conditions using a 14 cm serpentine chip design with LIF is shown in Figure 4.4. The final separation buffer was 50 mM boric acid and 6.5 mM SDS at pH 9.2. The applied voltage was +10000 V and +6000 V, with an injection time of 1 second.

4.4.2 On-Chip derivatization with dual LIF and EC detection:

Electrochemical detection has become an increasingly popular method of detection with MCE devices due to recent developments in fabrication methods allowing

for the integration of the miniaturized detector on chip.[19,22] In this research, amperometric detection was used with in-channel electrode alignment. Amperometric detection was accomplished by applying a constant potential to the working electrode with the current response being measured as a function of time.

The sample introduced into the derivatization channel consisted of a sample containing 10 μM Arg, Asp, GABA, Glu, Gly, Ser, Tau, and 1 mM hydrogen peroxide. Hydrogen peroxide detection was accomplished using electrochemical detection at a platinum electrode set to +1.0 V. Arg, Asp, GABA, Glu, Gly, Ser, and Tau were detected using LIF detection following on chip derivitization as seen in Figure 4.5. This dual detection experiment was repeated in combination with a microdialysis probe as shown in Figure 4.6.

4.4.3 Electrochemical detection

Peroxide was used as the model electroactive compound. In future studies more physiologically relevant electroactive compounds such as ascorbic acid, nitric oxide, and catecholamines will be added to the study. Peroxide was simply used as a model compound to test and evaluate the system to ensure that the chip design would function and that oxidizing agents in the sample would not reduce the signal achieved from the CBI derivatives. The NDA derivatized amino acids were not detected via electrochemical detection despite being electrochemically active. The amino acids were at a concentration of 10 μM, which is at the lower end of the reported limit of detection for the electrodes used in this device.[19] Also the oxidation of the CBI derivatives is not as favorable on a platinum electrode as compared to carbon fiber electrodes.[23,24]

4.4.4 On-line derivatization with dual detection on a microdialysis microchip electrophoresis system

The design for the complete integrated device was highly complex with many sections that had to be individually optimized. This chapter takes those previously optimized sections and combines them into a functional proof of concept device. The ability to successfully fabricate and execute an online MD-MCE-EC-LIF device with a built-in micromixer for on-chip derivatization demonstrates the idea of multiplexing and proves the ever-increasing functionality of a single, planar, microfluidic device. The primary design challenge with this device was matching the flow rates of the 3 syringe pumps to effectively derivatize the analytes of interest while still being able to establish a gate for sample injection into the separation channel. Not only did a gate need to be established and maintained, but the overall field strength inside the separation channel needed to correlate to that of the optimized separation parameters in order to maintain the integrity of the separation. The chip also needed to be characterized in terms of reagent mixing with sample via hydrodynamic flow for on-line derivatization with standards.

The optimal derivatization of the analytes was accomplished in pH 9.2 borate buffer and the separation buffer consisted of was 50 mM boric acid and 6.5 mM SDS at pH 9.2. This allowed for the maximum derivatization of the analytes within the micro-mixer without giving any statistically significant difference between the signal intensity of the on-chip and off-line derivatization reaction.

4.5. Conclusion

The primary goal of this study was to develop and fabricate a microdialysis microchip electrophoresis device with an integrated micro-mixer using dual detection. The designs were optimized for this system and characterized with final analysis using the complete device. The ultimate goal for this device was to achieve near real-time analysis for in-vivo monitoring of amino acid neurotransmitters and non-derivatizable electro active neurotransmitters, in an effort to achieve a more versatile analysis of the system. Future experiments conducted with this microfluidic device will be performed on a more complex sample matrix. An example would be using a microdialysis probe to sample in the brain extra cellular fluid (ECF) for the detection of amino acid neurotransmitters along with, ascorbic acid, glutathione, and nitric oxide. Other electrode materials that exhibit lower limits of detection for organic compounds also needs to be explored. Ideally a boron doped diamond or graphene electrode will be incorporated into the microfluidic device. These electrodes have been shown to have lower limits of detection and have a better oxidation potential for catecholamines.[25] This would also allow for the electrochemical detection of the CBI derivatives.

4.6 References:

[1] Dittrich, P. S., Tachikawa, K. & Manz, A. Micro total analysis systems. Latest advancements and trends. *Anal. Chem.* **12**, 3887-908 (2006).

[2] Manz, A., Graber, N. & Widmer, H. M. Miniaturized total chemical analysis systems: A novel concept for chemical sensing. *Sensors and Actuators B: Chemical* **1,** 244–248 (1990).

[3] Rohrman, B. A. & Richards-Kortum, R. R. A paper and plastic device for performing recombinase polymerase amplification of HIV DNA. *Lab Chip* **12**, 3082-3088 (2012).

[4] Bani-Yaseen, A. D., Kawaguchi, T., Price, A. K., Culbertson, C. T. & Jankowiak, R. Integrated microfluidic device for the separation and electrochemical detection of catechol estrogen-derived DNA adducts. *Analytical and Bioanalytical Chemistry* **399,** 519–524 (2011).

[5] Orwar, O., Fishman, H. A., Ziv, N. E., Scheller, R. H. & Zare, R. N. Use of 2, 3-naphthalenedicarboxaldehyde derivatization for single-cell analysis of glutathione by capillary electrophoresis and histochemical localization by fluorescence microscopy. *Anal. Chem.* **67,** 4261–4268 (1995).

[6] Bowden, M., Sequiera, M., Krog, J. P., Gravesen, P. & Diamond, D. Analysis of river water samples utilising a prototype industrial sensing system for phosphorus based on micro-system technology. *J. Environ. Monitor.* **4,** 767–771 (2002).

[7] Watson, C. J., Venton, B. J. & Kennedy, R. T. In vivo measurements of neurotransmitters by microdialysis sampling. *Anal. Chem.* **78,** 1391–1399 (2006).

[8] Giannitsis, A. T. Microfabrication of biomedical lab-on-chip devices. A review.

Estonian Journal of Engineering **2**, 109-139 (2011).

[9] Capretto, L., Cheng, W., Hill, M. & Zhang, X. Micromixing within microfluidic devices. *Top Curr Chem* **304,** 27–68 (2011).

[10] Wang, Y. Numerical study of rapid micromixers for lab-on-a-chip applications. 1-27 (2007).

[11] Giuri, E., Ricci, A. & Ricciardi, C. Influence of Geometry on Mixing in a Passive Micromixer. *COMSOL Users Conference* 1–24 (2006).

[12] Nandi, P., Scott, D. E., Desai, D. & Lunte, S. M. Development and optimization of an integrated PDMS based-microdialysis microchip electrophoresis device with on-chip derivatization for continuous monitoring of primary amines. *Electrophoresis* **6**, 895-902 (2013).

[13] Li, X., Tong, Y. L., Liu, C., Li, O. L. & Yang, X. J. Dual Detection Methods for Microchip and Conventional Capillary Electrophoreses. *Chinese Journal of analytical chemistry* **37**, 1547-1554 (2009).

[14] Lapos, J. A., Manica, D. P. & Ewing, A. G. Dual Fluorescence and Electrochemical Detection on an Electrophoresis Microchip. *Anal. Chem.* **74,** 3348–3353 (2002).

[15] Nandi, P., Kuhnline, C. D. & Lunte, S. M. Analytical consideration for microdialysis sampling. - *Applications of Microdialysis in Pharmaceutical Science* 39-76 (2011).

[16] Sandlin, Z. D., Shou, M., Shackman, J. G. & Kennedy, R. T. Microfluidic electrophoresis chip coupled to microdialysis for in vivo monitoring of amino acid neurotransmitters. *Anal. Chem.* **77,** 7702–7708 (2005).

[17] Wang, M., Roman, G. T., Schultz, K., Jennings, C. & Kennedy, R. T. Improved temporal resolution for in vivo microdialysis by using segmented flow. *Anal. Chem.* **80,** 5607–5615 (2008).

[18] Shou, M., Smith, A. D., Shackman, J. G., Peris, J. & Kennedy, R. T. In vivo monitoring of amino acids by microdialysis sampling with on-line derivatization by naphthalene-2,3-dicarboxyaldehyde and rapid micellar electrokinetic capillary chromatography. *Journal of Neuroscience Methods* **138,** 189–197 (2004).

[19] Scott, D. E., Grigsby, R. J. & Lunte, S. M. Microdialysis sampling coupled to microchip electrophoresis with integrated amperometric detection on an all-glass substrate. *ChemPhysChem* **14,** 2288–2294 (2013).

[20] Huynh, B. H., Fogarty, B. A., Nandi, P. & Lunte, S. M. A microchip electrophoresis device with on-line microdialysis sampling and on-chip sample derivatization by naphthalene 2, 3-dicarboxaldehyde/2-mercaptoethanol *Journal of pharmaceutical and Biomedical Analysis* **42,** 529–534 (2006).

[21] Weinberger, R. Practical Capillary Electrophoresis (2nd Ed.) Weinberger Robert: Librairie Lavoisier. (1993).

[22] Crain, M. M. *et al.* Fabrication of a glass capillary electrophoresis microchip with integrated electrodes. *Methods Mol. Biol.* **339,** 13–26 (2006).

[23] Zhang, L. Y., Liu, Y. M., Wang, Z. L. & Cheng, J. K. Capillary zone electrophoresis with pre-column NDA derivatization and amperometric detection for the analysis of four aliphatic diamines. *Anal. Chim. Acta* **508**, 141-145 (2004).

[24] Lamba, S., Pandit, A., Sanghi, S. K., Gowri, V. S. & Tiwari, A. Determination of aliphatic amines by high-performance liquid chromatography-amperometric

detection after derivatization with naphthalene-2,3-dicarboxaldehyde. **614**, 190-195 *Analytica chimica* (2008).

[25] Tan, S. M., Poh, H. L., Sofer, Z. & Pumera, M. Boron-doped graphene and boron-doped diamond electrodes: detection of biomarkers and resistance to fouling. *Analyst* **138,** 4885–4891 (2013).

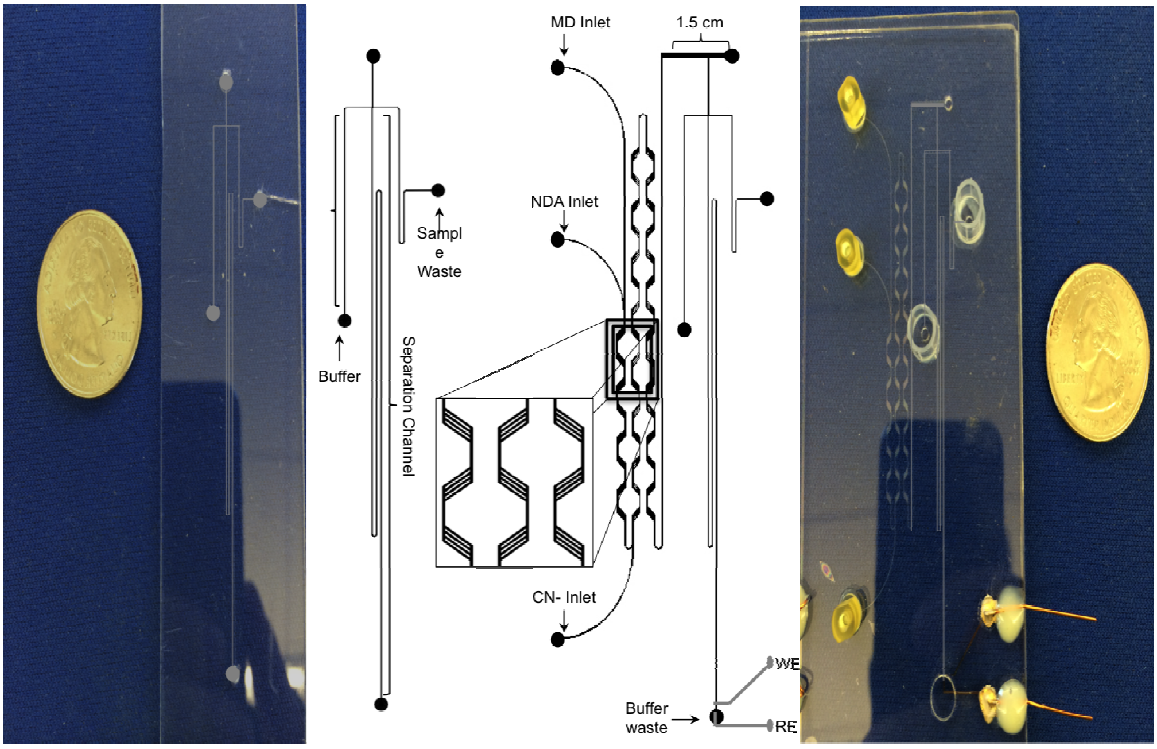

Figure 4.1: A) Schematic of the microchip design with 14 cm serpentine channel for separation optimization using LIF. B) Schematic of microchip design with electrode placement and derivatization channel for flow-through studies MD-MCE-EC-LIF studies with channel dimensions. All microfluidic channels were etched to 15 μm deep and 40 μm wide, except for the microdialysis flow through channel, which was 500 μm wide.

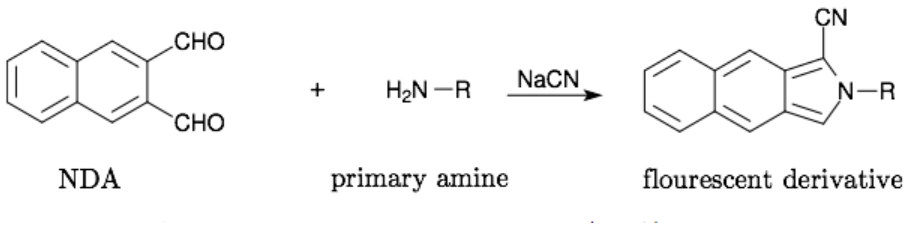

Figure 4.2: Reaction scheme for NDA with primary amine CN- to produce CBI derivative with the analytes of interest

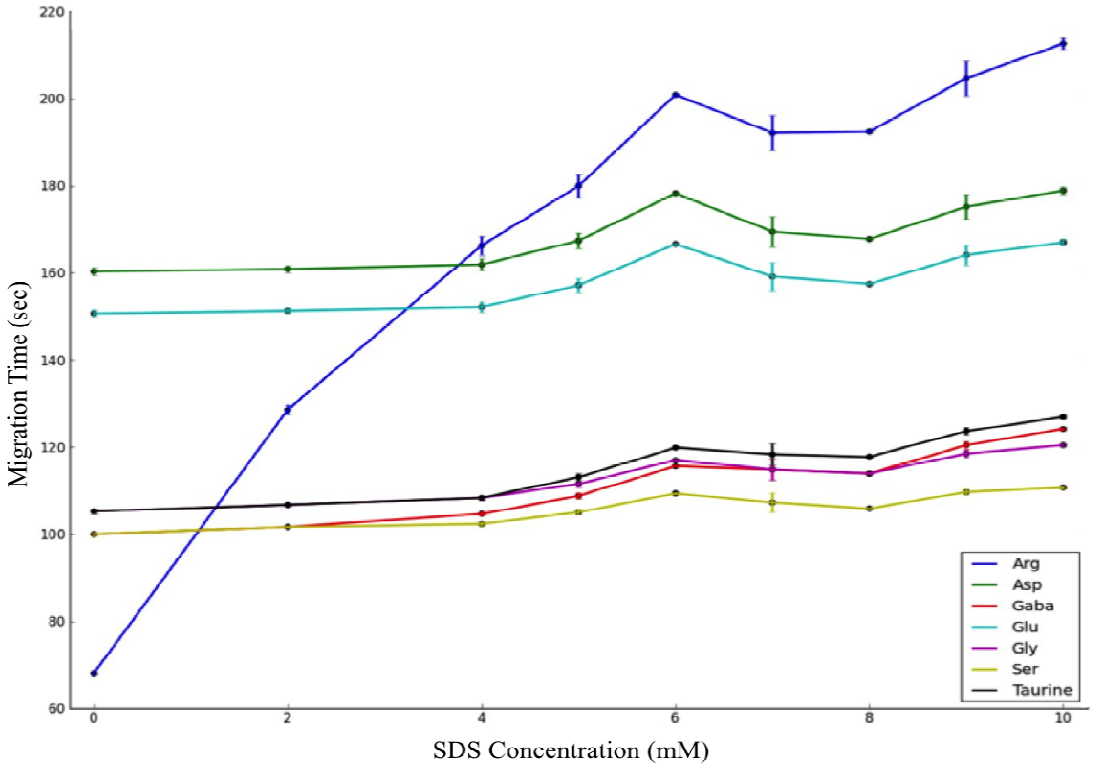

Figure 4.3: Separation optimization showing the effect of SDS concentration on the migration time of the target analytes. Separation buffer: 50 mM boric acid at pH 9.2, 2 μM Arg, Asp, Gaba, Glu, Gly, Ser, and Tau. The applied voltage was 10000 V and 6000 V with an injection time of 1 second. (courtesy of Simon Pfeiffer)

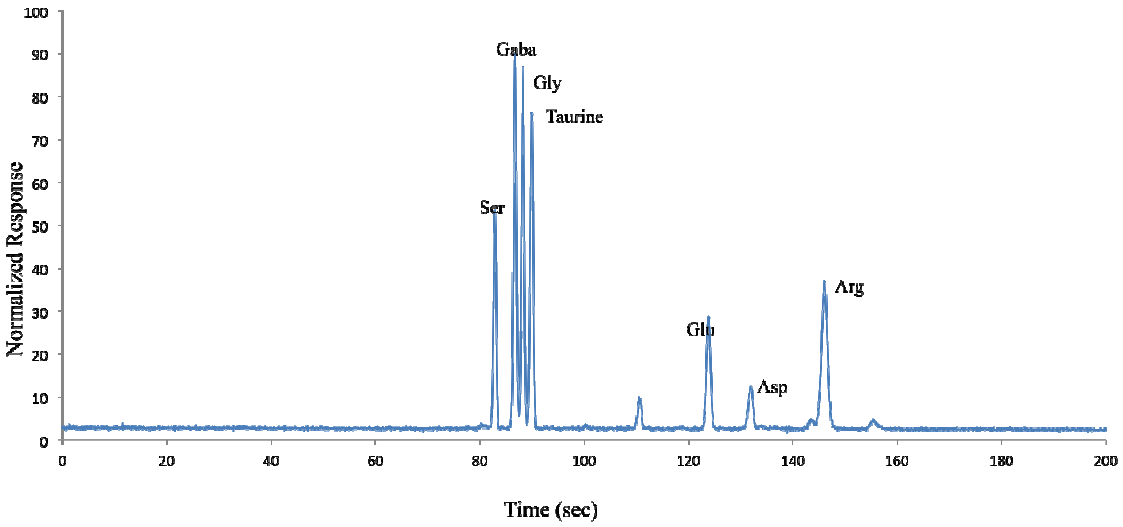

Figure 4.4: Optimized separation of prederivatized 10 μM Arg, Asp, Gaba, Glu, Gly, Ser, and Tau with NDA/CN^- using a 14 cm serpentine chip design with LIF. Separation buffer: 50 mM boric acid and 6 mM SDS at pH 9.2. All other conditions are identical to Figure 4.3.

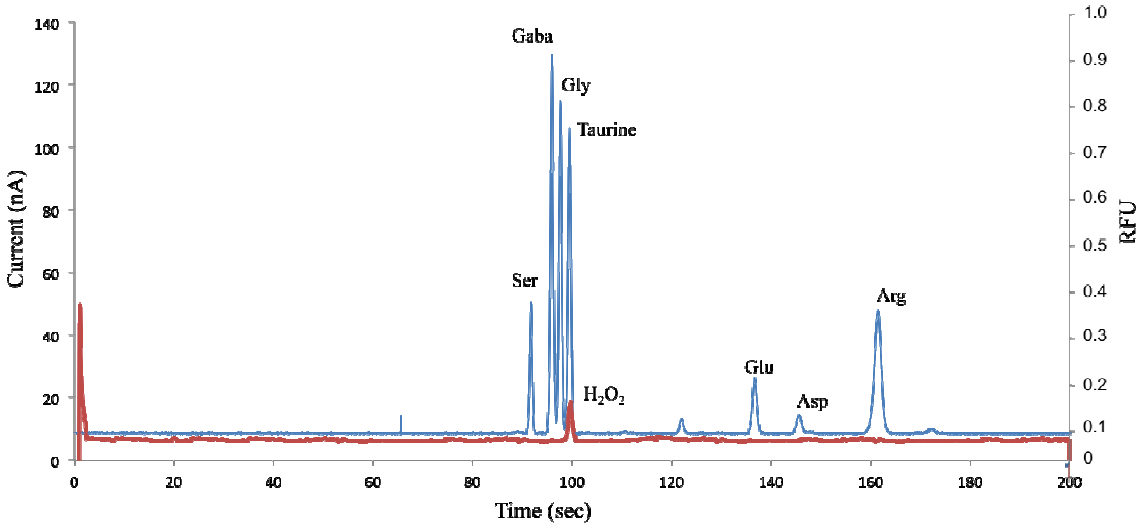

Figure 4.5: Detection of 1 mM hydrogen peroxide using electrochemical detection and separation of 10 μM Arg, Asp, Gaba, Glu, Gly, Ser, and Tau using LIF with on chip derivatization in normal polarity using direct perfusion. Separation buffer was made up of 50 mM boric acid and 6 mM SDS at pH 9.2. The applied voltage was +10000 V with a 1 second injection. 15 μm embedded platinum electrode at 1.1 V vs. an embedded platinum reference electrode

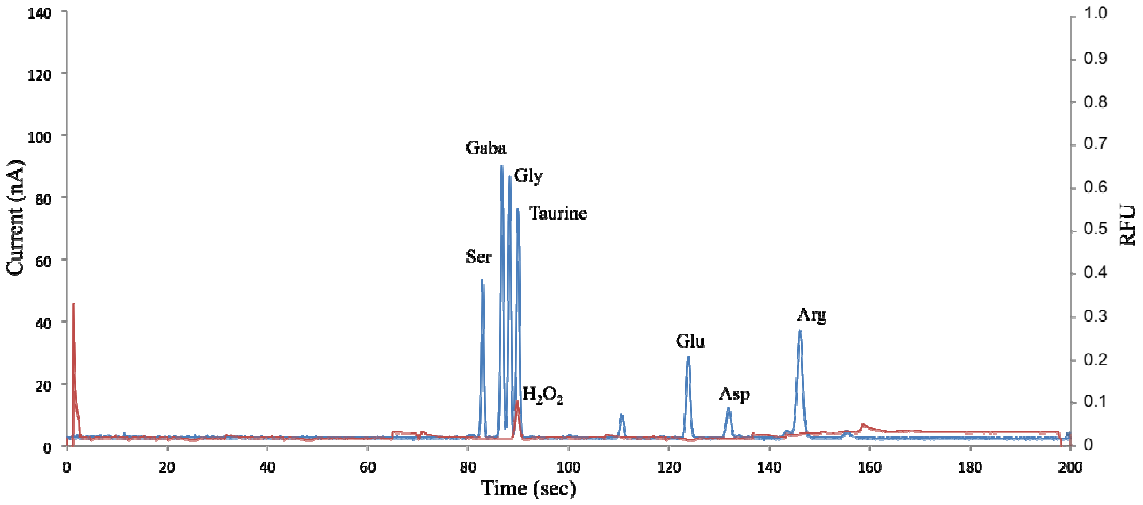

Figure 4.6: On-line microdialysis sampling with detection of 1 mM hydrogen peroxide using electrochemical detection and separation of 10 µM Arg, Asp, Gaba, Glu, Gly, Ser, and Tau using LIF with on chip derivatization in normal polarity. Separation buffer 50 mM boric acid and 6 mM SDS at pH 9.2. The applied voltage was +10000 V with a 1 second injection. 15 µm embedded platinum electrode at 1.1 V vs. an embedded platinum reference electrode. Syringe pump was set at a flow rate of 1 µL/min for microdialysis sampling.

Chapter 5

Future Directions

5.1 Summary

During the course of this dissertation the development and application of an on-line microdialysis microchip electrophoresis system has been described. Chapter two primarily focused on the fabrication of an all glass device with a flow gated interface design for microdialysis sampling coupled to microchip electrophoresis with electrochemical detection. The system was evaluated *in vitro* for continuous analysis of nitrite. Chapter three describes the first report of a miniaturized MD-MCE-EC system for on-animal sensing via telemetry control. The system was tested for ruggedness and long-term stability of the electrode along with *in vivo* testing in both rats and sheep for the production of nitrite in response to nitroglycerin. Control studies were also described for the collection of microdialysis samples off-line and analysis by conventional LC-EC. In chapter four the chip design and the detection scheme was further modified to facilitate dual EC and LIF detection. A serpentine separation channel was incorporated into the device along with an on chip micro-mixer for on chip sample derivatization. This design was employed for both electrochemical and fluorescence detection. The incorporation of both detection schemes allows for the possibility of simultaneous monitoring of easily derivatizable excitatory neurotransmitters as well as non-derivatizable electroactive species.

5.2 Future directions of projects

Most of the work described in this dissertation, are proof-of-concept studies with the goal of developing a miniaturized total analysis system for on-animal analysis. Work still remains in regards to the design and fabrication of this device, particularly with the

design of the micro-mixer for the LIF detection. The design and layout of the mixer can be improved for more efficient mixing using computer-modeling software like COMSOL Multiphysics®, to ensure that the derivatization reaction can occur efficiently within the smallest possible surface area.

In addition to improving the design of the mixer, the total reaction time for forming fluorescently labeled compounds for LIF detection can be enhanced. In regards to using NDA, other nucleophiles that are faster reacting and more stable can be explored in an effort to replace CN^-. A faster reaction time could shorten the derivatization channel thus reducing the lag time, as well as allowing for better temporal resolution and reducing the total size of the device. Detection limits remain a major concern in that some analytes are reported to be in nanomolar concentration ranges with our reported LOD's being in the μM range.[1] To improve the sensitivity and limits of detection with the fluorescently labeled compounds, the use of pinhole filters for focusing the laser can be used.

In chapter 4, the combination of electrochemical detection and LIF detection was discussed. This chapter focused on detection of a single analyte for the EC module. This needs to be expanded to multiple analytes, especially in the category of biogenic amines. The optimization of a separation for detection of both catecholamines and amino acid neurotransmitters is still needed in the future for this device. This would allow for a large number of analytes with different chemical characteristics to be simultaneously detected, giving greater insight than with a single analytical method. With the dual detection system, other dyes or derivatizing agents also need to be explored, considering that NDA derivatives will also be detected using electrochemical detection.

5.2.1 Microchip and electrode fabrication

One of the most important areas of the chip fabrication process needing to be optimized and improved is the electrode fabrication. Many parameters of the electrode deposition process can be optimized. Installing a more powerful vacuum pump and making sure all seals are stable, the base pressure can be decreased. Decreasing the base pressure increases the stability and uniformity of the thin film. Controlling the base pressure allows a higher degree of control for the deposition process. Pressure and film stability are intrinsically linked and can easily be controlled. Also, the rate of deposition and the total ionization energy increases at lower deposition pressures, which allows the thin film to be deposited faster and more efficiently. Any leak in the system or loss of vacuum pressure can be catastrophic to deposition rates and thus affects the viability of the thin film being deposited.

A heating element or baking step also needs to be added to the deposition process. By simply baking the chamber, the chamber degasses quickly and removes a large portion of gas and water that have adsorbed to the metal side-walls of the vacuum chamber. These trapped gasses and excess water, if not evacuated by baking, continually leach out during the deposition process and contaminate the thin films being deposited. This leaching effect drastically reduces the efficacy of the thin film. Ultimately, new types of electrodes and electrode materials needs to be explored.

Throughout this dissertation, platinum was used as the primary electrode material for the working and counter electrodes. Platinum can easily be modified in an effort to increase the sensitivity of the working electrode. It has become an increasingly popular

method to electro-deposited platinum black in a process called platinization to platinum electrodes.[2,3] This surface modification of the original electrode material produces an electrode with a higher sensitivity and lower limits of detection. However, platinum blacks primary benefit to platinized electrodes is the increase in surface area.[4] Three-dimensional electrodes take advantage of the ability to add height and increase the available surface area of a traditionally planar electrode. Increasing the overall surface area of the electrode allows for more electrode material, which increase the available space for electron exchange thus increasing the sensitivity of the electrode.[5,6]

Boron doped diamond and graphene electrodes are of particular interest as electrode materials to be used in the microfluidic devices discussed in this dissertation. Doping carbon with boron can change its electrochemical behavior and has been shown to require lower oxidation potentials for biomolecules such as dopamine and ascorbic acid.[7] These electrodes have also been demonstrated to have low capacitive currents with stable and reproducible current response for nanomolar concentrations of $Fe(CN)_6^{4-}$.[8] These lower limits of detection are essential to quantitatively measure analytes of interest that exist in a biological system at low μM to nM concentrations.

5.2.2 Point of care

The devices described within this dissertation lend themselves well to creating a deployable on-site monitoring system with near-real time analysis capability. This can either be directed toward a point of care or bedside device for the constant monitoring of

patients for diagnostics and injury prevention especially in the case of ischemic reperfusion injury and traumatic brain injury. The ability to gain insight into biological functions in near real time allows for the administration of therapeutic measures during critical and life threatening events. In chapter 4, the microfluidic device was developed to monitor a large spectrum of analytes with a dual detection system. This can easily be coupled with the telemetry device discussed in chapter 3 with the addition of a miniaturized LIF detection system that is currently being developed in the lab.

An application for mobile devices with real-time data capture and device control can also be added to the system so that all data analysis and monitoring can be done remotely and immediately without having to be tethered to a stationary monitoring system. This will make the telemetry-enabled miniaturized system truly portable and remotely operated.

5.2.3 Environmental monitoring

Much consideration has also been given to modify the device for environmental monitoring. For example the MD-MCE system could be used for the monitoring of water quality, especially in the cases of industrial and agricultural waste. Adapting the device to continuously monitor trace levels of pollutants in the water would be especially beneficial to the environmental protection agency (EPA).[9,10] Nitrite is of particular interest in regards to agricultural runoff in waterways from pesticides, fertilizers, and animal waste.[11-13] The microfluidic device discussed in chapter 2 and 3 has already been optimized for the detection of nitrite in aqueous solution. By developing an

enclosed, weather-resistant case in conjunction with the proposed mobile application, a remote sensor can be established for monitor water quality.

5.3 References:

[1] Nandi, P., Scott, D. E., Desai, D. & Lunte, S. M. Development and optimization of an integrated PDMS based-microdialysis microchip electrophoresis device with on-chip derivatization for continuous monitoring of primary amines. *Electrophoresis* **34**, 895-902 (2013).

[2] Li, Y. *et al.* Highly Sensitive Platinum-Black Coated Platinum Electrodes for Electrochemical Detection of Hydrogen Peroxide and Nitrite in Microchannel. *Electroanalysis* **25,** 895–902 (2013).

[3] Selimovic, A. & Martin, R. S. Encapsulated electrodes for microchip devices: microarrays and platinized electrodes for signal enhancement. *Electrophoresis* **34,** 2092–2100 (2013).

[4] Feltham, A. M. & Spiro, M. Platinized platinum electrodes. *Chemical Reviews* **71**, 177-194 (1971).

[5] Chen, G., Bao, H. & Yang, P. Fabrication and performance of a three-dimensionally adjustable device for the amperometric detection of microchip capillary electrophoresis. *Electrophoresis* **26,** 4632–4640 (2005).

[6] Pai, R. S. *et al.* Fully Integrated Three-Dimensional Electrodes for Electrochemical Detection in Microchips: Fabrication, Characterization, and Applications. *Anal. Chem.* **81,** 4762–4769 (2009).

[7] Tan, S. M., Poh, H. L., Sofer, Z. & Pumera, M. Boron-doped graphene and boron-doped diamond electrodes: detection of biomarkers and resistance to fouling. *Analyst* **138,** 4885–4891 (2013).

[8] Hutton, L. A. *et al.* Examination of the factors affecting the electrochemical

performance of oxygen-terminated polycrystalline boron-doped diamond electrodes. *Anal. Chem.* **85,** 7230–7240 (2013).

[9] Bowden, M., Sequiera, M., Krog, J. P., Gravesen, P. & Diamond, D. Analysis of river water samples utilising a prototype industrial sensing system for phosphorus based on micro-system technology. *J. Environ. Monitor.* **4,** 767–771 (2002).

[10] Cleary, J., Maher, D. & Diamond, D. in *Sensors for Real-Time Water Quality* **4,** 125–148 (Springer Berlin Heidelberg, 2013).

[11] Mellor, R. B., Ronnenberg, J., Campbell, W. H. & Diekmann, S. Reduction of nitrate and nitrite in water by immobilized enzymes. *Nature* **355,** 717–719 (1992).

[12] Sáez, F., Pozo, C., Gómez, M. A., Rodelas, B. & Gónzalez-López, J. Growth and Nitrite and Nitrous Oxide Accumulation of Paracoccus Denitrifcans ATCC 19367 in the Presence of Selected Pesticides. *Environ Toxicol Chem* **22,** 1993-1997 (2003).

[13] Burkholder, J. *et al.* Impacts of Waste from Concentrated Animal Feeding Operations on Water Quality. *Environ Health Perspect* **115,** 308–312 (2006).

Appendix

Practical Notes and Standard Operating Procedures

A.1 Glass microchip fabrication

Dr. Bryan Huynh made progress in establishing a fabrication process for glass microfluidic devices. In this appendix, his previously established protocols for bonding parameters have been modified and optimized for specific substrates and updated in regard to equipment availability. The fabrication of an all-glass microfluidic device is extremely challenging and great care must be taken to successfully process to the end product. The fabrication of a glass microfluidic device can be broken down into three steps: development, etching, and bonding, but there are multiple processes involved in each of these steps. These fabrication processes have been previously described in chapter 2 and 4:

And are presented here in a step-by-step process.

A.1.1 Sodalime glass fabrication process:

1. Draw a negative tone mask using AutoCAD software (Autodesk, San Rafael, CA) and the transparency printed by Infinite Graphics, Inc., Minneapolis, MN).
2. Overlay mask on the 4" × 4"× 0.060" chrome and AZ1518 photoresist coated soda-lime glass blanks.
3. Create a photolithographic pattern using an I-line UV flood source with an exposure dose of 86 mJ cm^{-2} (ABM, Inc., Scotts Valley, CA), for 4 seconds
4. Develop in ~ 100 mL of AZ® 300 MIF for 3 minutes.
5. Wash with DI water and dry with N_2 gas.

6. Bake at 100°C for 10 minutes using a hot plate.
7. Etch exposed chrome layer using chrome etchant CR-7S etchant.
8. Drill fluid wells in the glass plate containing the microfluidic channels using a diamond drill bit (TrueBite, Inc., Vestal, NY) mounted in a drill press.

Note: The microfluidic wells and access holes should be drilled before the glass is etched. This will allow the etching process to smooth the splintering and roughness of the access holes caused during the drilling process, as well asremove any debris from the drilling process. This drilling must be done in a water bath while being careful to allow only the drill bit to be submersed in water. A sacrificial piece of glass should be used on the back side of the glass plate to prevent the edges of the drilled hole from shattering.

9. Etch the plates in a 20:14:66 solution (49% hydrofluoric acid: concentrated nitric acid: water) to a depth of 15 microns for the microfluidic.
10. Verify etch depth using an Alpha-Step 200 stylus profilometer (Tencor, Milpitas, CA).
11. Cut the patterned and etched glass into individual chips using a tungsten carbide cutting wheel.
12. Place etched plates in an acetone bath to dissolve the layer of AZ® 1518 photoresist.
13. Remove any remaining chromium from each piece using CR-7S etchant.

A.1.2 Electrode fabrication

1. To fabricate the embedded platinum electrodes follow steps 1-7 as stated above in the Soda-Lime glass fabrication process
2. Etch glass plates in 10:1 buffered oxide etchant (JT Baker, Austin, TX) to produce a trench with a depth of approximately 500 nm.
3. Wash with DI water and dry with N2 gas.
4. Bake at 100 °C for 10 minutes using a hot plate.
5. Expose to oxygen plasma (March Plasmod, Concord, CA) for 5 minutes.

Note: This is done in order to promote adhesion of the metal to the etched glass surface.

6. Place the glass plate directly into the vacuum chamber of the AXXIS DC magnetron sputtering system (Kurt J. Lesker Co.)
7. Pump down to a base pressure of 5.0 × 10-7 Torr.
8. Deposit a 40 nm adhesion layer of titanium.
9. Deposit a 460 nm layer of platinum metal for the electrode material.

Note: All deposition was done at a pressure of 2.4×10^{-3}Torr with applied power of 220 W and 200 W, respectively.

10. Remove excess metal around the electrodes in an acetone bath.
11. Remove the chromium layer with CR-7S etchant.

A.1.3 Bonding procedure for glass

1. Scrub the two halves of the microfluidic device with a fiber wipe soaked in 5% Aconox™ solution.
2. Rinse with DI water.
3. Wash again in a 5% Alconox™ /5% calcium acetate solution.
4. Gently rub etched sides of each plate together for approximately 2 minutes.
5. Repeat step 3 and 4 three times.
6. Rinse the glass plates with water and roughly align the electrodes and the microfluidic channels by hand.
7. Visually inspect the chips to ensure that no air bubbles are present between the glass plates.
8. More precisely align the electrodes under a microscope.

Note: Align the electrodes so that the front of the working electrode is positioned no more than five microns into the end of the separation channel.

9. Clamp the assembled chip together using binder clips to ensure that the electrode alignment does not shift during processing.
10. Place the clamped chip in a low temperature oven (Lindberg/Blue-M, SPX Thermal Product Solutions, Riverside, MI) at 65 °C for one hour.
11. Increase the temperature to 110 °C for a minimum of 2 hours.

Note: Longer curing times of up to 96 hours promote a significantly higher success rate for full thermal bonding of the substrates.

12. Inspect assembled chip for proper electrode alignment and for areas of nonspecific binding identified by Newton rings.

Note: In the case of electrode misalignment or the formation of Newton rings, the chip can easily be pried apart and reassembled by repeating the procedure above until all requirements are met.

13. Place chip in a programmable muffle furnace and set furnace to the provided bonding program as dictated in table A1 or A2 per substrate type.

Table A1: Temperature Bonding Program for Sodalime Glass

Step 1	Ramp to 540 °C at 3 °C min^{-1}
Step 2	Ramp to 630 °C at 4 °C min^{-1}
Step 3	Hold at 630 °C for 3 hours
Step 4	Ramp down to 540 °C at 3 °C min^{-1}
Step 5	Ramp down to 510 °C at 1.5 °C min^{-1}
Step 6	Hold at 510 °C for 30 minutes
Step 7	Ramp down to 460 °C at 0.5 °C min^{-1}
Step 8	Ramp down to room temp at 5 °C min^{-1}

Table A2: Temperature Bonding Program for Borosilicate Glass

Step 1	Ramp to 300 °C at 1.5 °C min^{-1}
Step 2	Hold at 300 °C for 2 hours
Step 3	Ramp to 610 °C at 1.5 °C min^{-1}
Step 4	Hold at 610 °C for 8 hours
Step 5	Ramp down to 300 °C at 1.5 °C min^{-1}
Step 6	Ramp down to room temp at 5 °C min^{-1}

Note: It has become common practice amongst many groups who use glass microfluidic devices to bond the glass substrates under pressure by using weights to promote adhesion of the substrates. This is a practice that should not be performed outside of bonding presses or vacuum pressure systems specifically manufactured for high-pressure low temperature bonding. Using weights while bonding induces strain into the glass, which causes the glass to become brittle and prone to fracturing as seen in Figure A.1 B.[1] Pressure applied to the glass substrate due to weight will deform the glass, warp the substrate, and possibly collapse the fluid channels, along with stamping the substrate with any pattern that the weight or the surface media may have causing patterns and hazing to appear as shown in Figure A.1 C.

Increasing the ramp rate at which the temperature increase can induce strain on the glass will cause the glass microfluidic devices to fracture.[2] Sodalime glass is more forgiving to these temperature fluctuations because it is a softer type of glass and easier to work with.[1] Borosilicate, on the other hand, is much harder to work with. Increasing the temperature above 610 °C will soften the glass too much and can risk imprinting the glass surface with any patterns on the ceramic tile, thus reducing the optical integrity of the device for LIF detection. Holding temperatures are also especially important in borosilicate glass due to the lower thermal conductivity of the glass to allow for equal and thorough heating of the substrate.[3] The overall goal for each of these methods that were developed in this dissertation is to maintain the optical and structural integrity of the glass, while simplifying and developing a greener process for chip fabrication.

An effort was made to make the fabrication process a greener process than what has previously been done in our group or by many groups conducting glass bonding. Many of these protocols for glass bonding use piranha based cleaning steps.[4-6] Piranha solutions are a very strong oxidizing agent and are used to strip organic compounds from the surface. The solution consists of sulfuric acid and hydrogen peroxide. This is a highly volatile solution and can be dangerous, with complicated cleanup and disposal procedures. By implementing a calcium-assisted bonding step and simply washing the glass with Alconox and calcium acetate, the success rate for bonding was dramatically increased along with eliminating the need for harsh chemicals to clean the glass to promote adhesion.

After the glass plates were bonded together, bonded port connectors and fittings were attached to the chip using LS EPOXY two-part adhesive (Labsmith, Livermore, CA) over one of the access holes for the microdialysis sampling channel. Copper wires were also connected to the platinum reference and working electrodes through the access holes using colloidal silver.

A.2 Adhesive bonding

During the course of this study several different adhesive materials were investigated, including cyanoacrylate, Sylgard 184 (PDMS), NOA61, and other UV adhesives of a variety of viscosities for glass-glass bonding. Multiple bonding strategies were tested for each material. Adhesive bonding is a low temperature bonding process for glass microfluidic devices. Schlautmann and Majumdar introduced a “stamp-and-

stick" method as a low temperature adhesive bonding approach.[7] For the stamping process a thin film of the adhesive material was spin coated on a sacrificial wafer. The glass substrate with the microfluidic channels was lowered onto the wafer containing the adhesive material and used as a stamp to apply to adhesive evenly to the glass chip. This process serves as a method to transfer a thin film of adhesive selectively onto the raised surfaces of the glass device. Once the substrate was stamped and the adhesive transferred, the glass plate was brought into contact with the other glass plate to complete the device.

This process using adhesive bonding has been primarily limited to fabricating static devices such as microarrays or pressure driven flow-through devices. So far, only one report has been made, where adhesive bonding has been used in a CE based microfluidic device.[2] The reason there have been so few reports on this is because the device needs to provide a stable and long-term performance value under high strain. Adhesives can be used to bond glass, but this reduces their thermal and chemical resistance. The adhesive will always be a weak point in the structure; it also creates an exposed surface of dissimilar materials that may interfere with the chip's function.

With each of the different adhesives used, a good seal was created, but a potential difficulty is that the liquid adhesive may run into the etched channels. Neither of these methods was very successful. In most cases, the adhesive did leak into the fluid channel, or there was incomplete bonding due to inadequate coverage of the adhesive. In almost all cases, the adhesive used leached into the fluid channel during testing. Most of the adhesives are auto-fluorescent, which made it impossible to do LIF detection. In cases

where the adhesive didn't leak into the channel, there was incomplete bonding around the fluid channel, causing fluid leakage in the chip, with no defined separation channel available for use.

The use of adhesive bonding does have advantages in that thermal bonding requires an extremely high degree of surface flatness for the bonding substrates and it is a time-consuming process due to the limitations on temperature control and the strain of the glass. Also with thermal bonding, the glass and microfluidic channels may distort if the bonding procedure has not been optimized correctly.

A.3 Metal deposition:

Magnetron sputtering is a commonly used vapor deposition technique for depositing thin film coatings, which can be done by either of two modes. Direct current (DC) sputtering is done with conducting materials. If the target is a non-conducting material, the positive charge will build up and stop sputtering. In direct-current magnetron sputtering, the power density on the cathode results in a low-density plasma. Under plasma conditions, material is sputter-ejected from a target and deposited on a substrate. The substrate, in this case glass plates, is placed in a vacuum chamber and pumped down to a specific process pressure. In order to initiate a plasma, a negative charge is applied to the target, or deposition material. Positive charged gas ions, in this case argon, created by the plasma are attracted to the target at a high rate of speed. A high-energy transfer due to the collision energy, which ejects the particles from the target

material, generates deposition of the target material on the substrate. These ejected particles then transfer to the surface of the substrate as a thin film.

For magnetron sputtering, Magnets are used to focus the electrons and increase the collision count of the electrons striking the argon gas atoms inside the plasma.[8] This focusing increases the length of the electron path significantly, thus increasing the particle ionization and particle transfer.[9] Magnets also aid in the deposition of thin films by lowering the voltage needed to strike a plasma by focusing the electrons. This focusing effect helps control the uniformity of the deposited thin film and increases the rate of deposition. This also aids in reducing the heat in the system caused by electron bombardment.

Controlled heating of the deposition chamber can be used as a tool to improve film adhesion. Many systems use internal or external heating elements to keep a constant temperature in the vacuum chamber. Optimal substrate temperature for thin film deposition usually ranges from 150 °C to 300 °C, depending on the substrate and the target material. Another tool used in thin film deposition is a baking step, in which the temperature of the vacuum chamber is increased to 500 °C and held during the pumping down process.[10] This baking step has become the standard in the semiconductor industry. Baking the chamber aids in outgassing the system from any impurities which have adhered to the metal walls of the chamber and releases all water vapor from the system.[11] Baking the chamber is not an optional method; metals rapidly absorb gas molecules into their structure.[12] In order to remove excess molecules, particularly water molecules from the system, it must be baked.

A.4 References

[1] Iles, A., Oki, A. & Pamme, N. Bonding of soda-lime glass microchips at low temperature. *Microfluid Nanofluid* **3,** 119–122 (2006).

[2] Carroll, S. *et al.* Room temperature UV adhesive bonding of CE devices. *Lab Chip* **8,** 1564-1569 (2008).

[3] Berthold, A., Laugere, F., Schellevis, H., De Boer, C.R., Laros, M., Guijt, R.M. Fabrication of a glass-implemented microcapillary electrophoresis device with integrated contactless conductivity detection. *Electrophoresis* **23,** 3511–3519 (2002).

[4] Huynh, B. H., Fogarty, B. A., Martin, R. S. & Lunte, S. M. On-Line Coupling of Microdialysis Sampling with Microchip-Based Capillary Electrophoresis. *Anal. Chem.* **76,** 6440–6447 (2004).

[5] Crain, M. M. *et al.* Fabrication of a glass capillary electrophoresis microchip with integrated electrodes. *Methods Mol. Biol.* **339,** 13–26 (2006).

[6] Raley, N. F., Davidson, J. C. & Balch, J. W. Examination of glass-silicon and glass-glass bonding techniques for microfluidic systems. *Proceedings of SPIE* **2639,** 40 (1995).

[7] Schlautmann, S. & Besselink, G. Fabrication of a microfluidic chip by UV bonding at room temperature for integration of temperature-sensitive layers. *Journal of Micromechanics and Microengineering* **13**, 581-584 (2003).

[8] Srinivasan, G., Babu, V. S. & Seehra, M. S. Magnetic properties of radio frequency sputtered thin films of La–Pb–Mn oxides. *Appl. Phys. Lett.* **67,** 2090 2098 (1995).

[9] Kurt, J. Kurt: Lesker Co. Axxis operations Manual., Kurt Lesker Co, *Pittsburgh* **3**, 1-69 (1993).

[10] Hobson, J. P. Physical adsorption isotherms extending from ultrahigh vacuum to vapor pressure. *J. Phys. Chem.* **73,** 2720–2727 (1969).

[11] Alpert, D. & Buritz, R. S. Ultra-High Vacuum. II. Limiting Factors on the Attainment of Very Low Pressures. *J. Appl. Phys.* **25,** 202 209 (1954).

[12] Hablanian, M. H. High-Vacuum Technology: A Practical Guide, Second Edition - Marcel Dekker. New York., 25-427 (1997).

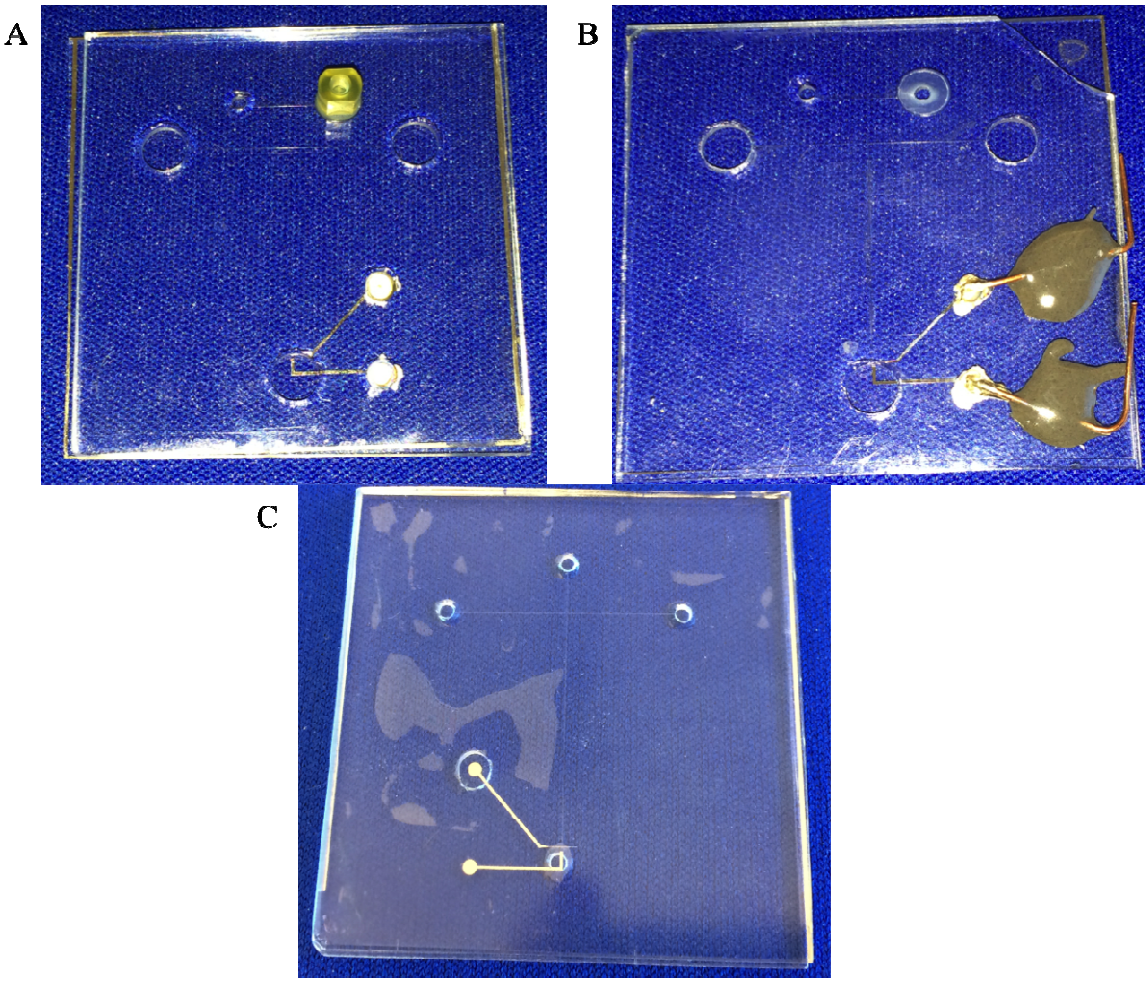

Figure A.1. Images illustrate the importance of using proper bonding procedures and their effects on chip quality. A) Shows an ideal chip with high optical clarity and complete bonding. B) Demonstrates how a chip can fracture and produce a slight haze along with completely collapsed channels due to weights being applied during the bonding process. C) Shows a chip with partially collapsed channels, incomplete bonding and severe optical hazing, due to weight being applied during the bonding procedure along with omitting the calcium assisted bonding step.